ACTA BIOLOGICA SLOVENICA

VOL. 61 ŠT. 2 LJUBLJANA 2018

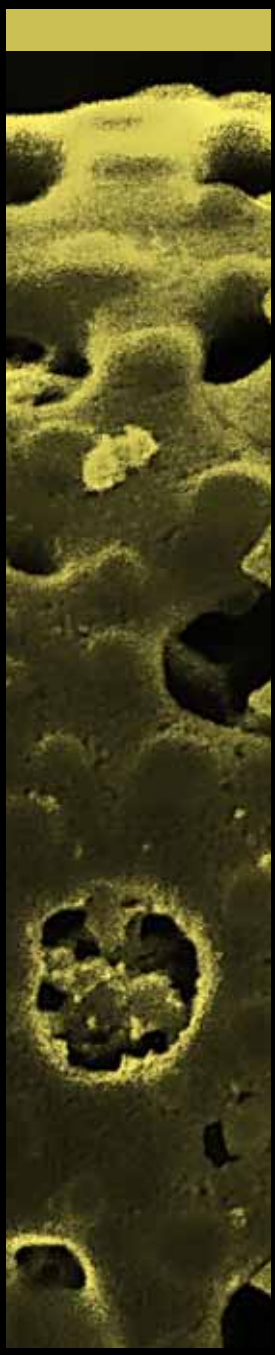

prej/formerly BIOLOŠKI VESTNIK

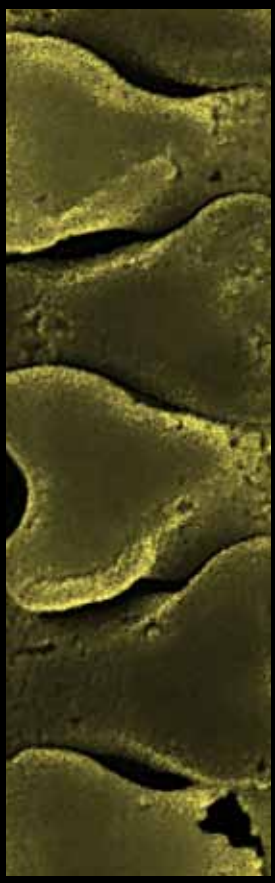

ISSN 1408-3671
UDK 57(497.4)

izdajatelj/publisher
Društvo biologov Slovenije

ACTA BIOLOGICA SLOVENICA

VOL. 61 ŠT. 2 LJUBLJANA 2018

prej/formerly BIOLOŠKI VESTNIK

ISSN 1408-3671
UDK 57(497.4)

izdajatelj/publisher
Društvo biologov Slovenije

ABS ACTA BIOLOGICA SLOVENICA
LJUBLJANA 2018 Vol. 61, Št. 2: 1–108

Acta Biologica Slovenica
Glasilo Društva biologov Slovenije – Journal of Biological Society of Slovenia

Izdaja – Published by
Društvo biologov Slovenije – Biological Society of Slovenia

Naslov uredništva – Address of Editorial Office
Acta Biologica Slovenica, Večna pot 111, SI-1001 Ljubljana, Slovenija
http://bijh.zrc-sazu.si/abs/

Zasnova oblikovanja – Design
Žare Vrezec

ISSN 1408-3671 UDK 57(497.4)

Natisnjeno – Printed on: 2018
Tisk – Print: Nonparel d.o.o., Škofja Loka
Naklada: 400 izvodov

Cena letnika (dve številki): 15 € za posameznike, 42 € za ustanove

Številka poslovnega računa pri Ljubljanski banki: 02083-142508/30

Publikacijo je sofinancirala Javna agencija za raziskovalno dejavnost Republike Slovenije

Acta Biologica Slovenica je indeksirana v – is indexed in: CAB Abstracts, Web of Knowledge – Thomson Reuters

ACTA BIOLOGICA SLOVENICA
LJUBLJANA 2018 Vol. 61, Št. 2: 3–13

In silico investigation of extracellular domain of RAGE receptor interaction with A-box and B-box of HMGB1 protein

In silico raziskava zunajcelične domene receptorja RAGE v interakciji z A-box in B-box proteina HMGB1

Safa Lotfi[a*], Marzieh Dehghan Shahsaltane[b]

[a] Department of Biotechnology, Institute of Science and High Technology and Environmental Sciences, Graduate University of Advanced Technology, Kerman, Iran
[b] Department of Biology, Faculty of Sciences, University of Zanjan, Zanjan, Iran

*correspondence: safalotfi@ut.ac.ir

Abstract: HMGB1 protein which is a non-histone chromosomal protein with two functional domains named A-box and B-box can also act as a signaling molecule after releasing from the cell and binding to the cell surface receptors such as RAGE. HMGB1 through its B-box domain binds to extracellular domain of RAGE and activates the signaling pathways involved in various pathological conditions like sepsis and tumor growth and metastasis. Interaction of recombinant HMGB1 A-box with RAGE antagonizes the RAGE activation by HMGB1. In the present study, interaction of human RAGE (hRAGE) extracellular domain (VC1C2) and B-box and A-box of human HMGB1 (hHMGB1) was investigated using a protein-protein docking software, HADDOCK. The results obtained were analyzed by PyMOL and LigPlot softwares. The results show B-box and A-box bind to different sites on the VC1 domain of RAGE and one of the B-box binding points is a positively charged groove located on the V domain surface which is also a major binding site for another RAGE ligand, Advanced Glycation End products (AGEs). The obtained results can be utilized to design new potent drugs for treatment of HMGB1-RAGE-related diseases such as cancer and sepsis.

Keywords: human HMGB1, human RAGE, HADDOCK software, cancer, sepsis

Izvleček: Protein HMGB1 je nehistonski kromosomski protein z dvema funkcionalnima domenama, A-box in B-box, ki lahko po sprostitvi iz celice deluje tudi kot signalna molekula in se veže na celično površino preko receptorjev kot je RAGE. HMBG1 se preko domene B-box veže na zunajcelično domeno RAGE in aktivira signalne poti, ki so vključene v različna patološka stanja kot so sepsa, rast tumorja in metastaze. Interakcija rekombinantnega proteina HMGB1 A-box z RAGE deluje antagonistično. V raziskavi smo preučevali interakcijo ekstracelularne domene (VC1C2) humanega RAGE (hRAGE) z B-box ter A-box humanega HMHB1 (hHMGB1). Uporabili smo računalniško orodje HADDOCK, pridobljene rezultate smo analizirali s programoma PyMOL in LigPlot. Rezultati so pokazali, da B-box in A-box vežeta na različna mesta domene VC1 na RAGE. Eno od vezavnih mest B-box je pozitivno nabita vdolbina na površini domene V in je hkrati glavno vezavno mesto za druge RAGE-ligande (Advanced Glycation End products – AGE). Rezultati raziskave so uporabni za načrtovanje novih zdravil za zdravljenje bolezni povezanih z interakcijami HMGB1-RAGE, kot sta rak in sepsa.

Ključne besede: humani HMGB1, humani RAGE, računalniški program HADDOCK, rak, sepsa

Introduction

Receptor for Advanced Glycation End products (RAGE) is a cell surface receptor belonging to the immunoglobulin superfamily (Neeper et al. 1992, Schmidt et al. 1992). RAGE receptor is involved in various pathological processes including inflammation (Orlova et al. 2007, Ramasamy et al. 2016), diabetic complications (Yamagishi et al. 2003, Litwinoff et al. 2015), cancer (Taguchi et al. 2000, Malik et al. 2015) and neurodegenerative disorders (Deane et al. 2003, Yan et al. 2003). The receptor structure is composed of 404 amino acids and three domains: an extracellular domain, a helical transmembrane domain and a short cytoplasmic domain. The extracellular domain which itself consists of three domains including a V-type immunoglobulin-like domain (V domain) and two tandem C-type immunoglobulin-like domains (C1 and C2 domains) is capable of binding to various biological ligands (Koch et al. 2010).

One of the RAGE ligands is High Mobility Group B1 (HMGB1) protein which binds to the V domain of extracellular part of RAGE receptor (Sorci et al. 2013, Musumeci et al. 2014). HMGB1 with 215 amino acids which also called HMG1 and amphoterin belongs to the superfamily of HMG proteins. The HMG proteins which were first isolated from calf thymus in 1973 are DNA-binding non-histone proteins with high content of acidic and basic amino acid residues (Goodwin et al. 1973). The highly evolutionary conserved HMGB1 protein in addition to the roles playing in the nucleus (Gerlitz et al. 2009, Lotfi et al. 2013), can act as a signaling molecule (cytokine) after releasing from the cell (Lotze and Tracey 2005). Today, the involvement of extracellular HMGB1 protein interaction with cell surface RAGE receptor in the various pathological states such as inflammation, sepsis (Zhu et al. 2010), growth and metastasis of tumor cells (Palumbo et al. 2004, Palumbo et al. 2009, Tang et al. 2010) and angiogenesis (Taguchi et al. 2000, Todorova and Pasheva 2012, He et al. 2017) has been confirmed.

HMGB1 structure consists of two tandem DNA-binding domains called HMG-box A and B (A-box and B-box) respectively and a long carboxylic tail rich in acidic residues. HMG-box domain which also exists in some other proteins, is consists of three alpha helices that are folded in the form of L, with an approximate angle of 80°. Although A and B boxes of HMGB1 have high similarity in structure, are functionally independent. As previously reported that the cytokine properties and the RAGE-binding site are located on the HMGB1 B-box (Huttunen et al. 2002, Tang et al. 2011). Surprisingly, the recombinant HMGB1 A-box can also bind to RAGE and antagonize the activation of RAGE by HMGB1 (Yang et al. 2004, LeBlanc et al. 2014).

In this study, the interaction of human RAGE (hRAGE) extracellular domain (VC1C2) with A-box and B-box of human HMGB1 (hHMGB1) has been investigated using protein-protein docking method. The results of this work show that B-box and A-box bind to distinct sites on the hRAGE VC1 domain and one of the binding pointes of B-box is a groove located on the V domain surface which also constitutes a main binding site for advanced glycation end products (AGEs). The results obtained from this work can be useful for designing new efficient drugs to treat HMGB1-RAGE-related diseases like sepsis and cancer.

Materials and methods

Searching PDB database to find the PDB structures

In order to study the interaction of A and B boxes of hHMGB1 with extracellular domain of hRAGE receptor (VC1C2) by protein-protein docking method, the PDB structures of three proteins were required. Thus, PDB website was searched to find the PDB structures corresponding to these proteins. The chain A of PDB entry 4LP5 (Yatime and Andersen 2013) which is the crystal structure of VC1C2 domain of hRAGE was selected as the receptor for the interaction study. The solution structure of hHMGB1 A-box (residues of 1 -84) has been also determined experimentally (PDB entry 2RTU) (Wang et al. 2013). 2RTU was used

as a ligand to study the interaction of A-box with extracellular domain of RAGE receptor.

Determination of three dimensional (3D) structure of B-box of hHMGB1 by I-TASSER web server

The I-TASSER server (Zhang-server) which operates based on the homology modeling method was ranked as No 1 protein structure prediction web server in CASP7, CASP8, CASP9 and CASP10 experiments (Yang and Zhang 2015). CASP (Critical Assessment of Techniques for Protein Structure Prediction) is a worldwide experiment for prediction of protein structure happening every two years since 1994 (Moult et al. 1995). The previous published data indicate that the residues of hHMGB1 which constitute the major site for hHMGB1-hRAGE interaction are located at the end of B-box and between B-box and C-terminal acidic tail (residues 150-183) (Huttunen et al. 2002). Although the structure of hHMGB1 B-box (residues 95-163) has been experimentally determined, there is no PDB structure covering all the residues responsible for the hHMGB1-hRAGE interaction. Thus, the 3D structure of residues 95-193 of hHMGB1 was determined by I-TASSER web server. For this purpose, the amino acid sequence corresponding to this part of hHMGB1 (UniProt entry: P094290) in FASTA format retrieved from UniProt website was given to the server. For each protein target, I-TASSER generates tens of thousands conformations (or decoys). I-TASSER clusters all the decoys according to the pairwise structure similarity and reports a total of five models corresponding to the five largest structure clusters. According to the Monte Carlo theory the largest clusters are related to the states of the largest partition function (lowest free energy) and thus possess the highest confidence. The confidence of each model created using I-TASSER is quantitatively measured by C-score. Although in most cases, the first model has higher C-score, since the top five models are ranked based on the cluster size, there is a possibility that the lower-rank models own a higher C-score. It is well known that the cluster size is more robust than C-score to rank the predicted models and therefore the first model is on average the most reliable and should be considered the best model unless there are certain biological and experimental reasons. C-score values vary between -5 to 2 (Yang et al. 2015). Between the five 3D models generated by I-TASSER, the first model (with highest C-score) was selected as the best model and applied for the interaction study as the B-box.

Study of interaction of hRAGE extracellular domain (VC1C2) with A-box and B-box of hHMGB1 using HADDOCK web server

HADDOCK 2.2 web server which is the most-cited data-driven protein-protein docking software was used for the protein-protein interaction study. In the data-driven docking methods such as HADDOCK, the available experimental data are used to set up the docking procedure and therefore the results obtained from these docking methods have more validity than *ab initio* docking methods (van Zundert et al. 2016). To perform the protein-protein docking process with HADDOCK, the easy interface of the web server was used. In addition to the PDB files of the interacting proteins, HADDOCK requires the active residues of them to perform the docking process. The HADDOCK software automatically finds the passive residues according to the given active residues. The active residues are directly contributing to the interaction process and surrounded by the passive residues which are not directly involved in this process. The active residues can be determined using the data obtained from the experimental methods or by means of CPORT web server (de Vries and Bonvin 2011). CPORT is an algorithm to predict the protein-protein interface residues. In fact, the CPORT is a combination of six interface prediction methods. For each HADDOCK run (Abox-VC1C2 and Bbox-VC1C2), the active residues of A-box and B-box were assigned according to the previously published experimental data (Huttunen et al. 2002, LeBlanc et al. 2014). Considering that there is no experimental data indicating that which residues of RAGE V domain are involved in the interaction with A-box and B-box, the active residues of 4LP5 chain A were predicted by CPORT server and only the active residues located in the V domain were selected for the docking process.

In each protein-protein docking run, HADDOCK generates hundreds of protein-protein conformations and classifies them into several clusters.

Each cluster specifies with a HADDOCK score. The HADDOCK score is a linear combination of various energies (van der Waals, electrostatic, desolvation and restraint violation) together with buried surface area (van Zundert et al. 2016). For each protein-protein docking (Abox-VC1C2, Bbox-VC1C2), the best conformation was selected according to the HADDOCK score and cluster size and analyzed by appropriate softwares.

The analysis of protein-protein interaction data

PyMOL software was applied to view and analyze the protein-protein complexes (Bbox-VC1C2 and Abox-VC1C2) obtained from HADDOCK software and LigPlot software (Wallace et al. 1995, Laskowski and Swindells 2011) was used to determine the amino acid residues involved in the protein-protein interaction process.

Results

The first I-TASSER model was selected as the B-box for the interaction study

As implied in the Materials and Methods, there is no PDB structure covering all the residues of hHMGB1 protein which are involved in the interaction with hRAGE receptor. Therefore, the 3D structure of residues 95-193 of hHMGB1 was determined by I-TASSER web server and the best model created by the web server was applied as the B-box for the interaction study. I-TASSER generated a total of five 3D models for B-box of hHMGB1. The model No. 1 with highest C-score (-1.16) was considered as the best model (Fig. 1). As shown in the Fig, B-box structure is composed of three alpha helices (I, II and III) connected with two loops and a long carboxylic tail.

hHMGB1 B-box through the residues located at helix III and C-terminal tail interacts with VC1 domain of hRAGE

As mentioned in the Materials and methods section, the Protein-Protein Docking Software, HADDOCK, was used to study the interaction of hHMGB1 Bbox with extracellular domain of hRAGE (VC1C2). To determine the residues involved in VC1C2-Bbox interaction, the results from HADDOCK were analyzed using DIMPLOT which is a part of the LIGPLOT software. DIMPLOT determines the residues of a protein-protein complex contributing to the formation of intermolecular hydrogen bonds. The results of this analysis are presented in Fig. 2. The surface representations of VC1C2 and B-box and the binding interface residues of two proteins (predicted by LigPlot) are shown in Fig. 3A. Figs. 3B and 3C represent the structure of HADDOCK VC1C2-Bbox complex in the surface and ribbon/sticks formats, respectively. As well seen in the Fig, the B-box binds to VC1C2 via the residues belonging to helix III and C-terminal tail. Although some Bbox-interacting residues of VC1C2 are located in C1 domain, most of the residues involved in the interaction belong to V domain.

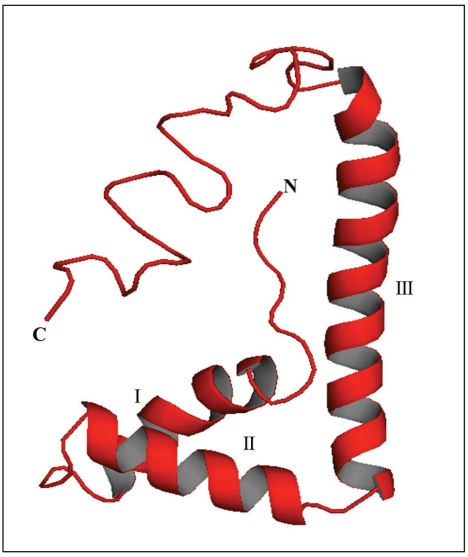

Figure 1: The best model created of residues 95-193 of hHMGB1 (referenced as the B-box in the text) by I-TASSER server.

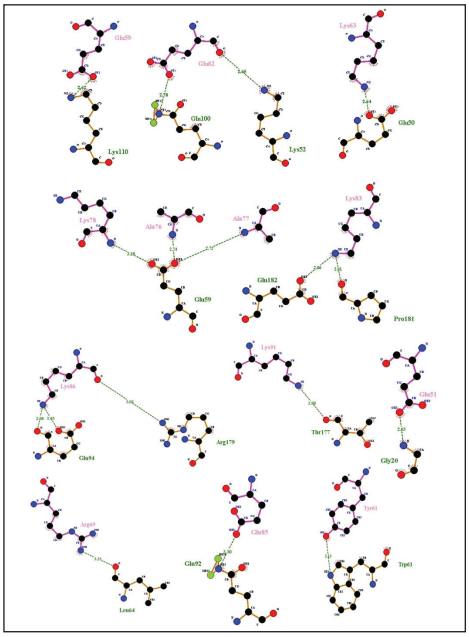

Figure 2: The amino acid residues of hHMGB1 B-box (titled with pink) and hRAGE VC1C2 (titled with green) interacting through hydrogen bonds in Bbox-VC1C2 HADDOCK complex predicted by LigPlot software. The hydrogen bonds are specified as green dotted line.

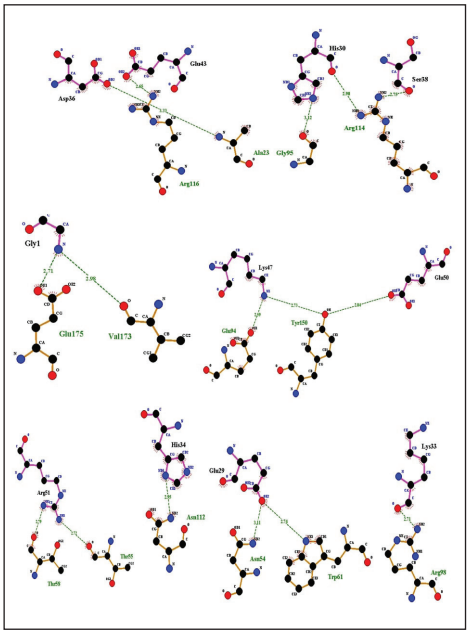

Figure 4: The amino acid residues of hHMGB1 A-box (titled with black) and hRAGE VC1C2 (titled with green) interacting through hydrogen bonds in Abox-VC1C2 HADDOCK complex predicted by LigPlot software. The hydrogen bonds are shown as green dotted line.

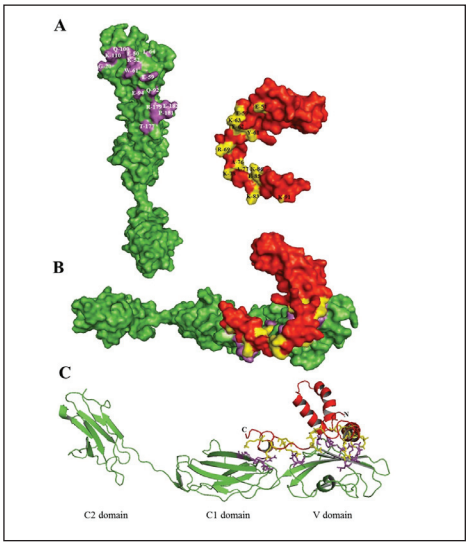

Figure 3: Illustration of VC1C2-Bbox interaction based on the protein-protein docking performed by HADDOCK and visualized by PyMOL. (**A**) The surface images of VC1C2 (green) and B-box (red) and the names and positions of their binding interface residues (predicted by LigPlot). The interfacial residues of VC1C2 and B-box are colored in purple and yellow, respectively. The surface (**B**) and ribbon/sticks (**C**) representations of the binding mode of VC1C2 protein (green) with B-box protein (red). The interfacial residues of two proteins (shown as sticks in the Figure 3C) are specified in purple and yellow, respectively.

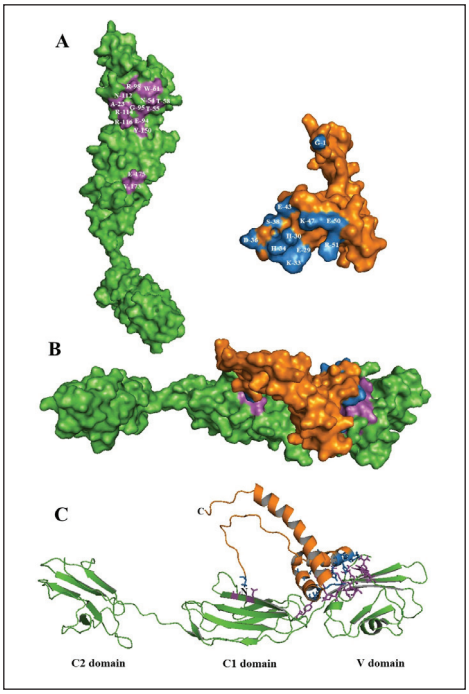

Figure 5: Illustration of VC1C2-Abox interaction based on the protein-protein docking performed using HADDOCK and viewed by PyMOL. (**A**) The surface presentations of VC1C2 (green) and A-box (orange) and the names and positions of their binding interface residues (predicted by LigPlot). The interfacial residues of VC1C2 and A-box are specified in purple and blue, respectively. The surface (**B**) and ribbon/sticks (**C**) representations of the binding mode of VC1C2 protein (green) with A-box protein (orange). The interfacial residues of two proteins (shown as sticks in the Figure 5C) are colored in purple and blue, respectively.

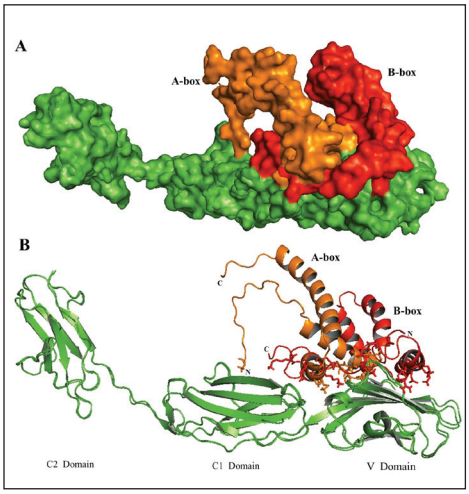

Figure 6: The superimposition of Bbox-VC1C2 and Abox-VC1C2 HADDOCK complexes using PyMOL software in surface (**A**) and ribbon/sticks (**B**) representations. In ribbon representation, the interfacial residues of B-box (red) and A-box (orange) are shown in sticks.

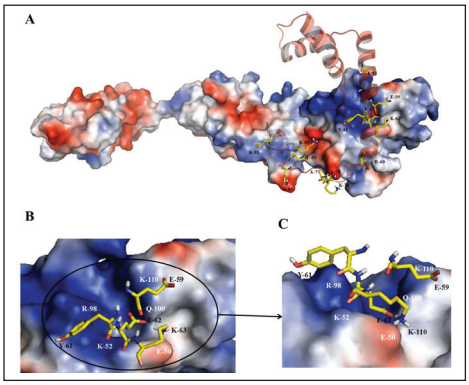

Figure 7: (**A**) The electrostatic potential surface of VC1C2 interacting with B-box (ribbon/sticks presentation). The names and positions of the binding interface residues of B-box (shown as sticks) are specified. (**B**) A close-up view showing that the VC1C2 surface groove created by Lys110, Arg98, Lys52, Glu50 and Gln100 constitutes one of the main B-box binding points. The names of the interfacial residues of B-box (shown in sticks) and VC1C2 are written in black and white, respectively. (**C**) The side chain of Glu62 fits into the groove.

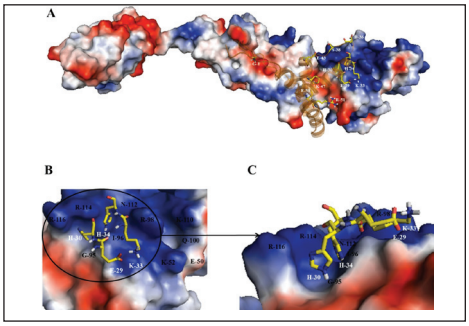

Figure 8: (**A**) The electrostatic potential surface of VC1C2 bound to A-box (ribbon/sticks format). The names and locations of the binding interface residues of A-box (shown in sticks) are specified. (**B**) A close-up view demonstrating that the groove generated by Lys110, Arg98, Lys52, Glu50 and Gln100 located on the VC1C2 surface does not constitute a binding point for A-box. The names of the interfacial residues of A-box (shown in sticks) and VC1C2 are written in white and black respectively. (**C**) The imidazole rings of His30 and His34 are located into the groove formed by the VC1C2 residues Arg114, Arg116, Asn112, Ile96 and Gly95.

Two first α-helices of A-box have a central role in the interaction with VC1C2

As mentioned before, the interaction of hHMGB1 Abox with VC1C2 domain of hRAGE was also investigated by means of HADDOCK software. The results of LigPlot analysis of VC1C2-Abox complex are shown in Fig. 4. In Fig. 5A, VC1C2 and Abox in the surface representation and the binding interface residues of two proteins (predicted by LigPlot) are shown. The structure of VC1C2-Abox complex obtained from HADDOCK software in the surface and ribbon/sticks formats are illustrated in the Figs. 5B and 5C, respectively. As it is clear from the results, in A-box, helix I, the first part of hellix II and the loop between them constitute the main site for biding to VC1C2 domain. The VC1C2 residues involved in the interaction are mostly from V domain, although a few residues from C1 domain participate in the interaction process.

A and B boxes of hHMGB1 interact with different regions of extracellular domain of hRAGE

Fig. 6 shows the VC1C2-Bbox and VC1C2-Abox complexes from HADDOCK software which are superimposed using PyMOL software in the surface (section A) and ribbon (section B) format. In the ribbon format, the residues of A-box and B-box involved in the interaction are shown as sticks. As seen in the Fig, A and B boxes of the hHMGB1 protein bind to different parts of the extracellular domain of hRAGE. Although the main binding site for both B-box and A-box is located on the V domain of hRAGE, the residues of this receptor interacting with these two proteins (Figs. 2 and 4), except for Trp61, are completely different. The B-box via its C-terminal half interacts with VC1C2 domain of hRAGE, whereas N-terminal half of the A-box participates in the interaction with this domain.

Discussion

As implied before in the text, residues 150-183 of hHMGB1 constitute the main binding site for the extracellular domain of hRAGE and the resulting activated signaling pathways contribute to the development of various cellular responses, such as inflammation and tumor growth and metastasis (Huttunen et al. 2002). In fact, the equivalents of these residues in the B-box created by I-TASSER are the residues 56-89. As it is clear in the Fig. 2, all the B-box residues contributing to the formation of intermolecular hydrogen bonds except for two residues (Glu51, Lys91) are compatible with the experimental published data. Analysis of the VC1C2 residues involved in the B-box interaction (Fig. 2) demonstrates that V domain constitutes the main interaction site, although some residues from C1 domain participle in this process.

According to the data published by LeBlanc et al. the A-box residues 23-50 are the main binding site for RAGE receptor and Abox-RAGE interaction antagonizes the activation of the receptor by HMGB1 protein (LeBlanc et al. 2014). The results obtained from investigation of Abox-VC1C2 interaction by HADDOCK are consistent with these experimental data. As mentioned in the

Materials and Methods, 2RTU which is the solution structure of hHMGB1 A-box, was selected as the A-box for the interaction study performed by HADDOCK. Of 87 residues of 2RTU, 1-3 are the protein expression tag and 4-87 are residues 1-84 (A-box) of hHMGB1 protein. Therefore, the RTU residues 26-53 are equivalent to the residues 23-50 (RAGE-binding site) of hHMGB1. The LigPlot analysis of the Abox-VC1C2 complex (Fig. 4) shows that all the A-box residues involved in the protein-protein interaction are located in this region (with the exception of Gly1). As mentioned above, this residue is not a major structural component of A-box and therefore, all the A-box residues participating in the interaction process are consistent with the experimental results already obtained (LeBlanc et al. 2014).

The electrostatic potential surface of VC1C2 protein created using the PyMOL software shows that the V domain molecular surface is mostly covered with positive charges. These positive charges in some areas are densely gathered and constitute a cationic center (Fig. 7A). One of these cationic centers is formed by Lys110, Arg98 and Lys52. These three residues together with Glu50 and Gln100 create a groove on the V domain surface (Figs. 7B and C). As obvious in the Fig. 7, this region of VC1C2 domain constitutes one of the main B-box binding points. The LigPlot analysis of the VC1C2-Bbox complex (Fig. 2) demonstrates that which residues of two proteins in this area contact with each other through hydrogen bonds. As it is clear, Glu59 of B-box makes a side chain-side chain hydrogen bond with Lys110 of VC1C2, Glu62 of B-box interacts with Gln100 and Lys52 of VC1C2 through a side chain-side chain and a backbone-side chain hydrogen bond respectively and Lys63 of B-box binds to Glu50 of VC1C2 by a side chain-side chain hydrogen bond. As seen in the Figs. 7B and C, the side chain of Glu62 is located inside the groove, while the side chains of Glu59 and Lys63 are in contact with the surface of the groove. It is worth noting that the experimental published data indicates that this groove is a major binding site for AGEs (Xue et al. 2011, Xue et al. 2014). AGEs are a heterogeneous class of compounds which are generated as a result of nonenzymatic protein Glycation. Today, it is well known that this group of RAGE ligands is linked to the complications of diabetes, chronic inflammation, cancer and Alzheimer's disease (Sorci et al. 2013).

Comparison of B-box and A-box binding sites on the extracellular domain of RAGE reveals that although both proteins interact with VC1 region, they bind to different locations of VC1C2 domain (Fig. 6). The groove created by Lys110, Arg98, Lys52, Glu50 and Gln100 on the surface of V domain does not play a role in the A-box-binding to the RAGE receptor. Although A-box binds to the vicinity of the groove and Arg98 makes a side chain-backbone hydrogen bond with Lys33 of A-box (Fig. 4), the side chain of any A-Box residues does not fit into the groove. However, the imidazole rings of His30 and His34 of A-box are located into the groove formed by the VC1C2 residues Arg114, Arg116, Asn112, Ile96 and Gly95 (Fig. 8).

Today, the design of protein-protein interaction inhibitors (PPIs) has been attracted much attention in the drug discovery. These inhibitors can include small molecules or peptides. The first step in PPI design process is to determine the binding interface of two proteins (Laraia et al. 2015). Given the fact that the role of HMGB1-RAGE interaction in various pathological states such as growth and metastasis of tumors (Palumbo et al. 2004, Palumbo et al. 2009, Tang et al. 2010) and sepsis (Zhu et al. 2010) is confirmed, the design of HMGB1-RAGE interaction inhibitors can lead to the development of promising drugs for the treatment of HMGB1-RAGE-related diseases. The results obtained from this study provide good information on HMGB1-RAGE interaction sites and the amino acid residues involved in the interaction process. Therefore, these results can be helpful to design the inhibitors which can efficiently block the interaction of these two proteins.

All amino acid residues involved in the protein-protein interaction do not have the same importance in the interaction process. A number of certain amino acid residues called hotspot residues participate more significantly in the binding affinity. Identification of these residues can help to design more specific and powerful inhibitors for the protein-protein interactions (Laraia et al. 2015). Nowadays, in addition to more costly and time-consuming experimental methods like point mutation, there are some computational methods such as molecular dynamics (MD) to detect the

hotspot residues (Morrow and zhang 2012). However, the performance of these additional researches will require more time and extensive studies in this area.

Conclusions

The results obtained from this work demonstrate that the A and B boxes of hHMGB1 bind to different locations of VC1 part of the extracellular domain (VC1C2) of cell surface RAGE receptor. Surprisingly, one of B-box binding points is a groove created by Lys110, Arg98, Lys52, Glu50 and Gln100 on the surface of VC1C2 which also constitutes a binding site for another ligand of RAGE receptor, AGEs. It should be noted that since the interaction of A-box and B-box with RAGE receptor leads to the activation of different signaling pathways, it is quite reasonable that these two proteins bind to different sites of the extracellular domain of the receptor. Considering that the involvement of HMGB1-RAGE interaction in the various pathological conditions has been confirmed, the results of this study can provide useful information to help design new potent drugs for HMGB1/RAGE-related pathologies.

Acknowledgements

We gratefully appreciate the research funding provided for this project (No. 7/5139) by Institute of Science and High Technology and Environmental Sciences, Graduate University of Advanced Technology, Kerman, Iran.

References

de Vries, S.J., Bonvin, A.M., 2011. CPORT: a consensus interface predictor and its performance in prediction-driven docking with HADDOCK. PloS One 6(3), e17695.

Deane, R., Du Yan, S., Submamaryan, R.K., LaRue, B., Jovanovic, S., Hogg, E., Welch, D., Manness, L., Lin, C., Yu, J., et al., 2003. RAGE mediates amyloid-beta peptide transport across the blood-brain barrier and accumulation in brain. Nature medicine 9(7), 907-913.

Gerlitz, G., Hock, R., Ueda, T., Bustin, M., 2009. The dynamics of HMG protein-chromatin interactions in living cells. Biochemistry and cell biology = Biochimie et biologie cellulaire, 87(1), 127-137.

Goodwin, G.H., Sanders, C., Johns, E.W., 1973. A new group of chromatin-associated proteins with a high content of acidic and basic amino acids. European journal of biochemistry / FEBS 38(1), 14-19.

He, S.J., Cheng, J., Feng, X., Yu, Y., Tian, L., Huang, Q., 2017. The dual role and therapeutic potential of high-mobility group box 1 in cancer. Oncotarget 8(38), 64534-64550.

Huttunen, H.J., Fages, C., Kuja-Panula, J., Ridley, A.J., Rauvala, H., 2002. Receptor for advanced glycation end products-binding COOH-terminal motif of amphoterin inhibits invasive migration and metastasis. Cancer research 62(16), 4805-4811.

Koch, M., Chitayat, S., Dattilo, B.M., Schiefner, A., Diez, J., Chazin, W.J., Fritz, G., 2010. Structural basis for ligand recognition and activation of RAGE. Structure 18(10), 1342-1352.

Laraia, L., McKenzie, G., Spring, D. R., Venkitaraman, A. R., Huggins, D. J., 2015. Overcoming chemical, biological, and computational challenges in the development of inhibitors targeting protein-protein interactions. Chemistry and biology 22(6), 689-703.

Laskowski, R.A., Swindells, M.B., 2011. LigPlot+: multiple ligand-protein interaction diagrams for drug discovery. Journal of chemical information and modeling 51(10), 2778-2786.

LeBlanc, P.M., Doggett, T.A., Choi, J., Hancock, M.A., Durocher, Y., Frank, F., Nagar, B., Ferguson, T.A., Saleh, M., 2014. An immunogenic peptide in the A-box of HMGB1 protein reverses apoptosis-induced tolerance through RAGE receptor. The Journal of biological chemistry 289(11), 7777-7786.

Litwinoff, E., Hurtado Del Pozo, C., Ramasamy, R., Schmidt, A.M., 2015. Emerging Targets for Therapeutic Development in Diabetes and Its Complications: The RAGE Signaling Pathway. Clinical pharmacology and therapeutics 98(2), 135-144.

Lotfi, S., Rabbani-Chadegani, A., Ghadam, P., 2013. Evidence for the binding affinity of daunomycin to HMGB1 protein in chromatin and in solution. International journal of biological macromolecules 52, 206-211.

Lotze, M.T., Tracey, K.J., 2005. High-mobility group box 1 protein (HMGB1): nuclear weapon in the immune arsenal. Nature reviews. Immunology 5(4), 331-342.

Malik, P., Chaudhry, N., Mittal, R., Mukherjee, T.K., 2015. Role of receptor for advanced glycation end products in the complication and progression of various types of cancers. Biochimica et biophysica acta 1850(9), 1898-1904.

Morrow, J. K., Zhang, S., 2012. Computational prediction of protein hot spot residues. Current Pharmaceutical Design 18(9), 1255-1265.

Moult, J., Pedersen, J.T., Judson, R., Fidelis, K., 1995. A large-scale experiment to assess protein structure prediction methods. Proteins 23(3), ii-v.

Musumeci, D., Roviello, G.N., Montesarchio, D., 2014. An overview on HMGB1 inhibitors as potential therapeutic agents in HMGB1-related pathologies. Pharmacology & therapeutics 141(3), 347-357.

Neeper, M., Schmidt, A.M., Brett, J., Yan, S.D., Wang, F., Pan, Y.C., Elliston, K., Stern, D., Shaw, A., 1992. Cloning and expression of a cell surface receptor for advanced glycosylation end products of proteins. The Journal of biological chemistry 267(21), 14998-15004.

Orlova, V.V., Choi, E.Y., Xie, C., Chavakis, E., Bierhaus, A., Ihanus, E., Ballantyne, C.M., Gahmberg, C.G., Bianchi, M.E., Nawroth, P.P., et al., 2007. A novel pathway of HMGB1-mediated inflammatory cell recruitment that requires Mac-1-integrin. The EMBO journal 26(4), 1129-1139.

Palumbo, R., Sampaolesi, M., De Marchis, F., Tonlorenzi, R., Colombetti, S., Mondino, A., Cossu, G., Bianchi, M.E., 2004. Extracellular HMGB1, a signal of tissue damage, induces mesoangioblast migration and proliferation. The Journal of cell biology 164(3), 441-449.

Palumbo, R., De Marchis, F., Pusterla, T., Conti, A., Alessio, M., Bianchi, M.E., 2009. Src family kinases are necessary for cell migration induced by extracellular HMGB1. Journal of leukocyte biology 86(3), 617-623.

Ramasamy, R., Shekhtman, A., Schmidt, A.M., 2016. The multiple faces of RAGE--opportunities for therapeutic intervention in aging and chronic disease. Expert opinion on therapeutic targets 20(4), 431-446.

Schmidt, A.M., Vianna, M., Gerlach, M., Brett, J., Ryan, J., Kao, J., Esposito, C., Hegarty, H., Hurley, W., Clauss, M., et al., 1992. Isolation and characterization of two binding proteins for advanced glycosylation end products from bovine lung which are present on the endothelial cell surface. The Journal of biological chemistry 267(21), 14987-14997.

Sorci, G., Riuzzi, F., Giambanco, I., Donato, R., 2013. RAGE in tissue homeostasis, repair and regeneration. Biochimica et biophysica acta 1833(1), 101-109.

Taguchi, A., Blood, D.C., del Toro, G., Canet, A., Lee, D.C., Qu, W., Tanji, N., Lu, Y., Lalla, E., Fu, C., et al., 2000. Blockade of RAGE-amphoterin signalling suppresses tumour growth and metastases. Nature 405(6784), 354-360.

Tang, D., Kang, R., Zeh, H.J., 3rd, Lotze, M.T., 2010. High-mobility group box 1 and cancer. Biochimica et biophysica acta 1799(1-2), 131-140.

Tang, D., Kang, R., Zeh, H.J., -3rd, Lotze, M.T., 2011. High-mobility group box 1, oxidative stress, and disease. Antioxidants and redox signaling 14(7), 1315-1335.

Todorova, J., Pasheva, E., 2012. High mobility group B1 protein interacts with its receptor RAGE in tumor cells but not in normal tissues. Oncology letters 3(1), 214-218.

van Zundert, G.C., Rodrigues, J.P., Trellet, M., Schmitz, C., Kastritis, P.L., Karaca, E., Melquiond, A.S., van Dijk, M., de Vries, S.J., Bonvin, A.M., 2016. The HADDOCK2.2 Web Server: User-Friendly Integrative Modeling of Biomolecular Complexes. Journal of molecular biology 428(4), 720-725.

Wallace, A.C., Laskowski, R.A., Thornton, J.M., 1995. LIGPLOT: a program to generate schematic diagrams of protein-ligand interactions. Protein engineering 8(2), 127-134.

Wang, J., Tochio, N., Takeuchi, A., Uewaki, J.I., Kobayashi, N., Tate, S.I., 2013. Redox-sensitive structural change in the A-domain of HMGB1 and its implication for the binding to cisplatin modified DNA. Biochemical and biophysical research communications 441, 701-706.

Xue, J., Rai, V., Singer, D., Chabierski, S., Xie, J., Reverdatto, S., Burz, D.S., Schmidt, A.M., Hoffmann, R., Shekhtman, A., 2011. Advanced glycation end product recognition by the receptor for AGEs. Structure 19(5), 722-732.

Xue, J., Ray, R., Singer, D., Bohme, D., Burz, D.S., Rai, V., Hoffmann, R., Shekhtman, A., 2014. The receptor for advanced glycation end products (RAGE) specifically recognizes methylglyoxal-derived AGEs. Biochemistry 53(20), 3327-3335.

Yamagishi, S., Takeuchi, M., Inagaki, Y., Nakamura, K., Imaizumi, T., 2003. Role of advanced glycation end products (AGEs) and their receptor (RAGE) in the pathogenesis of diabetic microangiopathy. International journal of clinical pharmacology research 23(4), 129-134.

Yan, S.S., Wu, Z.Y., Zhang, H.P., Furtado, G., Chen, X., Yan, S.F., Schmidt, A.M., Brown, C., Stern, A., LaFaille, J., et al., 2003. Suppression of experimental autoimmune encephalomyelitis by selective blockade of encephalitogenic T-cell infiltration of the central nervous system. Nature medicine 9(3), 287-293.

Yang, H., Ochani, M., Li, J., Qiang, X., Tanovic, M., Harris, H.E., Susarla, S.M., Ulloa, L., Wang, H., DiRaimo, R., et al., 2004. Reversing established sepsis with antagonists of endogenous high-mobility group box 1. Proceedings of the National Academy of Sciences of the United States of America 101(1), 296-301.

Yang, J., Yan, R., Roy, A., Xu, D., Poisson, J., Zhang, Y., 2015. The I-TASSER Suite: protein structure and function prediction. Nature methods 12(1), 7-8.

Yang, J., Zhang, Y., 2015. I-TASSER server: new development for protein structure and function predictions. Nucleic acids research 43(W1), W174-181.

Yatime, L., Andersen, G.R., 2013. Structural insights into the oligomerization mode of the human receptor for advanced glycation end-products. The FEBS journal 280(24), 6556-6568.

Zhu, S., Li, W., Ward, M.F., Sama, A.E., Wang, H., 2010. High mobility group box 1 protein as a potential drug target for infection- and injury-elicited inflammation. Inflammation & allergy drug targets 9(1), 60-72.

ACTA BIOLOGICA SLOVENICA
LJUBLJANA 2018 Vol. 61, Št. 2: 15–27

Stress tolerance of three opportunistic black yeasts

Toleranca na stres pri treh oportunističnih črnih kvasovkah

Janja Zajc[a], Cene Gostinčar[b,c], Metka Lenassi[d], Nina Gunde-Cimerman[b*]

[a] National Institute of Biology, Večna pot 111, SI-1000 Ljubljana, Slovenia
[b] Department of Biology, Biotechnical Faculty, University of Ljubljana, Jamnikarjeva ulica 101, SI-1000 Ljubljana, Slovenia
[c] Department of Molecular and Biomedical Sciences, Jožef Stefan Institute, Jamova cesta 39, SI-1000 Ljubljana, Slovenia
[d] Institute of Biochemistry, Faculty of Medicine, University of Ljubljana, Vrazov trg 2, SI-1000 Ljubljana, Slovenia

*correspondence: nina.gunde-cimerman@bf.uni-lj.si

Abstract: Many species of black yeasts can survive extremely harsh conditions and can quickly adapt to novel environments. These traits were proposed to have a role in the ability of some fungal species to colonise indoor habitats inhospitable for majority of microorganisms, and to cause (opportunistic) infections in humans. In order to better understand the stress tolerance of black yeasts and thereby their opportunism, we focused our research on the three model black yeasts: the polyextremotolerant *Aureobasidium melanogenum* and *Exophiala dermatitidis*, and the extremely halotolerant *Hortaea werneckii.* These black yeasts are shown to thrive at temperatures, salinities, pH values and, H_2O_2 concentrations that inhibit growth of mesophilic species. Most importantly, unlike their close relatives they can not only grow, but also synthesize siderophores (*E. dermatitidis*) or degrade proteins (*A. melanogenum*) at 37 °C - traits that are crucial for pathogenesis in humans. These results support the hypothesis that the ability to cope with various environmental stresses is linked to the opportunistic behaviour of fungi. Therefore, better understanding of the connections between the stress-tolerant biology of black fungi and their ability to cause disease is needed, in particular due to their changing interactions with humans and their emerging pathogenicity.

Keywords: melanised fungi, temperature, NaCl, pH tolerance, ROS, oligotrophism, proteolytic activity, capsule

Izvleček: Mnoge vrste črnih kvasovk lahko preživijo ekstremne razmere in se hitro prilagajajo novim okoljem. Te lastnosti imajo vlogo pri sposobnosti nekaterih vrst gliv, da lahko kolonizirajo negostoljubne habitate v notranjosti stavb in povzročijo (oportunistične) okužbe pri ljudeh. Raziskali smo toleranco na stres treh oportunističnih črnih kvasovk: poliekstremotolerantnih kvasovk *Aureobasidium melanogenum* in *Exophiala dermatitidis* ter izjemno halotolerantne kvasovke *Hortaea werneckii*. Vse tri črne kvasovke uspevajo pri temperaturah, koncentracijah NaCl, pH vrednostih in koncentracijah H_2O_2, ki zavrejo rast mezofilnih vrst. Še več, te vrste lahko v nasprotju s svojimi bližnjimi sorodniki ne le rastejo, temveč tudi sintetizirajo siderofore (*E. dermatitidis*) in razgrajujejo proteine (*A. melanogenum*) pri 37 °C, kar sta pomembni

lastnosti za patogenezo pri ljudeh. Ti rezultati se skladajo s hipotezo, da je sposobnost toleriranja različnih okoljskih stresov povezana z oportunističnim značajem gliv. Prav zato moramo bolje razumeti povezavo med biologijo tolerance na stres črnih gliv in njihovo sposobnostjo povzročanja bolezni, zlasti zaradi njihove spreminjajoče se interakcije z ljudmi in njihove porajajoče se patogenosti.

Ključne besede: melanizirane glive, termotoleranca, NaCl, pH toleranca, oksidativni stres, oligotrofizem, proteolitična aktivnost, kapsula

Introduction

Stress tolerance together with great adaptability enable some fungi to inhabit extreme natural environments, which makes them good candidates for colonizing novel habitats, especially those considered as generally hostile to abundant microbial growth (Gostinčar, Grube et al. 2011). Surveys of recently introduced indoor habitats have, for example, uncovered a surprising diversity of polyextremotolerant oligotrophic fungi (Hamada and Abe 2010, Lian and de Hoog 2010, Zalar, Novak et al. 2011). With the advances in technology and by making indoor habitats inhospitable to microbes to prevent their overgrowth, we are exposing microbes to new conditions, such as repeated cycles of thermal stress in dishwashers and novel chemicals such as aromatic pollutants, detergents and, biocides. These conditions appear to select for the most resilient and adaptable species, many of which can cause opportunistic human infections (Gostinčar, Grube et al. 2011, Gostinčar, Gunde-Cimerman et al. 2015).

Black yeasts are a phylogenetically diverse group of fungi with characteristically melanised cell walls that are found in several orders of *Dothideomycetes* and *Eurotiomycetes*. Melanisation and other physiological adaptations enable black yeasts to be highly resistant against different types of environmental stress (Gostinčar *et al.* 2012) and to cause infections in animals (including humans) and plants (Silveira & Nucci 2001, Garcia-Solache & Casadevall 2010, de Hoog *et al.* 2015). Three often neglected opportunistic pathogens belonging to black yeasts have been the subject of our research for several years: the polyextremotolerant *Aureobasidium melanogenum* and *Exophiala dermatitidis*, and the extremely halotolerant *Hortaea werneckii*.

Aureobasidium melanogenum (*Dothideales*, *Dothideomycetes*) is tolerant to various stresses such as low water activity, low and high temperature, fluctuating pH and oligotrophic conditions (Gostinčar, Ohm et al. 2014). It is common in tropical, temperate and polar areas, mainly in natural and anthropogenic aqueous environments, from tap water to household dishwasher interiors (Gostinčar, Ohm et al. 2014, Novak Babič, Zalar et al. 2016). Infections caused by *A. melanogenum* reported in the literature were caused by traumatic inoculation or involved severely immunocompromised patients (reviewed in de Hoog, Guarro et al. (2015)).

Exophiala dermatitidis (*Chaetothyriales, Eurotiomycetes*) can also resist various extremes, from low to high temperatures (Blasi, Tafer et al. 2015) and broad range of pH (Zalar, Novak et al. 2011). It has the greatest pathogenic potential among the three model black yeasts studied herein (de Hoog, Guarro et al. 2015), causing infections from superficial, cutaneous and subcutaneous, to visceral or systemic (de Hoog, Guarro et al. 2015) and subclinical pulmonary colonisation in patients with cystic fibrosis (Matos, Haase et al. 2003, Kondori, Lindblad et al. 2014, Sood, Vaid et al. 2014, de Hoog, Guarro et al. 2015). Like *A. melanogenum* it is frequently found in tap water (Novak Babič, Zalar et al. 2016), in household dishwashers (Zalar, Novak et al. 2011) and other indoor habitats, but it is rarely recovered from non-anthropogenic habitats (Sudhadham, Prakitsin et al. 2008).

Hortaea werneckii (*Capnodiales*, *Dothideomycetes*) is an extremely halotolerant fungus living in diverse habitats with increased salinity (Gunde-Cimerman, Zalar et al. 2000). It is the cause of *tinea nigra*, a superficial human infection of the palms, and sometimes the soles in tropical and

subtropical regions (Bonifaz, Gomez-Daza et al. 2010, de Hoog, Guarro et al. 2015). It is unable to degrade keratin, but it shows lipolytic activity (de Hoog and Gerrits van den Ende 1992, Göttlich, de Hoog et al. 1995). The systemic cases reported by Ng, Soo-Hoo et al. (2005) in patients with acute myelomonocytic leukaemia are a rare exception.

To better understand the stress-tolerance of black fungi and their pathogenic potential, we focused on the stress tolerance (to a combination of temperature and one additional stress factor) and few selected traits linked to the virulence of the three model black yeasts, such as proteolytic activity, production of siderophores and formation of capsule.

Materials and methods

Strains and culture conditions

Aureobasidium melanogenum (EXF-3378 / CBS 110374), *Exophiala dermatitidis* (EXF-10123 / CBS 525.76 / ATCC 34100) and *Hortaea werneckii* (EXF-2000 / CBS 100457) used in this study were isolated from different extreme environments: a public fountain in Bangkok (Thailand); a human sample (no additional data are available); and hypersaline water of solar salterns (Sečovlje, Slovenia), respectively. The strains are preserved in the Culture Collection Ex (Department of Biology, Biotechnical Faculty, University of Ljubljana, Infrastructural Centre Mycosmo, MRIC UL), at the Westerdijk Fungal Biodiversity Institute (The Netherlands) and American Type Culture Collection (ATTC, USA).

Cultures were maintained on complex malt-extract agar medium MEA (pH 6.0), consisting of (all w/v) 2% malt extract (Biolife, Italy), 2% glucose (Kemika, Croatia), and 0.1% peptone from meat (Merck, Germany); and on defined yeast nitrogen base (YNB) medium (pH 7.0) consisting of (all w/v) 0.17% yeast nitrogen base, 0.08% complete supplement mixture (both Qbiogene), 0.5% ammonium sulphate (Sigma-Aldrich, Germany), 2% glucose (Kemika, Croatia), and 2% agar (Formedium Ltd, UK), in deionised water. The cell suspensions (OD_{600} 0.5) were diluted in sterile deionized water 10^{-2}, 10^{-3} and 10^{-4} and 10 µL was spotted on agar medium for stress tolerance tests. The composition of the specific media for morphological analysis, stress tolerance tests and enzymatic screening are specified below.

Tolerance to acid and alkaline pH

The black yeasts were tested for their tolerance to acid (3, 4) and alkaline pH (8, 9, 10) on MEA. Medium with pH 8 was prepared with 100 mM Sodium Phosphate Buffer (Na_2HPO_4 – NaH_2PO_4) (both Merck, Germany). For the media with pH 9 and pH 10 100 mM glycine - NaOH buffer (both Sigma-Aldrich, Germany) was used. For the media with pH 3 and pH 4 100 mM Citric Acid – Na_2HPO_4 buffer (Carl Roth GmbH+Co, Germany and Merck, Germany) was used. The media were prepared in two parts as follows: (i) malt extract, peptone and glucose were dissolved in appropriate buffer in half the total volume of the medium and filter sterilized (Minisart-Plus 0.20 µm, Sartorius Stedim Biotech GmbH, Germany); (ii) 2 (w/v) % agar was added to water (half of the final medium volume) and autoclaved. The two components were aseptically combined, mixed and poured into petri dishes.

Oligotrophic growth assessment and production of siderophores

The minimal medium consisted of 1% (w/v) glucose (Kemika, Croatia), with the addition of the macroelements (w/v) of 0.6% $NaNO_3$, 0.15% KH_2PO_4, 0.05% $MgSO_4 \times 7H_2O$ and 0.05% KCl, and the microelements (w/v) of 0.01% EDTA, 0.0044% $ZnSO_4$, 0.001% $MnCl_2 \times 4H_2O$, 0.00032% $CoCl_2 \times 6H_2O$, 0.00032% $CuSO_4 \times 5H_2O$, 0.00022% $(NH_4)_6Mo_7O_{24} \times 4H_2O$, 0.00147% $CaCl_2 \times 2H_2O$ and 0.001% $FeSO_4 \times 7H_2O$ (all Sigma-Aldrich, Germany), in ultrapure water. Autoclaved diluted minimal medium was prepared by diluting 1 part of the medium with 9 parts of ultrapure water.

The detection of siderophore production was performed on chrome azurole S (CAS) agar based on the modified assay developed by Neilands, Konopka et al. (1987). In short, the siderophore indicator solution (0.12 % (w/v) CAS in deionized water) was mixed with 10 mL of iron (III) Solution (1 mM $FeCl_3$, 10 mM HCl) and hexadecyltrimethylammonium bromide (HDTMA) solution (0.18% (w/v)) (all Sigma-Aldrich, Germany). Buffered

malt extract medium was prepared as follows: 3% (w/v) PIPES, 0.6 % of NaOH (both Sigma-Aldrich, Germany), 2% malt extract (Biolife, Italy), 0.1% pepton (Merck, Germany), 2% glucose (Kemika, Croatia) and 2% agar (Formedium Ltd, UK) was dissolved in 900 mL water. Both solutions were autoclaved separately, cooled to 55 °C, combined carefully to avoid foaming and poured into Petri dishes. After inoculation of the fungi and incubation at 15 °C, 24 °C and 37 °C the presence of siderophores were observed as yellow to orange discoloration of the otherwise blue medium.

Tolerance to salt and oxidative stress

To test the tolerance to salt stress, YNB agar plates with glucose were supplemented with 5% and 10% (w/v) NaCl. Oxidative stress was tested on YNB plates supplemented after with 5 mM and 20 mM of filter sterilized H_2O_2, which were added to the medium after autoclaving and cooling down to 50 °C (Sigma-Aldrich, Germany).

Proteolytic activity

Strains of *A. melanogenum, E. dermatitidis* and *H. werneckii* were tested for degradation of casein, gelatine and keratine without NaCl and with the addition of 5% and 10% (w/v) NaCl. One loop of 7-day-old cultures grown at 24 °C on MEA were resuspended in physiological solution (0.9% [w/v] NaCl) to OD_{600} 0.5, and used for three-point inoculations by dropping 3 µL cell suspensions onto the agar surface, and by inoculation of the media in test tubes with 10 µL cell suspensions. All of the cultures were incubated at 15, 30 and 37 °C for 4 weeks. All of the experiments were carried out in duplicate.

Casein degradation was performed according to Brizzio et al. (2007) and the proteolytic activities of each species was considered positive if a clarification zone around the colonies on otherwise opaque agar was observed (Brizzio, Turchetti et al. 2007, de Garcia, Zalar et al. 2012). Keratinolytic activity was tested on azure dye-impregnated sheep's wool keratin (keratin azure; Sigma-Aldrich, Germany), as previously described by Scott et al. (2004). Briefly, tubes were first filled with 2 mL of agar basal medium without keratin, and then overlaid with 1 mL alkaline (pH 9) keratin azure medium. After incubation, the tubes were examined for the release and diffusion of the azure dye into the lower layer of basal medium (Scott and Untereiner 2004).

The activity of gelatinases was tested in 5 mL nutrient gelatine tubes composed of 12% (all w/v) gelatine (Sigma-Aldrich, Germany), 0.3% beef extract (Becton Dickenson, USA) and 0.5% peptone (Merck, Germany) (Hankin and Anagnostakis 1975), and inoculated with an a loop of the tested black yeasts. After the incubation, the tubes were placed to 4 °C for 30 min to check for liquefaction of the gelatine.

Morphological analysis

Microscopic characteristics were observed on slides of 7-day-old cultures of fungi grown at 30 °C on potato dextrose agar (Biolife, Italy) plates using a light microscope (Olympus BX51) equipped with a digital camera (Olympus DP73). For observation of extracellular polysaccharide (EPS) capsules and layers, negative staining with India ink was used (Becton, Dickinson and Company; Mexico) (Yurlova and de Hoog 2002).

Results

We systematically tested *A. melanogenum*, *E. dermatitidis* and *H. werneckii* for their tolerance to saline (5% and 10% (w/V) NaCl), pH 3-10 and oxidative stress induced by 5 mM and 20 mM H_2O_2 at various temperatures (15, 24, 37 °C) (Figs. 1, 2 and 3 respectively), growth at oligotrophic conditions and the ability to produce siderophores (Fig. 4), all conditions with clinical relevance. Additionally we examined the morphological features and presence of extracellular polysaccharide capsules (Fig. 5) of the *A. melanogenum*, *E. dermatitidis* and *H. werneckii* and tested their proteolytic activity (Tab. 1), which also play important roles in infectivity (Yike 2011, Seyedmousavi, Netea et al. 2014).

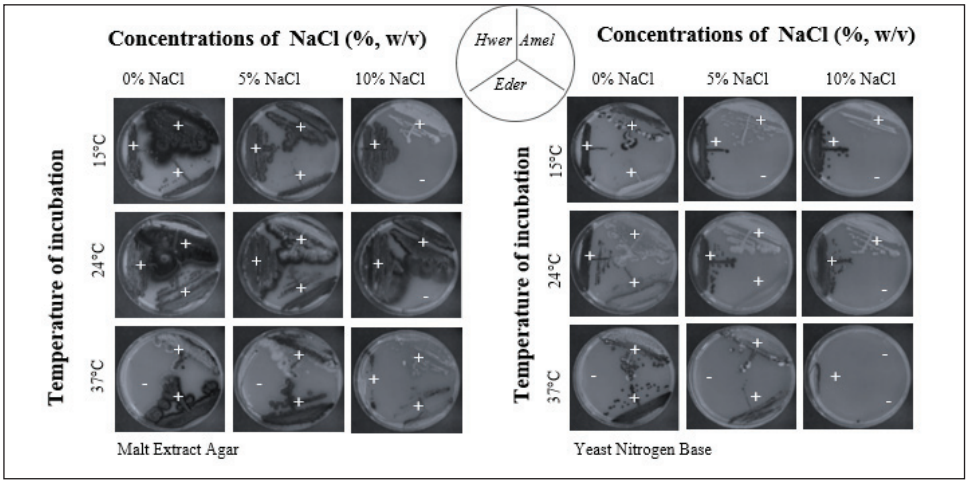

Figure 1: Growth of *Aureobasidium melanogenum* (Amel), *Hortaea werneckii* (Hwer) and *Exophiala dermatitidis* (Eder) at different temperatures and salt concentrations. Left panel -growth on malt extract agar medium (MEA)); right panel - growth on yeast nitrogen base medium with glucose (YNB).

Slika 1: Rast *Aureobasidium melanogenum* (Amel), *Hortaea werneckii* (Hwer) in *Exophiala dermatitidis* (Eder) pri različnih temperaturah in koncentracijah soli. Levo- rast na bogatem gojišču s sladnim ekstraktom (MEA); desno - rast na definiranem gojišču z dušikovo osnovo in glukozo (YNB).

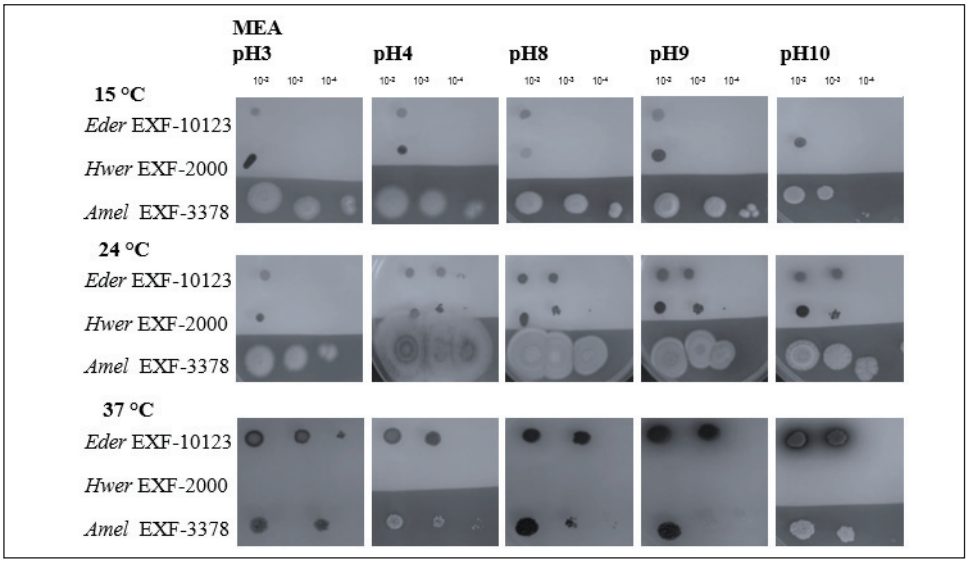

Figure 2: Growth of *Exophiala dermatitidis* (Eder), *Hortaea werneckii* (Hwer) and *Aureobasidium melanogenum* (Amel) at various temperatures and pH values.

Slika 2: Rast *Exophiala dermatitidis* (Eder), *Hortaea werneckii* (Hwer) in *Aureobasidium melanogenum* (Amel) pri različnih temperaturah in pH vrednostih.

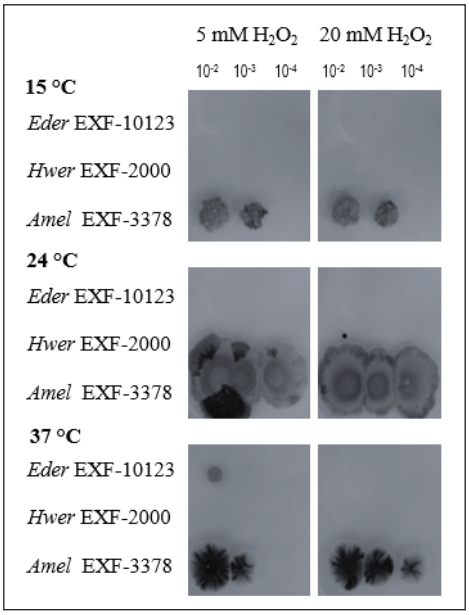

Figure 3: Temperature and H_2O_2 tolerance of *Exophiala dermatitidis* (Eder), *Hortaea werneckii* (Hwer) and *Aureobasidium melanogenum* (Amel).

Slika 3: Temperaturna toleranca in toleranca na H_2O_2 *Exophiala dermatitidis* (Eder), *Hortaea werneckii* (Hwer) in *Aureobasidium melanogenum* (Amel).

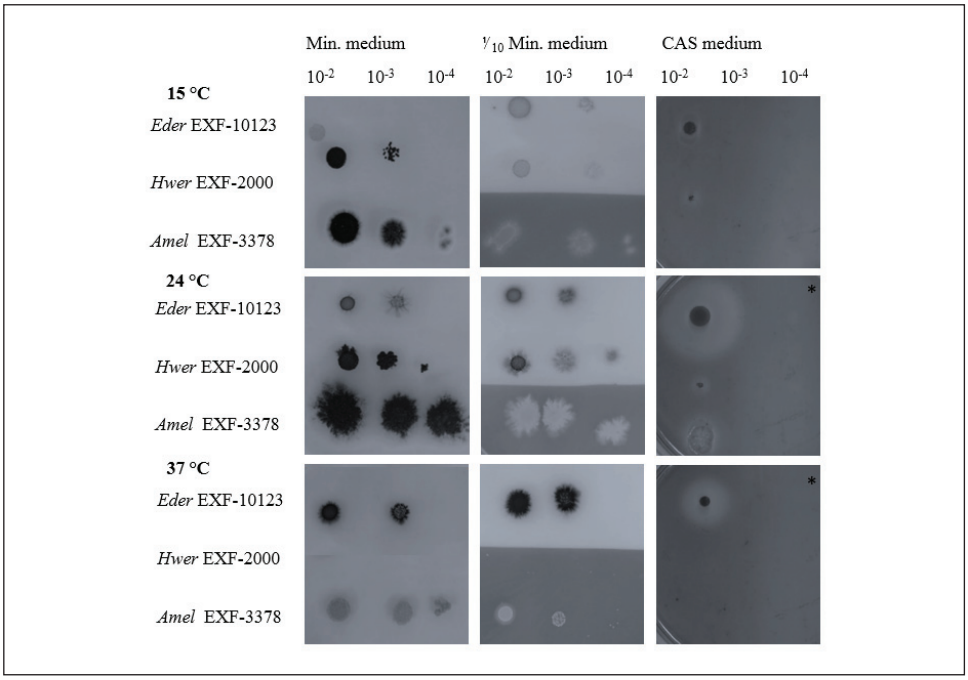

Figure 4: Oligotrophism and siderophore production (on chrome azurole S agar; CAS) of *Exophiala dermatitidis* (Eder), *Hortaea werneckii* (Hwer) and *Aureobasidium melanogenum* (Amel).

Slika 4: Oligotrofizem in proizvodnja sideroforov (na krom azurol S agarju; CAS) *Exophiala dermatitidis* (Eder), *Hortaea werneckii* (Hwer) in *Aureobasidium melanogenum* (Amel).

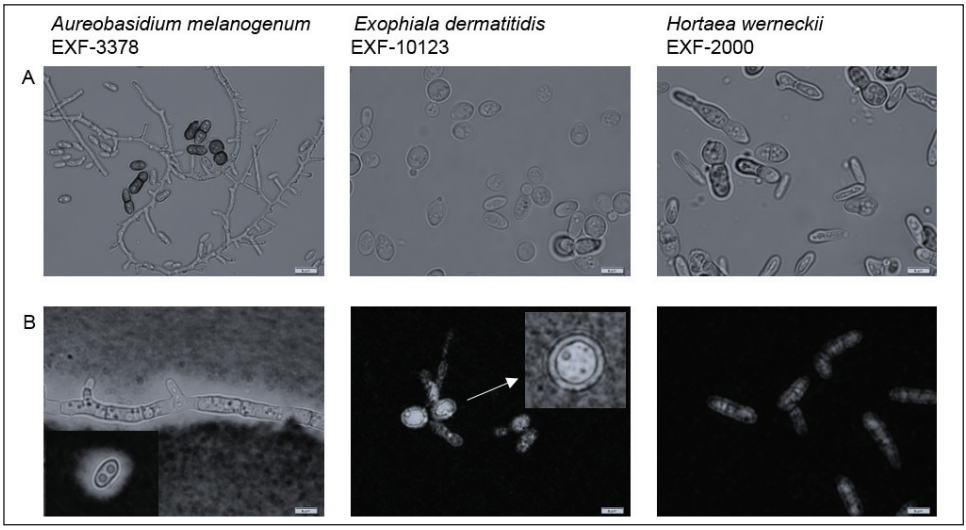

Figure 5: Representative micromorphologies of *Aureobasidium melanogenum*, *Exophiala dermatitidis* and *Hortaea werneckii*. A - Native phase-contrast micrographs. B - Extracellular polysaccharides or capsules negatively stained with India ink. Scale bar: 5 µm.

Slika 5: Reprezentativna mikromorfologija *Aureobasidium melanogenum*, *Exophiala dermatitidis* in *Hortaea werneckii* . A - Nativna fazno-kontrastna mikrografija. B - Zunajcelični polisaharidi ali kapsule, ki so negativno barvani z India črnilom. Merilce: 5 µm.

Table 1: Proteolytic activities of the three black yeasts, *Aureobasidium melanogenum*, *Hortaea werneckii* and *Exophiala dermatitidis* without NaCl and at 5% and 10% NaCl (w/v). Legend: +, activity; -, no activ ity; ng, no growth.

Tabela 1: Proteolitične aktivnosti treh črnih kvasovk, *Aureobasidium melanogenum*, *Hortaea werneckii* in *Exo phiala dermatitidis* brez NaCl in pri 5% in 10% NaCl (m / v). Legenda: +, aktivnost; -, ni aktivnosti; ng, ni rasti.

		A. melanogenum			*H. werneckii*			*E. dermatitidis*		
Proteolytic activity	Temperature \ Substrate	15°C	24°C	37°C	15°C	24°C	37°C	15°C	24°C	37°C
general	kasein	+	+	+	-	+	ng	-	-	-
	kasein + 5% NaCl	±	-	-	-	+	ng	-	-	-
	kasein + 10% NaCl	-	-	ng	-	+	-	ng	ng	ng
keratinase	keratin	-	-	-	-	-	ng	-	-	-
	keratin + 5% NaCl	-	-	-	-	-	ng	-	-	-
	keratin + 10% NaCl	-	-	ng	-	-	-	ng	ng	ng
gelatinase	gelatine	+	-	-	-	-	ng	-	-	-
	gelatine + 5% NaCl	+	-	-	-	-	ng	-	-	-
	gelatine + 10% NaCl	-	-	-	-	-	-	ng	ng	ng

Our data show that *E. dermatitidis* grows best at 37 °C under all of the tested salinities and pH conditions, whereas *A. melanogenum* and *H. werneckii* grow best at 24 °C (Fig. 2). *E. dermatitidis* grew well with 5% NaCl, while at 10% NaCl it grew only at its optimal growth temperature of 37 °C. The growth of *E. dermatitidis* at 37 °C was documented previously (de Hoog, Guarro et al. 2015), whereas the growth of *H. werneckii* above 35 °C at elevated salinity was observed only recently (Zupančič and Gunde-Cimerman, unpublished data). Here, the growth at 37 °C in the presence of NaCl was confirmed on both of the tested (MEA and YNB) media, although the growth of *H. werneckii* on the defined yeast nitrogen base (YNB) medium was very slow, with little growth even after 40 days of incubation (Fig. 1). The minimum concentration of NaCl that supported growth of *H. werneckii* at 37 °C was 10% (w/v) NaCl. All three black yeasts also grow well across a wide pH range, from pH 3 to pH 10. Our growth tests additionally confirmed that *A. melanogenum* is the most adaptable of the three species tested, not only to the combination of temperatures and salinities (Fig. 1), but also to the combination of temperatures and pH (Fig. 2).

Increasing salinity and/or temperatures reduced the degree of melanisation of *A. melanogenum*, whereas this was not the case for *H. werneckii* and *E. dermatitidis* (Fig. 1). Interestingly, at alkaline pH, a pigmented substance appeared to be leaking from the colonies of *E. dermatitidis*, forming diffuse dark areas around the colonies (Fig. 2).

Tolerance to H_2O_2 in the growth medium (chronic exposure) was greatest in *A. melanogenum*, which grew at both 5 mM H_2O_2 and 20 mM H_2O_2 (Fig. 3). *E. dermatitidis* grew at 5 mM H_2O_2 at optimal temperature (37 °C), while *H. werneckii* did not.

The oligotrophic characters of these three species were assessed on a minimal medium that was diluted to 10% of the original recipe (Fig. 4). All three species grew well on this medium at all tested temperatures (except for *H. werneckii*, which was unable to grow at 37 °C), therefore confirming their oligotrophic nature. The colonies of *H. werneckii* and *A. melanogenum* were smaller and less pigmented on the diluted minimal medium, whereas the colonies of *E. dermatitidis* were comparable in both size and melanisation on the minimal and diluted minimal media. Additionally, the discoloration of otherwise blue CAS agar showed the ability of siderophore production for all three species (Fig. 4). Given the largest halo area around the colony of *E. dermatitidis*, it is considered as the most potent producer of siderophores and importantly it was the only one able to produce siderophores at 37 °C.

Proteolytic activities were tested as the ability to degrade casein, gelatine and keratin supplemented with 0, 5% and 10% NaCl at 15 °C, 24 °C and 37 °C (Tab. 1). The results showed that of these three species, only *A. melanogenum* and *H. werneckii* were able to degrade casein and gelatine at certain conditions, whereas *E. dermatitidis* showed no proteolytic activity. The yeast *A. melanogenum* degraded casein in the absence of NaCl at all three temperatures of incubation and in the presence of 5% NaCl only weakly at 15 °C. *H. werneckii* on the other hand was the only species showing proteolytic activity on casein in the presence of both 5% and 10% NaCl but exclusively at 24 °C (Tab. 1).

We observed extracellular polysaccharides (EPS) covering the cells of *A. melanogenum* and *E. dermatitidis* (Fig. 5) under light microscopy after negative staining with India ink. The EPS layer around all *E. dermatitidis* cells was uniformly thick and well defined, whereas EPS was completely absent in the case of *H. werneckii*. In the case of *A. melanogenum* EPS layer took the form of irregularly thick masses surrounding the individual (or even groups of) chlamydospores and hyphae, whereas no EPS capsules or layers were observed around the non-pigmented yeast cells of *A. melanogenum* (Fig. 5).

Discussion

Species can differ in the depth of their extremotolerance (how extreme a particular type of stress can be before it causes cessation of growth and death), but also in its width (how many different types of stress and their combinations they endure). For the latter type Gostinčar, Grube et al. (2011) introduced the concept ‘polyextremotolerance’. Polyextremotolerant fungi are able to colonise entirely different substrates and endure a variety

of environmental conditions. A typical example of such species is *Aureobasidium melanogenum*, one of the few fungi in its phylogenetic group that is regularly encountered as an agent of human opportunistic infection. *A. melanogenum* is tolerant to high temperature, UV and ionising irradiation, lack of nutrients and other types of stress, resulting in its ability to colonise all kinds of habitats, from the municipal water supply system to window glass or Arctic ice (Gostinčar, Ohm et al. 2014). Nutritional versatility can include the ability to degrade aromatic hydrocarbons, a phenomenon particularly common in the order Chaetothyriales (Prenafeta-Boldu, Summerbell et al. 2006). This is also the order with the highest number of opportunistic species compared to the total number of species known in the order. A similar degree of extremotolerance is seen in *Exophiala dermatitidis*, which is commonly found in anthropogenic habitats such as tap water, dishwashers and creosoted railway sleepers or gasoline-rich environments, while, interestingly, in nature it is found only rarely (Zalar, Novak et al. 2011). On the other side of the spectrum, the monodirectional counterpart of polyextremotolerance might be referred to as 'monoextremotolerance'. *Hortaea werneckii* is a typical representative of this type of ecology, as it is almost invariably selected by presence of high concentrations of NaCl in its natural habitat — despite the fact that *in vitro* it grows well even without added salt (Gunde-Cimerman, Zalar et al. 2000).

Our results confirm that *A. melanogenum* has the widest ecological amplitude of the three investigated species. This is reflected in a combination of temperatures and salinities (Fig. 1) and of temperatures and pH (Fig. 2) supporting its growth. The fungus is well known to employ extensive stress-combating molecular mechanisms (reviewed in Gostinčar, Ohm et al. (2014)). The highest tolerance to H_2O_2 was seen in *A. melanogenum*, which was previously reported to tolerate short-term exposure to 640 mM H_2O_2 (Castiglia and Kuhar 2015); here we tested chronic exposure, which is more toxic to the cells. The inability of *H. werneckii* to grow in the presence of 5 mM H_2O_2 supports the previous observation (Kejžar, Gobec et al. 2013), while the growth of *E. dermatitidis* at 5 mM H_2O_2 was recently also reported by Song, Laureijssen-van de Sande et al. (2017). *E. dermatitidis* is not exceptionally tolerant to NaCl as it grows poorly at 10% NaCl, but can cope with a wide pH range, from 3-10 at all three temperatures of incubation. Interestingly, at high pH (9 and 10) brown halos appeared around the colonies indication diffusion of the (presumably) melanin pigment from the cell walls. This most probably indicates the effect of alkaline stress on the cell wall as was previously observed in *Saccharomyces cerevisiae* (Serrano, Martin et al. 2006).

Although *E. dermatitidis* does not grow as well in the presence of H_2O_2 as *A. melanogenum* (but exceeds the tolerance to H_2O_2 of *H. werneckii*), it is the most virulent of the three. The fungus shows exceptional temperature tolerance and grows well above its optimal 37 °C (and even at 45-57 °C) (Zalar, Novak et al. 2011, Blasi, Tafer et al. 2015) and is still metabolically active at 1 °C (Blasi, Tafer et al. 2015). It is enriched in habitats that are generally hostile to microbial growth, resulting in a lowered species diversity. This suggests that the fungus has a decreased competitive ability and is pushed to environments where few other microbes survive.

H. werneckii is unable to grow at temperatures above 35 °C (de Hoog and Gerrits van den Ende 1992, Chen, Xing et al. 2012). However, an additional challenge of 10% NaCl (w/v), the salinity that was previously determined as the optimal for *H. werneckii* (Kogej, Ramos et al. 2005), enables the fungus to grow at 37 °C (Zupančič and Gunde-Cimerman, unpublished data; and also confirmed here). The medical relevance of this observation remains to be investigated.

Limitation of nutrients also presents a stressful condition and microorganisms employ various mechanisms to prevent starvation. One of such is the production of siderophores, high affinity iron-chelating organic compounds (Neilands 1993), that have a role both in stress response and in virulence (Johnson 2008). All three here studied black yeasts are oligotrophic, *A. melanogenum* and *E. dermatitidis* also at 37 °C, and able to produce siderophores to overcome iron starvation. Importantly, of the three species *E. dermatitidis* appears to be the most potent siderophores producer and the only one able to produce siderophores at 37 °C. This is of great importance during the establishment of the infection in humans where phagocytes

release mediators that sequester iron and prevent the growth of non-siderophore-producing fungi (Hamad 2008).

Digestion of protein substrates plays an important role in growth and survival of both saprophytic and pathogenic fungi. Extracellular serine, aspartic, and metalloproteases are considered virulence factors of many pathogenic species (Monod, Capoccia et al. 2002, Yike 2011). Secreted proteases are of great importance for the ability of dermatophytes to colonise the surface of skin (*stratum corneum*, nails or hair) and of visceral pathogens, where they are involved in the adherence process and penetration of tissues and in interactions with the immune system of the infected host (Yike 2011). However, in the case of the three black yeasts studied here the proteolytic activities do not appear to be the deciding factor in their pathogenesis. For instance, the most virulent species *E. dermatitidis* showed no proteolytic activity at all, whereas *A. melanogenum* and *H. werneckii* degraded casein and gelatine only under certain conditions. Only *A. melanogenum* showed proteolytic activity at 37 °C, a trait most probably relevant to its pathogenesis.

Several fungi can produce EPS, either in the form of a well-defined layer surrounding the cell (*i.e.* a capsule), or as a more diffuse EPS covering of the cells (Yurlova & de Hoog 2002). This physical barrier interferes with phagocytosis and immune responses of the host, by inhibiting the production of proinflammatory cytokines and the binding of complement components, and by reducing the migration of leukocytes to the site of inflammation (Kent & Juneann 1998). Furthermore, these EPSs can protect the microorganisms from detrimental conditions by aiding in the formation of a gel-like matrix that promotes their adherence to surfaces and formation of biofilms (Ravella *et al.* 2010). The production of EPS is thus an important virulence factor. This is well-demonstrated for the pathogen *C. neoformans*, for which it was shown that mutants without the EPS capsule are typically avirulent, whereas the capsular strains show (various levels of) virulence (Fromtling *et al.* 1982). The EPS production of our studied strains (Fig. 5) correspond to their pathogenic potential: *E. dermatitidis* had yeast cells enclosed in a rather uniform EPS layer, *A. melanogenum* hyphae and chlamydospores were surrounded by irregular, thick EPS masses, while no EPS were visible around *H. werneckii*. The absence of the EPS capsule or layers for *H. werneckii* corresponds to its non-invasive pathogenic potential reflected in infections resticted to the *stratum corneum*, where immune responses are rarely activated. Without an EPS layer, the cells can retain a high degree of the cell wall hydrophobicity and promote the lipophilic adhesion of the cell wall to the human skin and to the surfaces of plastic medical devices (Göttlich, de Hoog et al. 1995).

If black yeasts are indeed pre-adapted for causing (opportunistic) infections (Gostinčar, Grube et al. 2011, Gostinčar, Muggia et al. 2012), their high stress tolerance might be useful as a marker that indicate species or groups with the potential to thrive in novel anthropogenic habitats and to enter into harmful interactions with humans. Our results clearly demonstrate the (poly)extremotolerance of the three respesentatives of black yeasts and importantly compare their ability of tolerance to a combination of two stress factors at the same time – a condition that is relevant to the pathogenesis of warm-bloded hosts; and uncovered certain traits linked to their pathogenic potential (*e.g.* synthesis of siderophores and degradation of proteins at human body temperature.

Povzetek

Črne kvasovke so filogenetsko raznovrstna skupina gliv iz redov Dothideomycetes in Eurotiomycetes, za katere so značilne melanizirane celične stene, številne med njimi pa so tudi izredno tolerantne na enega ali več različnih stresov. Črne kvasovke lahko tolerirajo različne okoljske strese, kot so visoke in nizke temperature, spremembe v pH, oksidativni stres, pomanjkanje hranil in ionizirajoče sevanje, in sicer do različnih mej. Toleranca na širok spekter ekstremov v okolju se imenuje poliekstremotoleranca, medtem ko lahko toleranco na enega ali nekaj dejavnikov stresa pojmujemo kot monoekstremoleranco.

V raziskavi smo ovrednotili in primerjali toleranco na strese, ki so relevantni za oportuno patogenost pri človeku pri treh črnih kvasovkah, in sicer pri poliekstremotolerantnih vrstah *Aureobasidium melanogenum* in *Exophiala dermatitidis* ter pri monoekstremoterantni *Hortaea werneckii*.

Te tri črne kvasovke so bile izpostavljene kombinaciji različnih temperatur (15, 24 ° C in 37 ° C) in dodatnega stresnega faktorja, kot je NaCl (5 in 10% NaCl), pH 3-10 in prisotnost 5 mM in 20 mM H_2O_2, ki je povzročil kronični oksidativni stres. Poleg tega smo testirali njihov oligotrofen značaj ter proizvodnjo spojin, ki kelirajo železo (siderofori), njihovo proteolitično aktivnost in proizvodnjo zunajceličnih polisaharidnih kapsul. Vse naštete lastnosti so povezane s patogenostjo.

Naši rezultati kažejo, da lahko obravnavane črne kvasovke uspevajo pri nizkih temperaturah (15 °C) in pri temperaturi človeškega telesa (37 °C), pri povišani slanosti, ekstremnih pH vrednosti in H_2O_2 do različnih mej. Vse kažejo oligotrofni značaj, saj lahko rastejo tudi pri zelo omejeni razpoložljivosti hranil in proizvajajo siderofore za vezavo železa. Vrsta *A. melanogenum* je bila najbolj prilagodljiva in edina vrsta, ki je kazala proteolitično aktivnost pri 37 °C, medtem ko je vrsta *E. dermatitidis* edina tvorila siderofore pri 37 °C; dve lastnosti, ki sta ključnega pomena za virulenco pri ljudeh.

Črne kvasovke so se razlikovale tudi glede tvorbe zunajceličnih polisaharidov: pri vrsti *E. dermatitidis* smo okrog celic opazili razločno oblikovane kapsule, pri *A. melanogenum* je bil okoli celic in hif prisoten obilen in nepravilno oblikovan sloj EPS, pri *H. werneckii* pa ni bilo opaznih EPS. To je v skladu s patogenim potencialom teh vrst: *H. werneckii* je namreč neinvaziven patogen na površini kože, kjer je za kolonizacijo potrebna lipofilna adhezija, medtem ko *A. melanogenum* in *E. dermatitidis* lahko povzročita subkutane, visceralne, ter celo sistemske okužbe, pri katerih je vloga EPS pomembna za oteževanje imunskega odziva in fagocitoze gostitelja.

Čeprav je glede na literaturo izrazita proteolitična aktivnost gliv lastnost, ki je tesno povezana s patogenezo pri ljudeh, naši rezultati tega ne podpirajo. Najbolj patogena vrsta *E. dermatitidis* ni pokazala nobene proteolitične aktivnosti ne na kazeinu ne na želatini, vrsta *A. melanogenum* pa je edina razgrajevala kazein pri 37 °C.

Pričujoča študija kaže, da so stopnja tolerance na stres in oligotrofizem, delno pa tudi proteolitična aktivnost, povezane z naraščajočim oportuno patogenim potencialom, vendar pa so za boljše razumevanje te povezave potrebne dodatne raziskave.

Acnowledgements

This study was supported by the state budget of the Slovenian Research Agency (Research Programmes P1-0170 and P1-0207, Infrastructural Centre Mycosmo, MRIC UL, and Postdoctoral Project Z7-7436 to J. Zajc).

References

Blasi, B., Tafer, H., Tesei, D., Sterflinger, K., 2015. From glacier to sauna: RNA-Seq of the human pathogen black fungus *Exophiala dermatitidis* under varying temperature conditions exhibits common and novel fungal response. Plos One 10(6).

Bonifaz, A., Gomez-Daza, F., Paredes, V., Ponce, R.M., 2010. Tinea versicolor, tinea nigra, white piedra, and black piedra. Clinics in Dermatology 28(2), 140–145.

Brizzio, S., Turchetti, B., de García, V., Libkind, D., Buzzini, P., van Broock, M., 2007. Extracellular enzymatic activities of basidiomycetous yeasts isolated from glacial and subglacial waters of northwest Patagonia (Argentina). Canadian Journal of Microbiology 53(4), 519–525.

Castiglia, V.C., Kuhar, F., 2015. Deterioration of expanded polystyrene caused by *Aureobasidium pullulans var. melanogenum*. Revista Argentina De Microbiologia 47(3), 256–260.

Chen, J., Xing, X.K., Zhang, L.C., Xing, Y.M., Guo, S.X., 2012. Identification of *Hortaea werneckii* isolated from mangrove plant *Aegiceras comiculatum* cased on morphology and rDNA sequences. Mycopathologia 174(5-6), 457–466.

de Garcia, V., Zalar, P., Brizzio, S., Gunde-Cimerman, N., van Broock, M., 2012. *Cryptococcus* species (Tremellales) from glacial biomes in the southern (Patagonia) and northern (Svalbard) hemispheres. Fems Microbiology Ecology 82(2), 523–539.

de Hoog, G.S., Gerrits van den Ende, A.H., 1992. Nutritional pattern and eco-physiology of *Hortaea werneckii,* agent of human tinea nigra. Antonie Van Leeuwenhoek 62(4), 321–329.

de Hoog, G.S., Guarro, J., Gené, J., Figueras, M.J., 2015. Atlas of Clinical Fungi. The ultimate benchtool for diagnostics, Blackwell Publishing Ltd.

Gostinčar, C., Grube, M., Gunde-Cimerman, N., 2011. Evolution of fungal pathogens in domestic environments? Fungal Biology 115(10), 1008–1018.

Gostinčar, C., Gunde-Cimerman, N., Grube, M., 2015. Polyextremotolerance as the fungal answer to changing environments. Microbial evolution under extreme conditions. C. Bakermans. Berlin, de Gruyter, 185–208.

Gostinčar, C., Muggia, L., Grube, M., 2012. Polyextremotolerant black fungi: oligotrophism, adaptive potential, and a link to lichen symbioses. Frontiers in Microbiology 3, 390.

Gostinčar, C., Ohm, R.A., Kogej, T., Sonjak, S., Turk, M., Zajc, J., Zalar, P., Grube, M., Sun, H., Han, J., Sharma, A., Chiniquy, J., Ngan, C.Y., Lipzen, A., Barry, K., Grigoriev, I.V., Gunde-Cimerman, N., 2014. Genome sequencing of four *Aureobasidium pullulans* varieties: biotechnological potential, stress tolerance, and description of new species. BMC Genomics 15(1), 549.

Göttlich, E., de Hoog, G.S., Yoshida, S., Takeo, K., Nishimura, K., Miyaji, M., 1995. Cell-surface hydrophobicity and lipolysis as essential factors in human *tinea nigra*. Mycoses 38, 489–494.

Gunde-Cimerman, N., Zalar, P., de Hoog, S., Plemenitaš, A., 2000. Hypersaline waters in salterns - natural ecological niches for halophilic black yeasts. FEMS Microbiology, Ecology 32(3), 235–240.

Hamad, M., 2008. Antifungal immunotherapy and immunomodulation: A double-hitter approach to deal with invasive fungal infections. Scandinavian Journal of Immunology 67(6), 533–543.

Hamada, N., Abe, N., 2010. Comparison of fungi found in bathrooms and sinks. Biocontrol Science 15(2), 51–56.

Hankin, L., Anagnostakis, S.L., 1975. The use of solid media for the detection of enzyme production by fungi. Mycologia (67), 597–607.

Johnson, L., 2008. Iron and siderophores in fungal-host interactions. Mycological Research 112, 170–183.

Kejžar, A., Gobec, S., Plemenitaš, A., Lenassi, M., 2013. Melanin is crucial for growth of the black yeast *Hortaea werneckii* in its natural hypersaline environment. Fungal Biology 117(5), 368–379.

Kogej, T., Ramos, J., Plemenitaš, A., Gunde-Cimerman, N., 2005. The halophilic fungus *Hortaea werneckii* and the halotolerant fungus *Aureobasidium pullulans* maintain low intracellular cation concentrations in hypersaline environments. Applied Environmental Microbiology 71(11), 6600–6605.

Kondori, N., Lindblad, A., Welinder-Olsson, C., Wenneras, C., Gilljam, M., 2014. Development of IgG antibodies to *Exophiala dermatitidis* is associated with inflammatory responses in patients with cystic fibrosis. Journal of Cystic Fibrosis 13(4), 391–399.

Lian, X., de Hoog, G.S., 2010. Indoor wet cells harbour melanized agents of cutaneous infection. Medical Mycology 48(4), 622–628.

Matos, T., Haase, G., Gerrits van den Ende, A.H., de Hoog, G.S., 2003. Molecular diversity of oligotrophic and neurotropic members of the black yeast genus *Exophiala*, with accent on *E. dermatitidis*. Antonie Van Leeuwenhoek 83(4), 293–303.

Monod, M., Capoccia, S., Lechenne, B., Zaugg, C., Holdom, M., Jousson, O., 2002. Secreted proteases from pathogenic fungi. International Journal of Medical Microbiology 292(5-6), 405–419.

Neilands, J.B., 1993. Siderophores. Archives of Biochemistry and Biophysics 302(1), 1–3.

Neilands, J.B., Konopka, K., Schwyn, B., Coy, M., Francis, R.T., Paw, B.H., Bagg, A., 1987. Comparative biochemistry of microbial iron assimilation. Iron Transport in Microbes, Plants and Animals. G. Winkelmann, D. Van der Helm and J. B. Neilands. New York, VCH Publishers.

Ng, K.P., Soo-Hoo, T.S., Na, S.L., Tay, S.T., Hamimah, H., Lim, P.C., Chong, P.P., Seow, H.F., Chavez, A.J., Messer, S.A., 2005. The mycological and molecular study of *Hortaea werneckii* isolated from blood and splenic abscess. Mycopathologia 159(4), 495–500.

Novak Babič, M., Zalar, P., Ženko, B., Džeroski, S., Gunde-Cimerman, N., 2016. Yeasts and yeast-like fungi in tap water and groundwater, and their transmission to household appliances. Fungal Ecology 20, 30–39.

Prenafeta-Boldu, F.X., Summerbell, R., de Hoog, G.S., 2006. Fungi growing on aromatic hydrocarbons: biotechnology's unexpected encounter with biohazard? FEMS Microbiol Rev 30(1), 109–130.

Scott, J.A., Untereiner, W.A., 2004. Determination of keratin degradation by fungi using keratin azure. Medical Mycology 42(3), 239–246.

Serrano, R., Martin, H., Casamayor, A., Arino, J., 2006. Signaling alkaline pH stress in the yeast *Saccharomyces cerevisiae* through the Wsc1 cell surface sensor and the Slt2 MAPK pathway. Journal of Biological Chemistry 281(52), 39785-39795.

Seyedmousavi, S., Netea, M.G., Mouton, J.W., Melchers, W.J.G., Verweij, P.E., de Hoog, G.S., 2014. Black yeasts and their filamentous relatives: Principles of pathogenesis and host defense. Clinical Microbiology Reviews 27(3), 527-542.

Song, Y.G., Laureijssen-van de Sande, W.W.J., Moreno, L.F., van den Ende, B.G., Li, R.Y., de Hoog, S., 2017. Comparative ecology of capsular *Exophiala* species causing disseminated infection in humans. Frontiers in Microbiology 8.

Sood, S., Vaid, V.K., Sharma, M., Bhartiya, H., 2014. Cerebral phaeohyphomycosis by *Exophiala dermatitidis*. Indian Journal of Medical Microbiology 32(2), 188–190.

Sudhadham, M., Prakitsin, S., Sivichai, S., Chaiyarat, R., Dorrestein, G.M., Menken, S.B.J., de Hoog, G.S., 2008. The neurotropic black yeast *Exophiala dermatitidis* has a possible origin in the tropical rain forest. Studies in Mycology(61), 145–155.

Yike, I., 2011. Fungal proteases and their pathophysiological effects. Mycopathologia 171(5), 299–323.

Yurlova, N.A., de Hoog, G.S., 2002. Exopolysaccharides and capsules in human pathogenic *Exophiala* species. Mycoses 45(11-12), 443–448.

Zalar, P., Novak, M., De Hoog, G.S., Gunde-Cimerman, N., 2011. Dishwashers - A man-made ecological niche accommodating human opportunistic fungal pathogens. Fungal Biology 115(10), 997–1007.

ACTA BIOLOGICA SLOVENICA
LJUBLJANA 2018 Vol. 61, Št. 2: 29–37

Combined use of chlorophyll a and phycocyanin fluorescence sensors for quantification and differentiation of phytoplankton: a useful approach for small surface water bodies

Kombinirana uporaba klorofilnega in fikocianinskega senzorja fluorescence za kvantifikacijo in kvalifikacijo fitoplanktona: uporaba v majhnih vodnih telesih

Tinkara Rozina[a], Tina Eleršek[b], Maja Zupančič Justin[c], Andrej Meglič[d*]

[a] Envit d.o.o., Vojkova cesta 63, 1000 Ljubljana, Slovenia
[b] Department of Genetic Toxicology and Cancer Biology, National Institute of Biology, Večna pot 111, 1000 Ljubljana, Slovenia
[c] Arhel d.o.o., Pustovrhova ulica 15, 1000 Ljubljana, Slovenia
[d] Biotechnical Faculty, University of Ljubljana, Večna pot 111, 1000 Ljubljana,

*correspondence: andrej.meglic@bf.uni-lj.si

Abstract: Sensors based on *in vivo* measurements of photosynthetic pigments fluorescence enable real-time phytoplankton monitoring with high spatial and temporal resolution. A combination of chlorophyll a (CHL) and phycocyanin (PC) fluorescence sensors was used for phytoplankton quantification and differentiation in two small water bodies, Koseze Pond and pond in Hotinja vas. The high correlation of CHL and PC fluorescence signals with biovolume was confirmed during the two-year monitoring in a natural pond environment in spite of a seasonal succession of the phytoplankton. Additionally, disturbances of the sensors were investigated. Water bodies containing predominantly algae yielded false positive signals of the PC sensor, which reached up to 1% of the intensity of the CHL signal. Similarly, underestimated counts of cyanobacteria measured with CHL fluorescence sensor can be adjusted using PC fluorescence sensor.

Keywords: small water bodies, algae, cyanobacteria, fluorescence sensors, biovolume

Izvleček: Senzorji za merjenje *in vivo* fluorescence fotosintetskih pigmentov omogočajo meritve fitoplanktona z visoko časovno in prostorsko ločljivostjo. Kombinacijo klorofilnega (CHL) in fikocianinskega (PC) senzorja smo uporabili za kvantitativno in kvalitativno spremljanje fitoplanktona v dveh majhnih vodnih telesih, Koseškem bajerju in ribniku v Hotinji vasi. Kljub spreminjanju vrstne sestave je ostala korelacija med signalom CHL senzorja in biovolumnom visoka. Opredelili smo tudi napake senzorjev. V primeru vodnih teles z visoko koncentracijo zelenih alg je PC senzor dajal lažen pozitiven signal v velikosti 1 % signal CHL senzorja. S kombinacijo obeh senzorjev je mogoče odpraviti tudi podcenitev koncentracije cianobakterij, do katere pride ob uporabi le CHL senzorja.

Ključne besede: mala vodna telesa, alge, cianobakterije, senzorji fluorescence, biovolumen

Introduction

Phytoplankton determination is according to EU Water Framework Directive (Directive 2000/60/EC) compulsory for the evaluation of ecological water status. Spectrophotometric analysis following extraction with organic solvents provides good estimates of the total chlorophyll *a* (CHL). However, CHL as an indicator of the total phytoplankton biovolume does not enable distinguishing between different groups of phytoplankton, for example between algae and cyanobacteria. The later are problematic due to formation of biologically active and often toxic substances and therefore deserve special attention and faster identification. Because of specific migration patterns on a daily, seasonal and weather-induced basis, occasionally taken samples in traditional monitoring approaches may give misleading results of phytoplankton and cyanobacteria population (Walsby et al. 2004).

Monitoring of the presence of toxic cyanobacteria became compulsory with the Bathing Water Directive 2006/7/EC. However, the Directive only requires a control of the presence of cyanotoxins. Monitoring sites with other recreational activities than bathing are not included in the Directive (Brient 2008). Among them are small lakes, ponds and urban water bodies covering only a few hectares or less. Despite their prevalence and rich biological diversity, they have received little attention in the EU Water Framework Directive (Directive 2000/60/EU, Biggs et al. 1999, Oertli et al. 2002, Williams et al. 2003). They are subjected to increasing negative environmental impacts, such as stormwater nutrient and contaminant loading. One of the greatest concerns in such water bodies are cyanobacterial blooms, leading to unpleasant odours and occasional animal poisoning (Sedmak et al. 1994, Lürling and Faassen 2013). In such sites, faster and simple monitoring methods are needed, giving real-time results on a detailed spatial and temporal scale.

One of the characteristics of cyanobacteria are accessory photosynthetic pigment. With their help, the available light can be used more efficiently than other phytoplankton organisms (Raps et al. 1983). In fresh waters, cyanobacteria are the only organisms producing significant amounts of PC (Wetzel 2001). In the marine environment, PC is also present in Cryptophyceae and Rodophyceae (Wetzel 2001).

In recent years, advances in technology allow fluorometric measurements *in situ*. Submersible PC fluorescence sensors enable quantitative evaluation of cyanobacteria abundance in freshwater bodies (Kong et al. 2013, Kasinak et al. 2015, Zamyadi et al. 2014). Field probes measuring the *in-vivo* fluorescence of CHL and PC may present an interesting approach for fast detection of changes in the planktonic population (Bastien et al. 2011, Seppälä et al. 2007).

For proper use of fluorescence field sensors in water monitoring, their limitations should be considered. The signal can be affected by different factors such as water turbidity, uneven distribution of cyanobacteria due to the formation of colonies, the presence of biological and mineral particles in the water and the growth status of cyanobacteria and algae (Chang et al. 2012, McQuaid et al. 2011, Zamyadi et al. 2012). Errors can also occur if sensors are used without proper calibration (Bowling et al. 2012, Song et al. 2013).

In this study, we weekly measured CHL and PC fluorescence in Koseze Pond and compared the results with phytoplankton biovolume – a combination that gave the highest uniformity in the previous study (Rozina et al. 2017). Due to the negligible occurrence of cyanobacteria we took additional samples of water from the pond in Hotinja vas with a predominant population of cyanobacteria and also measured some laboratory algae and cyanobacteria cultures. We consider the necessity of simultaneous measurements with PC and CHL sensors to avoid the underestimation or overestimation of cyanobacterial biomass.

Materials and methods

Sampling sites

Koseze Pond is a small, shallow artificial water body used also as a fishpond, situated in Ljubljana, Slovenia (46°04` 02.33``N; 14°28` 07.78``E) and is a part of the recreational area. The pond was selected due to the occasional presence of cyanobacteria in the past. It has an approximately 37,000 m^2 surface area and 55,000 m^3 volume. Maximum depth is 3 m. Water samples were collected weekly

from beginning of May to the end of September in 2014 and 2015 from the middle of the pond. As the preliminary tests showed even distribution of phytoplankton on different locations and depths of the pond, grab water samples were collected from a depth of 30 cm. Samples were kept in plastic containers and measured immediately after arrival in the laboratory.

The pond in Hotinja vas (46° 28` 03.85``N; 15° 40` 39.67``E) is a small, shallow water body situated in the centre of the village in the eastern part of Slovenia, with a 9,300 m^2 surface area, not deeper than one meter and used also as a fishpond. Untreated surrounding sewage is occasionally discharged into the water body leading to regular large-scale occurrences of cyanobacteria. Sampling was performed four times in summer 2015. Both water bodies are not included in the national monitoring.

In addition to environmental samples, we also measured laboratory cultures of green algae and cyanobacteria. We used *Desmodesmus communis* 276-4b, *Chlorella vulgaris* 211-11b ans *Arthrospira platensis* 85.79 from the SAG collection (Goettingen, Germany) and *Microcystis aeruginosa* PCC 7806 from the Institute Pasteur (Paris, France). All laboratory cultures were grown at room temperature and maintained under axenic conditions in 100 mL flasks in 50 mL Jaworski's medium exposed to natural daylight.

Fluorescence measurements

For fluorescence measurement a portable KM 245 water quality flow-through chamber (Arhel, Slovenia) fitted with CHL and PC fluorescent sensors (Cyclops 7, Turner, U.S.A.) were used. The sensors were installed in a black, non-reflective measuring chamber, equipped with a brush that automatically cleaned the lenses of the sensors (Fig. 1). The CHL sensor excites CHL at 465 ± 85 nm and measures emission at 696 ± 22 nm while the PC sensor excites the cyanobacterial PC below 595 nm and measures fluorescence emission above 630 nm. To prevent interferences optimal distance from the walls of the chamber and between both sensors was determined in a series of tests.

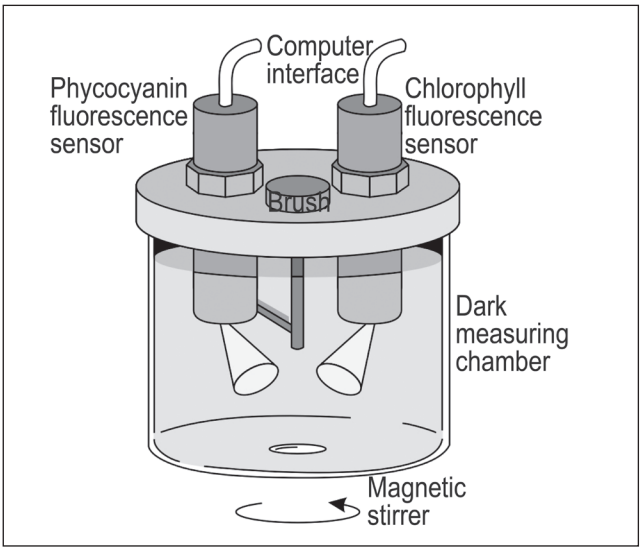

Figure 1: Portable KM 245 water quality system (Arhel, Slovenia) with dark measuring chamber fitted with CHL and PC fluorescent sensors, magnetic stirrer, brush and interface to personal computer, which serves as data logger and data display.

Slika 1: Prenosni sistem KM 245 za nadzor kvalitete vode (Arhel, Slovenija). V črni merilni komori sta CHL in PC senzor fluorescence, magnetno mešalo, metlica in povezava z osebnim računalnikom, ki je namenjen shranjevanju in prikazovanju podatkov.

For experimental purposes, 800 mL of water sample was poured into the measuring chamber. Settling was prevented using a magnetic stirrer. Data sampling frequency was set to 4.5 Hz. Each sample was measured for 5 minutes, and the average signal was calculated. The results were presented in relative units (r.u.) corresponding the voltage output of the sensor. The same water sample was used for biovolume and taxonomic determination.

Phytoplankton quantification and taxonomic determination

Environmental samples were concentrated in 100 mL glass cylinders (Hydro Bios, Germany) under darkness for 24 hours. Plankton was taxonomically determined under an Eclipse TE300 inverted microscope (Nikon, Japan). Material fixed in 4% (v/v) formalin was used for counting and biovolume calculations. Depending on the phytoplankton composition and concentration, a Nageotte (Assistent, Germany) or Sedgewick-Rafter (PhycoTech, U.S.A.) counting chamber was used. The biovolume of phytoplankton culture was calculated from the average biovolume of individual cells, taking into account the geometry of the cells (Hillebrand et al., 1999). General procedures for the use of sedimentation chambers, preservation and storage of samples and evaluation of cell density were followed according to the European standard (CEN EN 15204, 2006). Algal species were identified following the keys and articles of John et al. (2002), Komárek and Anagnostidis (2000, 2005) and Hindak (1976).

Results

Correlation between CHL fluorescence and biovolume

Measurements of CHL and PC fluorescence, expressed in relative units (r.u.), were compared to total biovolume. The seasonal dynamic of phytoplankton in the Koseze pond was followed from the beginning of May to the end of September in 2014 and 2015 (Fig. 2). The peak of the phytoplankton density was in August 2014 and 2015. In later the phytoplankton development was slightly slower and reached lower pick values. The CHL fluorescence followed the biovolume (Fig. 2).

Throughout the entire 2014 and 2015 monitoring period, the measurements of CHL fluorescence showed a high correlation (r=0.95, n=21 for 2014 and r=0.92, n=18) with phytoplankton biovolume (Fig. 3). Moreover, most of the measurements from 2015 fall into the prediction band made for 2014.

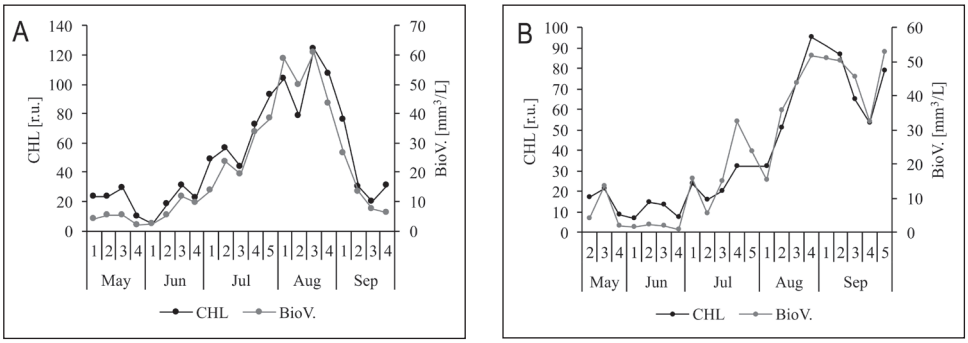

Figure 2: Seasonal changes of chlorophyll (CHL) fluorescence and total phytoplankton biovolume (BioV) in Koseze Pond from the beginning of May to the end of September 2014 (A) and 2015 (B). Numbers on x-axis indicate week of the month.

Slika 2: Sezonsko spreminjanje fluorescence CHL in celokupnega biovolumna fitoplanktona (BioV.) v Koseškem bajerju med začetkom maja in koncem septembra 2014 (A) in 2015 (B). Številke na x osi označujejo tedne v mesecu.

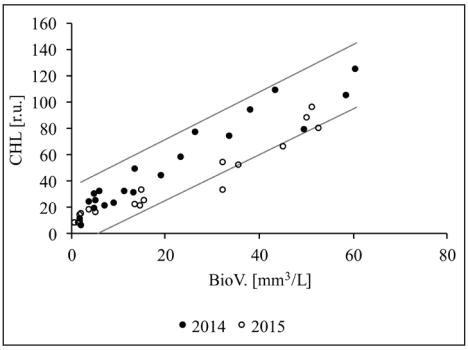

Figure 3: Chlorophyll (CHL) fluorescence as a function of total phytoplankton biovolume (BioV). Black circles represent samples taken from Koseze Pond in season 2014 and hollow circles samples from the 2015 season. Grey lines indicate prediction band of 2014 measurements.

Slika 3: Fluorescenca klorofila (CHL) kot funkcija celokupnega biovolumna fitoplanktona (BioV.). Črni polni krogi predstavljajo vzorce Koseškega bajerja iz sezone 2014, prazni krogi pa iz sezone 2015. Sivi črti označujeta predikcijski interval meritev iz 2014.

The correlation between CHL fluorescence and total biovolume in the pond remained high during both observation periods (Fig. 3), in spite of the phytoplankton seasonal succession (Fig. 4). In the 2014 season, a significant change in species composition occurred in the second week of July, with a growing abundance of filamentous green algae *Planctonema lauterbornii* (*Trebouxiophyceae*) (Fig. 4A). This species dominated in the 2015 summer season as well (Fig. 4B).

The taxonomic analyses from 2014 and 2015 showed that the cyanobacteria population barely reached 2% of the total biovolume (average 0.45%, range 0.04-2.82% for 2014 and average 0.41%, range 0.01-2.0% for 2015). In addition, values from the phycocyanin sensor were also low, most of the time below 1% of the CHL fluorescence indicating almost complete absence of cyanobacteria in the pond. Monthly taxonomic analysis have shown the presence of turbulent and the absence of colonial species of cyanobacteria.

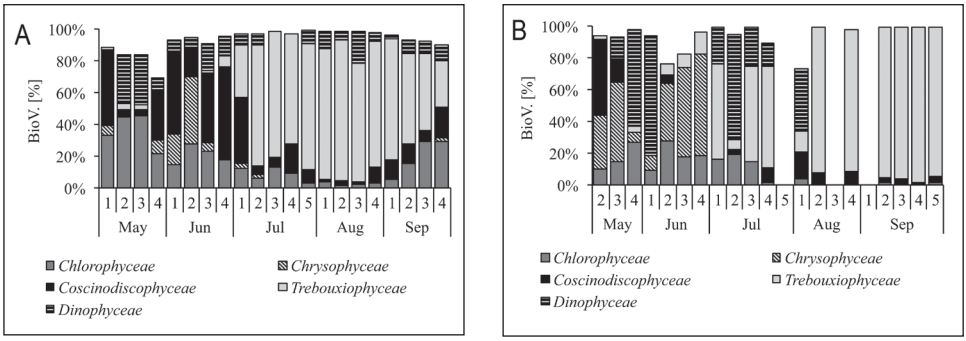

Figure 4: Seasonal succession of the biovolume (BioV) in Koseze pond in 2014 (A) and 2015 (B). Data are represented as a relative share of five main phytoplankton classes. The class *Trebouxiophyceae* was represented by the species *Planctonema lauterbornii.*

Slika 4: Sezonsko spreminjanje biovolumna (BioV.) v Koseškem bajerju leta 2014 (A) in 2015 (B). Podatki so predstavljeni kot relativen delež petih najpogostejših razredov fitoplanktona. Razred *Trebouxiophyceae* je zastopala vrsta *Planctonema lauterbornii.*

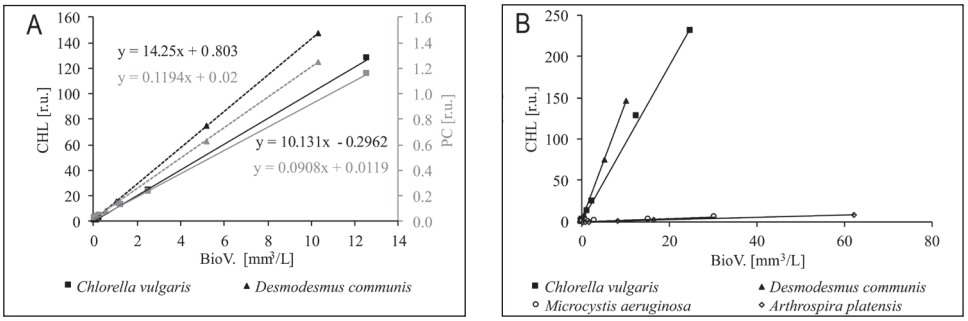

Figure 5: Laboratory cultures. (A) Phycocyanian (PC) - grey lines and chlorophyll (CHL) fluorescence - black lines - of green algae *Desmodesmus communis* and *Chlorella vulgaris* as a function of cell biovolume. The ratio between PC and CHL fluorescence signals is approximately 1:100. (B) Relationship between CHL fluorescence and biovolume (BioV.) of four axenic laboratory cultures – green algae *Desmodesmus communis* and *Chlorella vulgaris* and cyanobacteria *Microcystis aeruginosa* and *Arthrospira platensis*. The suspension of each culture was gradually diluted to 1000 cells/ml.

Slika 5: Laboratorijske kulture. (A) Fluorescenca fikocianina (PC) – sive črte in klorofila (CHL) – črne črte pri algah vrste *Desmodesmus communis* in *Chlorella vulgaris* v odvisnosti od biovolumna. Razmerje med fluorescenco PC in CHL je približno 1:100. (B) Odvisnost fluorescence CHL od biovolumna (BioV.) štirih akseničnih laboratorijskih kultur – zelenih alg vrste *Desmodesmus communis* in *Chlorella vulgaris* ter cianobakterij vrste *Microcystis aeruginosa* in *Arthrospira platensis*. Suspenzija vsake kulture je bila postopoma redčena na 1000 celic/ml.

CHL and PC fluorescence in cyanobacterial reach pond

Four water samples from the pond in Hotinja vas with cyanobacteria biovolume ranging from 53 and 81 percent were analysed. Although the correlation between CHL fluorescence and biovolume remained high (r=0.96) the slope of the linear fit was much lower than in the case of Koseze Pond (0.6 compared to 1.6). The correlation between the PC fluorescence signal and cyanobacteria biovolume was high (r=0.95) although higher number of samples should be collected to confirm the significance (Fig. 5).

Discussion

Linear relationship and high correlation between fluorescence and biovolume have been confirmed in many studies. However, most of the studies with PC and CHL fluorescence sensors were made using laboratory phytoplankton cultures and only a few were made using environmental samples (Loisa 2015, Kong 2013, Izydorczyk 2009).

In the case of Koseze Pond, the measurements of CHL fluorescence showed a high correlation with phytoplankton biovolume throughout the entire 2014 and 2015 monitoring period. Calibration curve from 2014 could be used for 2015 samples, although, for a more accurate calculation of the biovolume, calibrations in the environmental water sample should be repeated every season. The fluorescence system therefore constitutes the upgrade to the current monitoring system, providing information of phytoplankton dynamics in real time. The correlation stayed high despite the changes in the phytoplankton composition. Different species composition should also result in different slope of a linear fit because the concentration of CHL depends on phytoplankton species. This can be explained by the adaptation of the pigment concentration of the phytoplankton organisms according to environmental light conditions and was also confirmed by Gregor et al. (2007) with measurements performed at different lake depths. In our case, all the samples were taken from the same pond location and depth. Organisms in a small turbid shallow water body, as in our case, were exposed to the same environmental condi-

tions. It can be concluded that due to comparable ecological niches, the *in-vivo* CHL fluorescence of various species was similar and the correlation with biovolume remained high. This additionally argues in favour of fluorescent measurements and their application for biovolume quantification. Results of fluorescence measurement on green algae (laboratory cultures) have showed low PC signal although green algae do not contain PC (Fig. 5a). Gregor et al. (2007) also reported in their study that falsely positive signals of the PC sensor at a high eukaryotic algae presence in water might occur. There was about 10-11 fold higher PC signal response from cyanobacteria than algae and vice versa, a much higher CHL signal response received from eukaryotic algae than cyanobacteria in their study. In the measurements with our equipment and settings, the PC signal of the green algae represented only 1% of their CHL signal. Therefore, the ratio between the CHL and PC signals should be taken as an important criterion in the evaluation of the cyanobacteria presence. By using both PC and the CHL sensors during on-site monitoring, we can avoid overestimation of the presence of cyanobacteria.

Long-term observations in Koseze Pond, confirmed that in the case of a parallel increase of PC and CHL fluorescence signals, with a 100 times lower PC signal than the CHL one, the real presence of cyanobacteria is probably negligible and the value of the PC signal shows only interferences.

An opposite problem is found in water bodies with the prevailing cyanobacteria population (Hotinja vas fishpond). Despite their high biomass, cyanobacteria have a low CHL fluorescence response (Figure 5b) that can be explained by a weak absorption of blue light (Campbell et al. 1998, Gregor et al. 2007). In contrast to green algae where the antenna pigments that harvest light for photosystem II are CHL, accessory chlorophylls and carotenoids (Green and Durnford 1996), cyanobacterial photosystem II contains only 10 to 20 % of the total CHL (Bryant 1986). The major part of cyanobacterial CHL is located in photosystem I, which does not dissipate energy through fluorescence. The measurement of the PC fluorescence is, therefore, a better approach to cyanobacterial biovolume determination compared to CHL fluorescence measurements as this prevents cyanobacteria underestimation.

Performed measurements demonstrated the need for simultaneous measurements with PC and CHL fluorescence sensors to accurately quantify cyanobacteria and green algae in mixed populations.

Conclusion

The study demonstrates that seasonal phytoplankton development and the presence of cyanobacteria can be monitored with combined use of PC and CHL fluorescence sensors. Correlation between CHL fluorescence and biovolume in remained stable even after significant changes in the phytoplankton species composition and allowed relatively accurate quantification of cell biovolume. This reduces the need for standard analyses and allows qualitative differentiation of phytoplankton with a reliable prediction of cyanobacteria even in small ponds and lakes with quickly changing biovolume and species composition. False positive signals of the PC sensor in the case of the predominant eukaryotic algal population in the water body, reaching up to 1% of the intensity of the CHL signal, as it was the case with our instruments and settings, could be recognised and disregarded. Similarly, underestimated counts of cyanobacteria measured with CHL fluorescence sensor can also be adjusted using PC fluorescence sensor.

Povzetek

Cvetenje cianobakterij predstavlja izjemno tveganje za okolje. Njihovo zgodnje odkrivanje in nadzorovanje je zato ključnega pomena za upravljanje z vodnimi telesi. Standardne metode spremljanja fitoplanktona imajo številne omejitve, zato je potrebna nadgradnja z metodami, ki dajejo rezultate v realnem času. V našem delu smo pokazali, da lahko z uporabo CHL in PC senzorja fluorescence določimo koncentracijo alg in cianobakterij v vodnem telesu. Meritve fluorescence CHL na Koseškem bajerju so pokazale visoke korelacije z biovolumnom fitoplanktona skozi celotno dvoletno obdobje izvajanja meritev kljub spremembam v vrstni sestavi. Opredelili smo tudi napake senzorjev. V primeru vodnih teles z visoko koncentracijo zelenih alg je PC

senzor dajal lažen pozitiven signal v velikosti 1 % signala CHL senzorja. Po drugi strani pa pride do podcenitve koncentracij cianobakterij ob uporabi le CHL senzorja. Ker so cianobakterije in zelene alge prisotne v istih okoljih je upoštevanje te napake pri meritvah bistvenega pomena. S sočasno uporabo CHL in PC S sočasno uporabo CHL in PC senzorja se lahko izognemo tako podcenitvi kot precenitvi številčnosti cianobakterijske populacije.

References

Bastien, C., Cardin, R., Veilleux, E., Deblois, C., Warren, A., Laurion, I., 2011. Performance evaluation of phycocyanin probes for the monitoring of cyanobacteria. Journal of Environmental Monitoring 13, 110-118.

Biggs, J., Fox, G., Nicolet, P., Whitfield, M., Williams, P., 1999. The value of the pond. The Freshwater Biological Association Newsletter 8, 1–3.

Bowling, L., Ryan, D., Holliday, J., Honeyman, G., 2012. Evalution of in situ fluoromety to determine cyanobacterial abundance in the Murray and lower Darling rivers, Australia. River Research Applications 29(8), 1059-1071.

Brient, L., Lengronne, M., Bertrand, E., Rolland, D., Sipel A., Steinmann, D., Baudin, I., Legeas, M., Le Rouzic, B., Bormans, M., 2008. A phycocyanin probe as tool for monitoring cyanobacteria in freshwater bodies. Journal of Environmental Monitoring 10, 248-255.

Bryant, D.A., 1986. The cyanobacterial photosynthetic apparatus, comparison to those of higher plants and photosynthetic bacteria. In, Platt, T., Li, W.K.W. (Eds.), Photosynthetic Picoplankton. Canadian Bulletin of Fisheries and Aquatic Sciences 214, 423-500.

Campbell, D., Hurry, V., Clarke, A.K., Gustafsson, P., Öquist, G., 1998. Chlorophyll fluorescence analysis of cyanobacterial photosynthesis and acclimation. Microbiology and Molecular Biology Reviews 62, 667-683.

CEN EN 15204, 2006. Water quality - Guidance standard on the enumeration of phytoplankton using inverted microscopy (Utermöhl technique). 42 pp.

Chang, D.W., Hobson, P., Burch, M., Lin, T.F., 2012. Measurement of cyanobacteria using in-vivo fluoroscopy – Effect of cyanobacterial species, pigments, and colonies. Water Research 46, 5037-5048.

Directive 2000/60/EC of the European Parliament and of the Council of 23 October 2000 establishing a framework for Community action in the field of water policy as amended by Decision 2455/2001/EC and Directives 2008/32/EC, 2008/105/EC and 2009/31/EC.

Directive 2006/7/EC of the European Parliament and of the Council of 15 February 2006 concerning the management of bathing water quality and repealing Directive 76/160/EEC.

Green, B.R., Durnford, D.G., 1996. The chlorophyll-carotenoid proteins of oxygenic photosynthesis. Annual Review of Plant Physiology and Plant Molecular Biology 47, 685-714.

Gregor, J., Maršalek, B., Šipkova, H., 2007. Detection and estimation of potentially toxic cyanobacteria in raw water at the drinking water treatment plant by in vivo fluorescence method. Water Research 41, 228–234.

Hillebrand, H., Dürselen, C.D., Kirschtel, D., Pollingher, U., Zohary, T., 1999. Biovo-lume calculation for pelagic and benthic microalgae. Journal of Phycology 35(2), 403–424.

Hindak J. F. 1976. Freshwater algae. Bratislava, Slovak Academic Publishing House, 157 pages.

Izydorczyk, K., Carpentier, C., Mrówczyński, J., Wagenvoort, A., Jurcak, T., Tarczyńska, M. 2009. Establishment of an Alert Level Framework for cyanobacteria in drinking water resources by using the Algae Online Analyser for monitoring cyanobacterial chlorophyll a. Water Research 43, 989-996.

John, D.M., Whitton, B.A., Brook, A.J. (Ed.), 2002. The Freshwater Algal Flora of the British Isles. An Identification Guide to Freshwater and Terrestrial Algae. Cambridge University Press, 702 pp.

Kasinak, J. M. E., Holt, B. M., Chislock M. F., Wilson A. E., 2015. Benchtop fluorometry of phycocyanin as a rapid approach for estimating cyanobacterial biovolume. Journal of Plankton Research 37(1), 248-257.

Komárek, J, Anagnostidis K., 2000. Freshwater flora of Central Europe 19/1. Elsevier Spektrum Akademischer Verlag, Berlin.

Komàrek, J., Anagnostidis, K., 2005. Cyanoprokaryota. 2. Teil, Oscillatoriales. Süsswasser- flora von Mitteleuropa 19/2. Elsevier, München,759 pp.

Kong, Y., Lou, I., Zhang, Y., Lou, C.U., Mok, K.M., 2013. Using an online phycocyanin fluorescence probe for rapid monitoring of cyanobacteria in Macau freshwater reservoir. Hydrobiologia 741, 33-49.

Loisa, O., Käärlä, J., Laaksonlaita, J., Niemi, J., Sarvala, J., Saario, J., 2015. From phycocyanin fluorescence to absolute cyanobacteria biomass, An application using in-situ fluorometer probes in the monitoring of potentially harmful cyanobacteria blooms. Water Practice &Technology 10 (4), 695-698.

Lühring, M., Faassen, E.J., 2013. Dog Poisoning Associated with a Microcystis aeruginosa Bloom in the Netherlands. Toxins 5(3), 556-567.

McQuaid, N., Zamyadi, A., Prevost M., Bird, D.F., Dorner, S., 2011. Use of in vivo phycocyanin fluorescence to monitor potential microcystin-producing cyanobacterial biovolume in a drinking water source. Journal of Environmental Monitoring 13, 455-463.

Oertli, B., Joyer, D. A., Catella, E., Juge, R., Cambin, D., Lachavanne, J. B., 2002. Does size matter the relationship between pond area and biodiversity. Biological Conservation 104, 59–70.

Raps, S., Wyman, K., Siegelman, H. W., Falkowski, P. G., 1983. Asaptation of the cyanobacterium *Microcystis aeruginosa* to light intensity. Plant Physiology 2(3),829-832.

Rozina, T., Sedmak, B., Zupančič Justin, M., Meglič, A., 2017. Evaluation of cyanobacteria biomass derived from upgrade of phycocyanin fluorescence estimation. Acta Biologica Slovenica 60(2), 21,28.

Sedmak, B., Kosi, G., Kolar B., 1994. Cyanobacteria and their relevance. Periodicum Biology 96, 428-430.

Song, K., Li, L., Tedesco, L., Clercin, N., Hall, B., Li, S., Shi, K., Liu, D., Sun, Y., 2013. Remote estimation of phycocyanin (PC) for inland waters coupled with YSI PC fluorescence probe. Environmental Science Pollution Research 20, 5330–5340.

Seppälä, J., Ylöstalo, P., Kaitala, S., Hällfors, S., Raateoja, M., Maunula, P., 2007. Ship-of-opputunity based phycocyanin fluorescence monitoring of the filamentous cyanobacteria bloom dynamics in the Baltic See. Estuarine, Costal and Shelf Science 73, 489-500.

Walsby, A.E., Ng, G., Dunn, C., Davis, P.A., 2004. Comparison of the depth where Planktothrix rubescens stratifies and the depth where the daily insolation supports its neutral buoyancy. New Phytologist 162, 133–145.

Wetzel, R. G., 2001. Limnology. 3rd ed. Philadelphia, Saunders College Publishing. 342 pages.

Williams, P., Whitfield, M., Biggs, J., Bray, B., Fox, G., Nicolet, P., Sear, D., 2003. Comparative biodiversity of rivers, streams, ditches and ponds in an agricultural landscape in Southern England. Biological Conservation 115, 329–341.

Zamyadi, A., McQuaid, N., Prevost, M., Dorner, S., 2012. Monitoring of potentially toxic cyanobacteria using an online multi-probe in drinking water sources. Journal of Environmental Monitoring 14(2), 579-558.

Zamyadi, A., Dorner, S., Ndong, M., Ellis, D., Bolduc, A., Bastien, C., Prévost, M., 2014. Application od in vivo measurments fort he management of cynobacteria breakthrough into drinking water treatment plants. Environmental Science; Processes & Impacts 16, 213-323.

ACTA BIOLOGICA SLOVENICA
LJUBLJANA 2018 Vol. 61, Št. 2: 39–46

‘Only introduced’ or ‘invasive’: spread of the alga *Aulacoseira ambigua* f. *japonica* from Asia to Africa and Europe

„Zgolj preseljena“ ali „invazivna“: širjenje alge *Aulacoseira ambigua* f. *japonica* iz Azije v Afriko in Evropo

Tina Eleršek

Department of Genetic Toxicology and Cancer Biology, National Institute of Biology, Večna pot 111, SI-1000 Ljubljana, Slovenia

Correspondence: tina.elersek@nib.si

Abstract: Many non-native algal species are found in waters all over the world. Many terms are used to describe such organisms that have expanded their distribution. However, a unified model or concept remains to be defined, as how biological ‘invasions’ are seen depends on the perspective. Understanding invasive organisms is important for biodiversity, science policy and water management. During monitoring sampling at Slivniško Lake (Slovenia) in 2016, the curved diatom *Aulacoseira ambigua* f. *japonica* Tuji & D.M. Williams was identified. This species originates from Japan, from where it was described more than 100 years ago. The chronology of the published distributions of *A. ambigua* f. *japonica* defines its spread from Japan to Asia, then to western Russia and South Africa, and now to central Europe. This study provides further evidence that *A. ambigua* f. *japonica* has become established in Europe (Slovenia), as supported by light microscopy and scanning electron microscopy. To the best of our knowledge, this is the first qualitative and quantitative description of *A. ambigua* f. *japonica* in Europe. It has been suggested that the shape of these algal colonies is significant for the interpretation of ecological information, and indeed, also in the present case, spiral colonies were found in this eutrophic water body. Although curved cells and colonies can also be interpreted as (sub)populations or morphological variants, only detailed molecular studies can reveal if these also have taxonomic significance.

Keywords: algae, *Aulacoseira ambigua* f. *japonica,* introduced species, invasive species, scanning electron microscopy

Izvleček: V vodah po vsem svetu najdemo veliko tujerodnih vrst. Za opis organizmov, ki se širijo, je v uporabi veliko različnih pojmov. Kaže se potreba po opredeliti enotnega modela ali koncepta, saj je videnje bioloških “invazij” odvisno od perspektive. Razumevanje invazivnih organizmov je pomembno za biotsko raznovrstnost, znanstveno politiko in upravljanje z vodami. Med spremljanjem vzorčenja na Slivniškem jezeru (Slovenija) leta 2016 smo med drugim določili tudi ukrivljeno diatomejo *Aulacoseira ambigua* f. *japonica* Tuji & D.M. Williams. Ta vrsta izvira iz Japonske, kjer je bila opisana pred več kot 100 leti. Kronologija objavljenih pojavljanj *A. ambigua* f. *japonica* opredeljuje njeno širjenje iz Japonske v Azijo, nato v zahodno Rusijo in Južno

Afriko, zdaj pa v osrednjo Evropo. Ta raziskava vsebuje dodatne dokaze, da se je *A. ambigua* f. *japonica* uveljavila v Evropi (v Sloveniji), podprte s svetlobno mikroskopijo in vrstično elektronsko mikroskopijo. Gre za prvi kvalitativni in kvantitativni opis *A. ambigua* f. *japonica* v Evropi. Oblika algnih kolonij je lahko pomembna za razlago ekoloških informacij; v danem primeru so bile v evtrofnem vodnem telesu najdene spiralne kolonije. Čeprav so ukrivljene celice in kolonije lahko interpretirane tudi kot (sub)populacije ali morfološke različice, lahko le natančne molekularne študije razkrijejo, če imajo ti morfotipi taksonomski pomen.

Ključne besede: alge, *Aulacoseira ambigua* f. *japonica,* vnesene vrste, invazivne vrste, vrstična elektronska mikroskopija

Introduction

Many terms are used to describe organisms that expand their distribution, including 'introduced', 'non-indigenous', 'non-native', 'invasive', 'exotic', and even 'alien'. This has made studies associated with biological invasion often difficult and confusing to follow (Kokocinski et al. 2017). After 20 years of studies of such organisms, a unified model or concept remains to be defined, particularly because how biological 'invasions' are seen is a matter of perspective (Heger et al. 2013). The term 'invasive' usually relates to a new species that spreads rapidly through a new environment, and this has a negative connotation. Thus an invasive organism is seen to have a tendency to spread to a degree that is believed to cause damage to the environment, or ecosystem services such as human economy or health. Indeed, the International Union for Conservation of Nature defines an invasive species as a widespread non-indigenous species that has adverse effects on the invaded habitat. Usually, man is commonly believed to be responsible for invasive organisms that have been introduced into places away from their natural range of distribution.

The conceptual model of the ecological impact of the invasion process can be divided into three stages: transport, establishment, and spread (Kokocinski et al. 2017). Many species are transported and become established, but their spread and any associated negative impact also rely on favourable natural conditions in the particular ecosystem. Nevertheless, it is difficult to define the spatial and temporal scale of such an expansion, and also the negative impact that is might have, as every invasive species has a different interaction with the ecosystem and its members. It is common sense that non-stressed ecosystems can more easily cope with changes, in comparison to ecosystems that are exploited by humans.

There are many published lists of local invasive algal species according to countries or regions, and these represent mostly cyanobacteria and other potentially toxic species (Kokocinski et al. 2017). For cyanobacteria, it is understandable that special attention must be paid, as some cyanobacterial species can produce potent toxins. Instead, it is rare that diatoms are considered as invasive. The best described case is the diatom *Didymospehnia geminata* (Taylor and Bothwell 2014), for which blooms have been reported in rivers worldwide that have been somewhat hastily attributed to their introduction. Here, the evidence indicates that such *D. geminata* blooms are probably not caused by their specific introduction, but rather by the environmental conditions in connection with the phosphorous concentrations, which promote excessive stalk production by this historically rare species (Taylor and Bothwell 2014). This emphasises how important it is to understand whether the successful dominance of a species is a result of its introduction or of changing environmental conditions that have facilitated what was an already existing population, or whether both processes apply. The origins of such invasive microorganisms are importance for science policy and management (Taylor and Bothwell 2014).

To date, few data have been published relating to the freshwater diatom *Aulacoseira ambigua* f. *japonica* (F. Meister) Tuji & D.M. Williams.

The very first description of this species was by Meister (1913), more than 100 years ago in Japan, who named it as *Melosira japonica*. The first record of the species with the current name was also in Japan, by Tuji and Williams (2007). According to AlgeBase (2017), the accepted basionym and homotypic synonym of *A. ambigua* f. *japonica* Tuji & D.M. Williams is *M. japonica* F. Meister. This species has also been referred to as *Melosira ambigua* f. *curvata* (Skabichevskii 1960), *Melosira ambigua* f. *spiroides* (Chalfina 1966), and *Melosira granulata* var. *tenuissima* f. *spiralis* (Wakabayaschi and Ichise 1982). In 2010 this species was reported for Korea (Joh 2010), and 6 years later, for South Africa (van Vuuren and Taylor 2016). Then only one year after that it was identified in France (Anon. 2017). Following this chronology and movement, the path that *A. ambigua* f. *japonica* has followed from its origins in Japan to initial spread to Asia, then western Russia and South Africa, and now central Europe.

Here we provide further evidence that *A. ambigua* f. *japonica* has become established in Europe (Slovenia). To the best of our knowledge, this is the first qualitative and quantitative description of *A. ambigua* f. *japonica* in Europe.

Study area, materials and methods

Study area

Slivniško Lake (Slivniško jezero) is located in the eastern part of Slovenia, near to Šentjur, which is 20 km from the Croatian–Slovenian border (GKY 534340, GKX 116230; 46°11′17″N, 15°26′48″E). Slivniško Lake has a surface area 840,000 m^2, a length of 5,000 m, and a width of 500 m. It is 292 m above sea level, and has a mean depth of 5 m, with maximum depth of 14 m. This accumulation is based on a carbonate geological base, with inflow from the Ločnica Stream, and outflow of Voglajna River. A reservoir was created in 1976 for industrial use, but due to technological development, for many years it has only been used as a floodwater retention buffer, and as a lake for fishing and tourism activities. Indeed, Slivniško Lake is famous for its fishing competitions, with a recent winning catfish of 255 cm in length, and 95 kg in weight.

The ecological characteristics of Slivniško Lake have been followed through the National Freshwater Monitoring Programme, with the data included here originally from national reports (Remec-Rekar 2011-2016). Slivniško Lake is described as a lowland accumulation with moderate ecological potential, with it included in the ecotype of shallow Pannonian plain with Alpine influence. The ecological status of Slivniško Lake has remained moderate, and it has never shown any cyanobacterial blooming. From 2011 to 2016, it had good chemical status. Over the period from 2011 to 2016, the mean total nitrogen and phosphorous through the water column was 519 µg L^{-1} and 113 µg L^{-1}, respectively. It had a mean biovolume of 4 mm^3 L^{-1}, mean annual chlorophyll *a* of 7 µg L^{-1}, and maximum chlorophyll *a* of 21 µg L^{-1} (in 2014). The mean Secci depth was 1 m. According to the Organisation for Economic Cooperation and Development criteria, from 2011 to 2016, this classification defined Slivniško Lake as a eutrophic water body.

Sampling and laboratory sample preparation

Sampling of the phytoplankton of Slivniško Lake was carried out in accordance with national methodologies, from a boat with an automated sampler, and for the euphotic zone in its deepest part. Immediately after sampling, the contents of a 100 mL tube was fixed with 4% formalin and transferred to the laboratory. The fixed samples were stored at 4 °C. Light microscopy analyse was carried out up to 5 months after the sampling, at 1,000× magnification (Microscope Nikon Eclipse TE300, Japan). A subsample for the examination of diatom frustules only was cleaned of organic material by addition of HNO_3, with heating leading to degradation of the organic matter, with only silicate (silica) frustules of the diatom species remaining.

Scanning electron microscopy

The cleaned samples were centrifuged and washed three times with acetone, and placed directly on a metal holder. After sputter coating with platinum, the algae were analysed using a scanning electron microscope (JSM-7500 F; JEOL, Japan). The sample was not as rich in *A.*

ambigua f. *japonica* as samples described by van Vuuren and Taylor (2016), and they were more fragmented due to the protocol with acid cleaning of the organic material, so only short chains were seen with the scanning electron microscopy. Nevertheless, the observation of fresh material also revealed long spiral colonies, although these were unfortunately not captured in the light microscopy images.

The species

Aulacoseira ambigua f. *japonica* was found in Slivniško Lake in 2016 during National Freshwater Monitoring. During this year, this diatom alga was found in phytoplankton, in March, July and October, with a mean concentration of 372 cells mL^{-1}, and with mean biovolume of 0.14 $mm^3 L^{-1}$, which represented 21% of total Bacillariophyta biovolume, and 2.3% of total phytoplankton biovolume. The lengths were measured using computer software (Nikon NIS Elements 3.22.15), with the arithmetic mean for diameter and length calculated from 20 separate cells.

These studies of Slivniško Lake during the National Freshwater Monitoring from 2011 to 2016 revealed a different dominant species each year. Relative annual mean abundance >2% was seen for: *Aphanocapsa* sp. (Nägeli 1849), *Aphanothece* sp. (Nägeli 1849), *Coelastrum* sp. (Nägeli 1849), *Cyanobium* sp. (Rippka & Cohen-Bazire 1983), *Eutetramorus planktonicus* (Korshnikov 1953), *Merismopedia tenuissima* (Lemmermann 1898), *Navicula minima* (Grunow 1880), *Oocystis lacustris* (Chodat 1897), *Pediastrum simplex* (Meyen 1829), *Peridinium umbonatum* (Stein 1883), *Phacotus lenticularis* (Diesing 1866), *Tetrastrum komarekii* (Hindák 1977) and *Woronichinia naegeliana* (Elenkin 1933). Relative annual mean biovolume >2% was seen for: *Aulacoseira granulate* (Simonsen 1979), *Ceratium hirundinella* (Dujardin 1841), *Chlamydomonas rigensis* (Skuja 1927), *Coelastrum* sp. (Nägeli 1849), *Cosmarium* sp. (Corda ex Ralfs 1848), *Cryptomonas obovata* (Czosnowski 1948), *Cyclotella* sp. (Brébisson 1838), *Dinobryon divergens* (Imhof 1887), *Euglena ehrenbergii* (Klebs 1883), *Euglena* sp. (Ehrenberg 1833), *Fragilaria ulna* (Lange-Bertalot 1980), *Koliella* sp. (Hindák 1963), *Lepocinclis ovum* (Lemmermann 1901), *Pandorina morum* (Bory 1824), *Pediastrum duplex* (Meyen 1829), *Pediastrum duplex* var. *gracillimum* (West & G.S.West 1895), *Pediastrum simplex* (Meyen 1829), *Phacotus lenticularis* (Diesing 1866), *Phacus longicauda* (Dujardin 1841), *Sphaerocystis schroeteri* (Chodat 189) and *Trachelomonas* sp. (Ehrenberg 1833).

Observations

Centric diatoms rarely form spiral colonies (van Vuuren and Taylor 2016), and therefore the spiral shaped diatom colonies with distinctly curved cells were relatively easy to determine. After investigation under light microscopy (Fig. 1) and scanning electron microscope (Fig. 2), the taxon from Slivniško Lake was identified as a special form of *A. ambigua*, defined as *A. ambigua* f. *japonica* (F. Meister) Tuji & D.M. Williams. The mantle of the cells of the *Aulacoseira* genus is much deeper than for other centric taxa, which gives the cells a cylindrical or tube-like structure. The cells are linked as valve face to valve face by short spines (van Vuuren and Taylor 2016). With mean diameter of 5 µm and length of 10 µm (Figs. 1, 2, 3), these matched the previously reported ranges of 3 µm to 12 µm in diameter, and 5 µm to 15 µm in length, with their characteristic hollow ringleiste and specific external rimoportulae (Potapova and English 2010).

Discussion

Aulacoseira ambigua f. *japonica* has never before been recorded for the locality of Slivniško Lake. In 2016, it was well established, but it had not become dominant. Such establishment of this species represents the second stage of the conceptual ecological model for an invasive species, with expansion of the invasion as the final stage (Kokocinski et al. 2017). Nevertheless, biological invasions are important parts of the functioning of aquatic and terrestrial ecosystems (Sukenik et al. 2015).

Previous studies have revealed decreases in species diversity after invasion by alien species, along with alterations to ecosystem functioning due to the reproduction and feeding behaviours

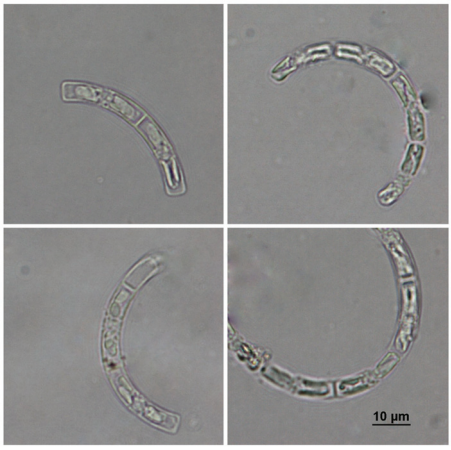

Figure 1: *Aulacoseira ambigua* f. *japonica* Tuji & D.M. Williams from Slivniško Lake (Slovenia), light microscopy with phase contrast. Scale bar of 10 µm is in the bottom right corner.
Slika 1: *Aulacoseira ambigua* f. *japonica* Tuji & D.M. Williams iz Slivniškega jezera (Slovenija), posnetek svetlobnega mikroskopa s faznim kontrastom. V spodnjem desnem kotu je merilce dolžine 10 µm.

of such organisms, and because of the release of new chemical compounds (e.g., cyanotoxins) after expanded invasion (Sukenik et al. 2015). Further studies are needed to enable us to recognize better and mitigate the potential threats associated with such invasive processes. Here the path followed in the travels of a species can also help in the determination of its origin, as the origins of such invasive microorganisms can be important for science policy and management (Taylor and Bothwell 2014).

Although curved cells and colonies of *A. ambigua* can be interpreted as a potential (sub) population (Potapova and English 2010) or a morphological variant (Tremarin et al. 2013), only detailed molecular studies can reveal if this truly has taxonomic significance or not. The morphological variations and the distributions of *A. ambigua* in Brazilian environments were described by Tremarin et al. (2013), although they only indicated long, slightly curved chains (with no curved individual cells). Tuji and Williams (2007) reported that the shape of such colonies is significant for the interpreting of ecological information. Indeed, ecological differences for *A. ambigua* and *A. japonica* (*M. japonica*) have been reported, whereby Tanaka (2002) defined straight colonies in mesotrophic waters, and Tuji and Williams (2007) defined spiral colonies with curved cells in eutrophic waters. This latter is confirmed also in the present case, as Slivniško Lake has been described as a eutrophic water body since 2011, and it showed only spiral colonies of *A. ambigua* f. *japonica* in 2016. However, it is important to bear in mind that such monitoring studies just provide a snap-shot in time, and that you cannot stop the evolution while studying the ecology.

This demonstrates that *A. ambigua* f. *japonica* has become established in Europe (Slovenia), with the support of light microscopy and scanning electron microscopy images. To the best of our knowledge, this is the first qualitative and quantitative description of *A. ambigua f. japonica* in Europe.

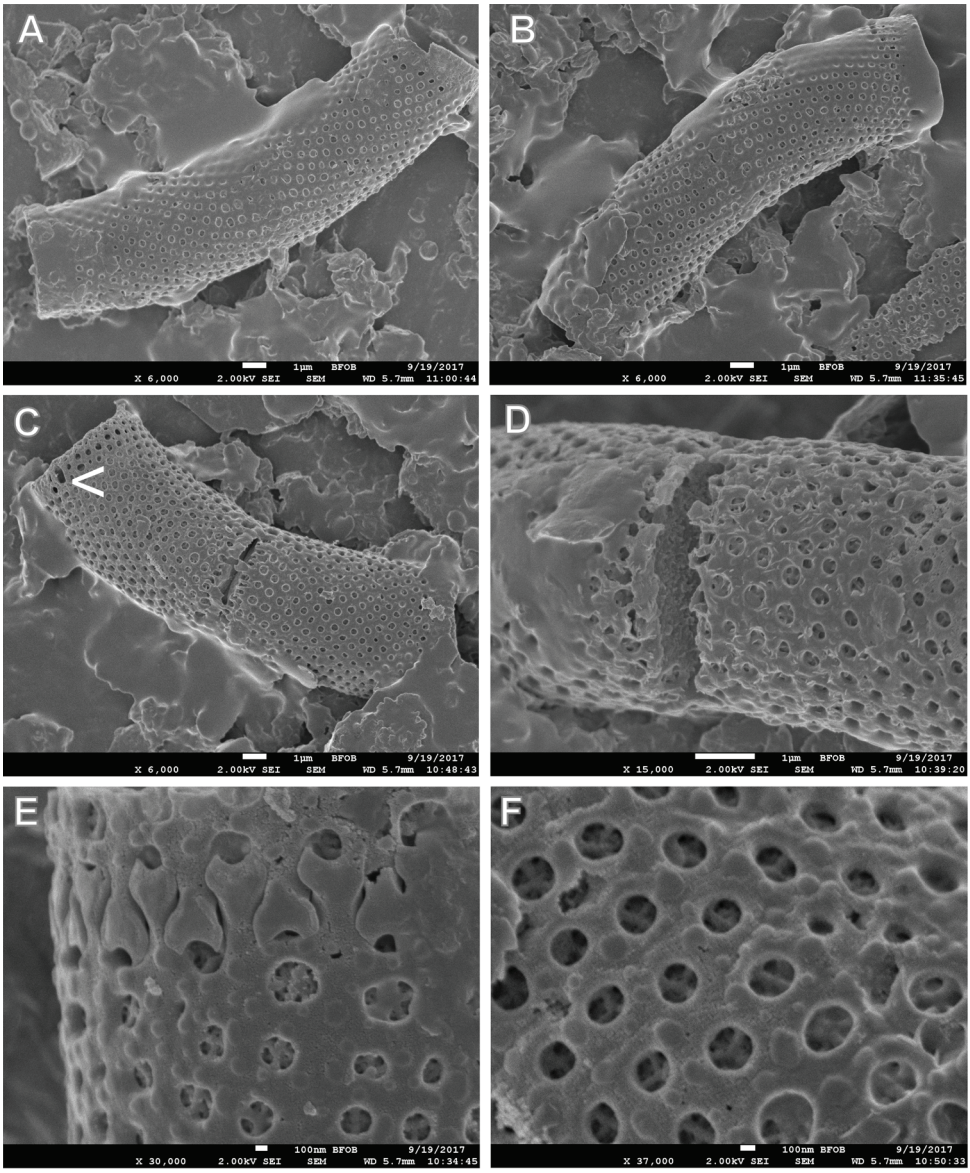

Figure 2: *Aulacoseira ambigua* f. *japonica* Tuji & D.M. Williams from Slivniško Lake (Slovenia), scanning electron microscopy. A, B - The curvature of the individual cells. B, C - Position and structure of the external rimoportulae (white arrow). D - Separation of the valves. E - Linking valve showing complex shape of the linking spines on the valve face. F - Detail of the mantle areolae. Scale bar is positioned at the bottom of every picture; A-D: 1 µm, E-F: 100 nm.

Slika 2: *Aulacoseira ambigua* f. *japonica* Tuji & D.M. Williams iz Slivniškega jezera (Slovenija), posnetek vrstičnega elektronskega mikroskopa. (A, B) Ukrivljenost posameznih celic. (B, C) Položaj in struktura zunanjih rimoportul (bela puščica). (D) Razmejitev silikatne lupinice. (E) Povezovalna struktura, ki prikazuje kompleksno obliko povezovalnih zobcev na čelni strani silikatne lupinice. (F) Podrobnosti ploskve. Merilce se nahaja na spodnjem robu vsake slike; A-D: 1 µm, E-F: 100 nm.ploskve. Merilce se nahaja na spodnjem robu vsake slike; A-D: 1 µm, E-F: 100 nm.

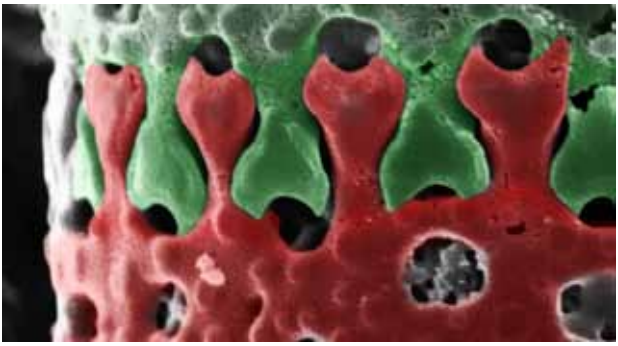

Figure 3: A detail of the cell joint structure - linking valve of alga *Aulacoseira ambigua* f. *japonica* Tuji & D.M. Williams from Slivniško Lake (Slovenia), scanning electron microscopy. Scale bar as on Figure 2E.

Slika 3: Detajl povezovalne strukture dveh lupinic alge *Aulacoseira ambigua* f. *japonica* Tuji & D.M. Williams iz Slivniškega jezera (Slovenija), posnetek vrstičnega elektronskega mikroskopa. Merilce kot na sliki 2E.

Summary

Biological migrations are important parts of the functioning of aquatic and terrestrial ecosystems. Alga *Aulacoseira ambigua* f. *japonica* has never before been recorded for the locality of Slivniško Lake. In 2016 this species at this location became well established, but it had not become dominant in the algal community. Only detailed molecular studies will reveal if this species with its morphological variation can be interpreted as a potential (sub)population or a morphological, or maybe even as ecological variant, with a link to the eutrophication of water body. The migration path of this species revealed some information, but further studies are needed to enable us to better recognize and mitigate the potential threats associated with invasive processes.

Povzetek

Biološke migracije so pomembni deli delovanja vodnih in kopenskih ekosistemov. Alga *Aulacoseira ambigua* f. *japonica* še nikoli prej ni bila zaznana na lokaciji Slivniškega jezera. Leta 2016 pa je ta vrsta na tej lokaciji postala dobro uveljavljena, vendar v algni združbi ni prevladala. Le podrobne molekularne študije bodo razkrile, ali je ta vrsta s svojimi morfološkimi različicami potencialna (sub)populacija ali morfološka oz. celo ekološka varianta, ki je povezana z evtrofikacijo vodnega telesa. Selitvena pot te vrste je razkrila nekatere informacije, vendar so potrebne nadaljnje študije, ki nam omogočajo boljše prepoznavanje in zmanjševanje potencialnih groženj, povezanih z invazivnimi procesi.

Acknowledgements

The sampling and laboratory analyses of this species received funding from the National Monitoring Scheme at the National Agency of Environment (funded by the Slovenian Ministry of the Environment and Spatial Planning) under grant agreement N° 2551-16-500150. The author thanks Karmen Stanič for field and laboratory technical assistance, Miloš Vittori for technical assistance with the scanning electron microscopy, and Christopher Berrie for reviewing the language and grammar.

References

AlgaeBase - Guiry, M.D., Guiry, G.M., 2017. World-wide electronic publication, National University of Ireland, Galway. http://www.algaebase.org; searched on 20 September 2017.

Anon, 2017. Inventaire national du Patrimoine naturel. Paris: Muséum National d'Histoire Naturelle. https://inpn.mnhn.fr/accueil/index; searched on 20 September 2017.

Chalfina, N.A., 1966. De speciebus generis Melosira Ag. e flumine Amur notula, Novitates systematicae plantarum non vascularium, pp. 43-46 (in Russian).

Heger, T., Saul, W.C., Trepl, L., 2013. What biological invasions 'are' is the matter of perspective. Journal of Natural Conservation 21(2), 93-96.

Joh, G., 2010. Algal flora of Korea: 3 (1). Chrysophyta: Bacillariophyceae: Centrales. Freshwater diatoms I. Incheon: National Institute of Biological Resources. pp. [1-6], 1-161.

Kokociński, M., Akçaalan, R., Salmaso, N., Stoyneva-Gärtner, M.P., Sukenik, A., 2017. Expansion of alien and invasive cyanobacteria. In: Meriluoto J., Spoof L., Codd G.A. (Eds.): Handbook of Cyanobacterial Monitoring and Cyanotoxin Analysis, pp. 28-39.

Meister, F., 1913. Beiträge zur Bacillariaceenflora Japan. Archiv für Hydrobiologie und Planktonkunde, Stuttgart, 8, 305-312, page(s): 305, 311; pl. 4, fig. 1.

Potapova, M., English, J., 2010. *Aulacoseira ambigua*. In: Diatoms of the United States. http://westerndiatoms.colorado.edu/taxa/species/aulacoseira_ambigua; searched on 25 September 2017.

Remec-Rekar, Š., 2011-2016. The assessment of the status of lakes in Slovenia. Ministry of the Environment and Spatial Planning, Environmental Agency of the Republic of Slovenia (in Slovenian).

Skabichevskii, A.P., 1960. Planktonnye diatomovye vodorosli presnykh vod SSSR (sistematika, ekologiya, rasprostranenie). Moscow: Izd. Mosk. Gos. Univ. (in Russian).

Sukenik, A., Quesada, A., Salmaso, N., 2015. Global expansion of toxic and non-toxic cyanobacteria: effect on ecosystem functionating. Biodiversity and Conservation 24(4), 889-908.

Tanaka, M., 2002. Illustrations of the Japanese freshwater plankton. The University of Nagoya Press, Nagoya, 584 p. (in Japanese).

Taylor, B.W., Bothwell, M.L., 2014. The origin of invasive microorganisms matters for science, policy, and management: the case of *Didymosphenia geminate.* Bioscience 64(6), 531-538.

Tuji, A., Williams, D.M., 2007. Type examination of Japanese diatoms described by Friedrich Meister (1913) from Lake Suwa. Bullets of National Museum of Natural Sciences, Ser. B, 33(2), 69-79.

van Vuuren, S.J., Taylor, J.C., 2016. A first record of *Aulacoseira ambigua* f. *japonica* (F. Meister) Tuji & D.M. Williams in South African freshwaters. African Journal of Aquatic Sciences 41(4), 369-375.

Tremarin, P.I., Ludwig, T.V., Torgan, L.C., 2013. Morphological variation and distribution of the freshwater diatom *Aulacoseira ambigua* (Grunow) Simonsen in Brazilian continental environments. IHERINGIA, Sér. Bot., Porto Alegre 68(1), 139-157.

Wakabayashi, T., Ichise, S., 1982. In: Negoro K. (Ed.) The plankton of Lake Biwa. The Shiga Prefectural Institute of Public Health and Environmental Science (in Japanese).

ACTA BIOLOGICA SLOVENICA
LJUBLJANA 2018 Vol. 61, Št. 2: 47–70

The vascular flora of Kopački rit Nature Park (Croatia)

Vaskularne rastline Naravnega parka Kopački rit (Hrvaška)

Vlatko Rožac[a], Dragan Prlić[b], Siniša Ozimec[c*]

[a] Public Institution Kopački rit Nature Park, Mali Sakadaš 1, Kopačevo, HR-31327 Bilje, Croatia
[b] Josip Juraj Strossmayer University of Osijek, Department of Biology, Cara Hadrijana 8/A, HR-31000 Osijek, Croatia
[c] Josip Juraj Strossmayer University of Osijek, Faculty of Agrobiotechnical Sciences Osijek, Vladimira Preloga 1, HR-31000 Osijek, Croatia

*correspondence: sozimec@pfos.hr

Abstract: Kopački rit Nature Park is a large fluvial-marshy floodplain, situated in the northeastern Croatia, between courses of the Danube and the Drava Rivers. Due to exceptional biological and ecological values of this floodplain area in the middle course of the Danube River, it had been protected since 1967; proclaimed as Nature Park in 1999 and from 2012 is a part of the UNESCO Transboundary Biosphere Reserve Mura-Drava-Danube. This paper lists a total of 522 vascular plant taxa, classified in 295 genera and 96 families, recorded for Kopački rit Nature Park. The list is completed according to checked literature records and data for 114 new taxa, found during the floristic investigation carried out from 2010 to 2018. Taxonomic, ecological and phytogeographical analyses are presented. Hemicryptophytes dominate (39.3%) in the biological spectrum, followed by therophytes (23.8%), geophytes (12.6%) and hydrophytes (12.5%). In the chorological spectrum, the most numerous are plants of Eurasian floral elenent (32.8%), followed by Cosmopolites (27.4%), and European floral element (10.7%). Out of 53 recorded allochthonous plants, 26 are invasive alien plant species. According to protection and conservation status at the national level, 55 taxa are listed in the Red Book of Vascular Plants of Croatia and 53 taxa are strictly protected. One species, *Marsilea quadrifolia*, is listed in Annex II of the Habitat Directive.

Key words: Kopački rit, Danube, flora, biodiversity

Povzetek: Naravni park Kopački rit je obsežna poplavna ravnica, ki se nahaja na severovzhodu Hrvaške, med rekama Donavo in Dravo. Zaradi izjemne biološke in ekološke vrednosti tega poplavnega območja v srednjem toku reke Donave je območje od leta 1967 zaščiteno. Naravni park je bil razglašen leta 1999 in od leta 2012 je območje del prekomejnega biosfernega rezervata UNESCO Mura-Drava-Donava. V Naravnem parku Kopački rit je bilo zabeleženih 522 vaskularnih rastlinskih taksonov, ki sodijo v 295 rodov in 96 družin. Seznam temelji na podatkih v literaturi, katerim smo dodali 114 novih taksonov, ki so bili popisani med florističnimi raziskavami, opravljenimi od leta 2010 do leta 2018. V prispevku so predstavljene taksonomske, ekološke in fitogeografske analize. Med taksoni prevladujejo hemikritopiti (39,3 %),

sledijo jim terofiti (23,8 %), geofiti (12,6 %) in hidrofiti (12,5 %). Najštevilčnejši so evrazijski florni elementi (32,8 %), sledijo kozmopolitske vrste (27,4 %) in evropski florni elementi (10,7 %). Od 53 zabeleženih alohtonih rastlin je 26 invazivnih tujerodnih rastlinskih vrst.

Ključne besede: Kopački rit, Donava, flora, biotska raznolikost

Introduction

Floristic studies in the area of Kopački rit Nature Park were only occasional in the past. Numerous records, sometimes with a description of geographically uncertain localities, are included in publications related to the wider area of the Slavonia and Baranja regions.

The earliest report about plants in the present-day Kopački rit area dates back to the 18th century. Count Luigi Ferdinando Marsigli collected information on the indigenous plants of the Danube region and presented it in the sixth volume of the monograph: Danubius Pannonico-Mysicus (Marsigli 1726). Among the listed plants and localities along the Danube course, the mouth of the Drava River ("circa influxum Fluvii Dravii") was recognised as the collection hot spot of several plants. Paul Kitaibel made field excursions in Baranja region in the period 1799 – 1808 (Purger and Csiky 2008), and some of his records were published by Neilreich (1866). Ádám Boros made a field visit in Kopački rit from 24 to 27 June 1944 and reported findings of *Urtica kioviensis* (Boros 1944a), *Veronica peregrina* (Boros 1944b) and *Marsilea quadrifolia* (Boros 1946).

Floristic studies have been renewed and intensified in the period from the1960s up to the end of 1980s (Jovanović 1965, Ilijanić 1968, Balátová-Tuláčková and Knežević 1975, Rauš et al. 1980, 1985). Trinajstić and Pavletić (1978) investigated the aquatic vegetation and made the first record of a neophyte *Azolla filiculoides* in Kopački rit. In the review of vegetation diversity in Kopački rit Special Zoological Reserve, Topić (1989) decribed structure of 37 associations, arranged into ten classes of aquatic, marshland, ruderal, meadow and forest vegetation. During the botanical surveys in the period 1986 – 1988, Panjković (1990) recorded 723 taxa for the flora of the Baranja region, including several taxa found in Kopački rit.

Topić (1999) summarised all available literature data about flora and vegetation in Kopački rit and made a list of 368 taxa for the flora of Kopački rit. Zahirović (2000) carried out from 1997 to 1999 an extensive field investigation of the rare and endangered plant species in northeastern Croatia, including the area of Kopački rit. Among 467 recorded taxa, 37 had been new for the flora of the Baranja region. Distribution and ecology of two rare aquatic plants in Kopački rit, *Azolla filiculoides* and *Wolffia arrhiza*, was described in details. Topić and Ozimec (2001) reported the first finding of *Typha laxmannii* as a new to the Croatian flora.

Latest discoveries treated two new taxa to the flora. An invasive aquatic species *Elodea nuttallii* was found in 2006 in the drainage channels in Kopački rit (Kočić et al. 2014). *Scirpus pendulus,* a neophyte originating from North America, was discovered in July 2011 on the muddy bottom in a wet ditch in the area between Kozjak and Tikveš (Ozimec and Topić 2018).

Public Institution Kopački rit Nature Park initiated and supported intensive floristic investigations in the period 2010 – 2018, combined with monitoring of rare and threatened plants and habitats. An important achievement of these activities is a complete list of the vascular flora, presented for the first time in this paper.

Material and methods

Study area

Kopački rit Nature Park is located in north-eastern Croatia, in the angular area formed by the confluence of the Danube and the Drava River (Fig. 1). The Park covers an area of 231 km^2 with an altitudinal range from 78 to 86 m a.s.l. This is a large fluvial-marshy floodplain formed during the late Quaternary (Bognar 1990).

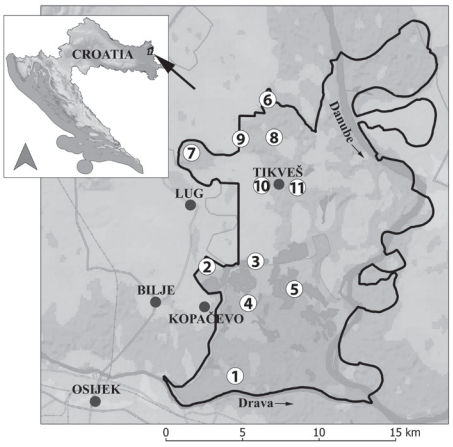

Figure 1: The area of Kopački rit Nature Park with position of localities where new taxa had been found.

Slika 1: Območje Naravnega parka Kopački rit z lokacijami, kjer smo našli nove taksone.

Data from the climatological station in Tikveš for the period 2004 – 2013 confirms that the climate is moderately warm and rainy (Cvitan 2014). Mean annual air temperature is 11.0 °C, the absolute minimum is – 25.1 °C, and the absolute maximum is 39.4 °C. The coldest month is January (0.4 °C) and warmest is July (21.9 °C). Mean annual precipitation amounts to 696 mm, the highest in June (89 mm), and lowest in January (44 mm). Mean relative humidity is 85%, highest in December and January (91% each), and lowest in July (79%). Mean annual number of days with frost is 53, and with dew is 142 days.

Floodwater enters the area from both the northern and southern parts when the Danube water level exceeds the value of 81.50 m a.s.l. (at Apatin gauging station), and at water level above 83.00 m a.s.l. the entire area is filled with water. The largest water body is the Kopačko Lake with the surface of 200–250 ha in the period out of flooding. The deepest one is the Sakadaš Lake with a mean depth of 7 m. The lakes are interconnected with rivers through a network of natural channels (Tadić 1999).

The inflow of the Danube floodwaters towards the Kopačko Lake is distributed by the 6 km long Hulovo Channel, which is connected with the Danube course near river km 1,388. In the northern part, floodwaters are distributed by the Vemeljski Dunavac, a Danube sidearm with upper end at river km 1,407 and lower end at river km 1,392 (Ozimec and Topić 2018).

Danube flooding and water stagnation are major pedogenetic factors of specific soil type characterised by fine texture and low hydraulic conductivity. The most prevalent are hydromorphic soils, particularly gleysols. Excessive wetting by floods and high subsurface water enables the evolution of hydromorphic soils (Tadić et al. 2014).

Regarding the phytogeographical position, the area belongs to the Eurosiberian – North American region and the Pannonian sector of the Central European province. This is a transitory region between the vegetation of the *Carpinion betuli* alliance and forest-steppe zone of the *Aceri tatarici – Quercion* alliance (Topić and Šegulja 2005). In the land use structure, freshwaters and marshland covers 40% of the total Park area, forests 30%, and the agricultural land 20% (Anonymous 2006).

The area of Kopački rit was firstly protected in 1967 under the category of Managed Natural Reserve. Its boundaries and protection categories had been changed during the fifty-year period. Existing protection status was established in 1999 by the Act of Kopački rit Nature Park (Anonymous 1999) at total area of 231 km^2 including 71 km^2 of Kopački rit Special Zoological Reserve and the Danube course between river km 1,412 and 1,382. In 1993, Kopački rit was designated on the List of Wetlands of International Importance under the Ramsar Convention. It is included in the ecological network Natura 2000 in Croatia, with a site code HR2000394 Kopački rit (Anonymous 2013a, 2015). The latest achievement in nature protection is the establishment of UNESCO Transboundary Biosphere Reserve Mura-Drava-Danube, proclaimed in July 2012, with Kopački rit Nature Park as the best-preserved natural floodplain of the entire Reserve.

Floristic study

Field investigations were carried out in the period from 2010 to 2018, with an approval for research and collection issued by the competent state authority for the nature protection.

Investigated localities (Fig. 1) where new taxa had been found are described as it follows:

1. Wet meadows near the left bank of the Drava River (19 May 2010, 26 May 2011, 25 May 2012, 29 August 2017), size about 83 ha, degraded meadow association *Veronico longifoliae – Euphorbietum lucidae*;
2. Fishponds "Podunavlje", basins A, D, and E and surrounding area (2 July 2010, 1 July 2011, 11 August 2011), size about 217 ha, channels and standing water with aquatic and marshland vegetation from classes *Lemnetea, Potamogetonetea* and *Phragmito-Magnocaricetea;*
3. Fishponds "Podunavlje", basins B and C and surrounding area (15 September 2010, 2 June 2014), size about 300 ha, standing water with aquatic and marshland vegetation from classes *Lemnetea, Potamogetonetea* and *Phragmito-Magnocaricetea*; periodically developed amphibious alliance *Nanocyperion*; meadow association *Arrhenatheretum elatioris* along the flood protection dyke;
4. Čonakut Channel and surrounding area (1 July 2011), size about 35 ha, channels and banks with vegetation from classes *Lemnetea, Potamogetonetea* and *Phragmito-Magnocaricetea;* periodically developed amphibious alliance *Nanocyperion*;
5. Kopačko Lake and surrounding area (12 July 2013, 24 August 2018), size about 200 ha, standing water with aquatic and marshland vegetation from classes *Lemnetea, Potamogetonetea* and *Phragmito-Magnocaricetea*; periodically developed amphibious alliance *Nanocyperion*;
6. Čarna Channel by the road bridge (15 September 2011), size about 1 ha, ruderal vegetation developed by the road;
7. Siget forest complex (10 June 2010, 7 April 2011, 30 September 2011), size about 443 ha, forest communities of pedunculate oak and common hornbeam, association *Carpino betuli-Quercetum roboris*;
8. Tikveš Castle complex and surrounding area (18 April 2011, 16 May 2011, 8 July 2011, 8 May 2012, 25 May 2012, 4 May 2017, 8 May 2018, 1 June 2018), size about 140 ha, forest communities of pedunculate oak and common hornbeam, association *Carpino betuli-Quercetum roboris*, Black walnut (*Juglans nigra*) plantation, meadow association *Arrhenatheretum elatioris*;
9. Melioration canals between settlement Kozjak and Tikveš Castle complex (23 July 2010, 18 August 2010, 18 August 2011, 15 September 2011), size about 8 ha, channels and banks with vegetation from classes *Lemnetea, Potamogetonetea* and *Phragmito-Magnocaricetea*;
10. Area between settlements Tikveš and Kozjak (13 July 2010, 1 July 2011, 10 August 2012, 20 August 2014), size about 40 ha, channels with vegetation from classes *Lemnetea, Potamogetonetea* and *Phragmito-Magnocaricetea*; shrubs from the class *Rhamno-Prunetea* at site of the former pasture;
11. Settlement Tikveš and Čarna Channel (10 August 2012, 23 September 2018), size about 16 ha, channels with vegetation from classes *Lemnetea*, *Potamogetonetea* and *Phragmito-Magnocaricetea* ruderal vegetation developed by the road.

The plant taxa were determined using the standard determination keys and iconographies (Domac 2002, Javorka and Csapody 1991, Knežević 2006, Pignatti 2002, Preston 1995, Rothmaler 2009). Agricultural and strictly ornamental plants have not been part of this research and are not presented in the results. Taxonomy and nomenclature had been adjusted according to the Flora Croatica Database (Nikolić 2018). Literature data on the presence of taxa were taken from the previously published papers and other printed sources.

A complete list of the flora of Kopački rit Nature Park contains taxa arranged in systematic order with families, genera, species and infraspecific taxa arranged alphabetically. Newly recorded taxa are marked with *, and invasive allien plant species with [1)].

Ecological and phytogeographical analyses

The plant life-forms are interpreted according to Raunkier (1937) and Pignatti (2002). The following abbreviations were used to define life forms: Ch – Chamaephyta, G – Geophyta, H – Hemicryptophyta, Hy – Hydrophyta, P – Phanerophyta, T – Therophyta. Chorological elements follow Horvatić (1963), Horvatić et al. (1967-1968) and Pignatti (2002). Floristic elements were described with the following abbreviations: Ce – Central European; Cir-H – Cicrcum-Holarctic; Cosm – Cosmopolites; Cul-ad – Cultivated and adventive; E – European; E-As – Eurasian; Ee-P – East European-Pontic, Med –Mediterranean; S-Eur – South European; Se-E – Southeast European.

Taxa included in the Red Book of Vascular Flora of Croatia (Nikolić and Topić 2005) are indicated by an abbreviation of the IUCN risk category: CR – Critically Endangered, EN – Endangered, VU – Vulnerable, NT – Near Threatened and DD – Data Deficient.

Taxa assigned as strictly protected species in Croatia under the Ordinance on Strictly Protected Species (Anonymous 2013b, 2016), are abbreviated as SP.

Allochthonous flora was determined and analysed according to Mitić et al. (2008), Nikolić et al. (2014) and Flora Croatica Database (Nikolić 2018). Invasive alien plant species and their areas of origin were attributed from Boršić et al. (2008) with abbreviations: AmS – South America, AmN – North America, As – Asia, EA – Eurasia, Am – Americas, M – Mediterranean, C – in culture.

Results

A total of 522 taxa (504 species and 18 subspecies) representing 295 genera and 96 families have been recorded for the vascular flora of Kopački rit Nature Park (Tab. 1). As an achievement of the field investigations, carried out from 2010 to 2018, the floristic diversity increased for additional 114 newly recorded taxa.

Table 1: Floristic list of Kopački rit Nature Park.
Tabela 1: Seznam flore Naravnega park Kopački rit.

List of taxa	Investigated locality	Life form	Floral element	Risk category / Protection statusw
PTERIDOPHYTA				
Azollaceae				
Azolla filiculoides Lam.		Hy	Cul-ad	
Equisetaceae				
Equisetum arvense L.		G	Cir-H	
Equisetum x *moorei* Newman		G	Cir-H	
Equisetum palustre L.		G	Cir-H	
Equisetum telmateia Ehrh.*	3	G	Cir-H	
Marsileaceae				
Marsilea quadrifolia L.		Hy	Cir-H	EN SP
Ophioglossaceae				
Ophioglossum vulgatum L.		G	Cir-H	NT
Salviniaceae				
Salvinia natans (L.) All.		Hy	E	NT SP
Woodsiaceae				
Athyrium filix-femina (L.) Roth*	8	H	Cosm	

List of taxa	Investigated locality	Life form	Floral element	Risk category / Protection statusw
SPERMATOPHYTA MAGNOLIOPHYTINA				
MAGNOLIOPSIDA (DICOTYLEDONAE)				
Aceraceae				
Acer campestre L.		P	E	
Acer negundo L.[I)]		P	Cul-ad	
Acer tataricum L.		P	Se-E	
Amaranthaceae				
Amaranthus retroflexus L.[I)]		T	Cosm	
Apiaceae				
Aegopodium podagraria L.		G	E-As	
Anthriscus sylvestris (L.) Hoffm.		H	E-As	
Chaerophyllum temulum L.		T	E-As	
Conium maculatum L.		H	Cosm	
Daucus carota L.		H	E-As	
Oenanthe aquatica (L.) Poir.		H	E-As	
Orlaya grandiflora (L.) Hoffm.*	8	T	S-Eur	
Pastinaca sativa L.		H	Cosm	
Pimpinella saxifraga L.		H	E-As	
Sanicula europaea L.*	8	H	Cosm	
Sium latifolium L.		Hy	Ce	
Torilis japonica (Houtt.) DC.		T	Cosm	
Trinia glauca (L.) Dumort.		H	Med	
Araliaceae				
Hedera helix L.*	7	P	E	
Aristolochiaceae				
Aristolochia clematitis L.		G	S-Eur	
Asclepiadaceae				
Asclepias syriaca L.[I)]		G	Cul-ad	
Asteraceae				
Achillea millefolium L.		H	Cosm	
Achillea pannonica Scheele		H	Se-E	
Ambrosia artemisiifolia L.[I)]		T	Cul-ad	
Anthemis cotula L.		T	Cosm	
Arctium lappa L.		H	E-As	
Artemisia annua L.		T	E-As	
Artemisia campestris L.		Ch	Cir-H	
Artemisia vulgaris L.		H	Cosm	
Aster novi-belgii L.		H	Cul-ad	
Bellis perennis L.		H	Ce	
Bidens cernuaw L.		T	E-As	
Bidens frondosa L.*[I)]	5	T	Cul-ad	
Bidens tripartita L.		T	E-As	
Carduus acanthoides L.		H	S-Eur	
Carpesium abrotanoides L.		H	E-As	
Carpesium cernuum L.		T	S-Eur	
Centaurea jacea L.		H	Cosm	
Centaurea micranthos S. G. Gmel.		H	Ee-P	
Centaurea rhenana Boreau		H	E	
Chamomilla recutita (L.) Rauschert		T	Cosm	
Chamomilla suaveolens (Pursh) Rydb.[I)]		T	Cosm	

List of taxa	Investigated locality	Life form	Floral element	Risk category / Protection statusw
Cirsium arvense (L.) Scop.		G	E-As	
Cirsium canum (L.) All.		G	Se-E	
Conyza canadensis (L.) Cronquist[I)]		T	Cul-ad	
Erigeron annuus (L.) Pers.[I)]		T	Cul-ad	
Eupatorium cannabinum L.		H	E-As	
Filaginella uliginosa (L.) Opiz		T	E-As	
Galinsoga parviflora Cav.[I)]		T	Cul-ad	
Inula britannica L.		H	E-As	
Inula ensifolia L.		H	Se-E	
Inula salicina L.		H	E-As	
Leucanthemum vulgare Lam.*	8	H	E-As	
Matricaria perforata Mérat*	8	T	E-As	
Pulicaria dysenterica (L.) Bernh.		H	S-Eur	
Pulicaria vulgaris Gaertn.		T	E-As	
Senecio aquaticus Hill		H	E	
Senecio paludosus L.		H	Cir-H	
Serratula tinctoria L.		H	E-As	
Solidago gigantea Aiton[I)]		H	Cul-ad	
Tanacetum vulgare L.		H	E-As	
Tussilago farfara L.		G	E-As	
Xanthium strumarium L. ssp. *italicum* (Moretti) D.Löve*[,I)]	2	T	Med	
Xanthium strumarium L. ssp. *strumarium*		T	Cul-ad	
Balsaminaceae				
Impatiens glandulifera Royle*[,I)]	8	T	Cul-ad	
Impatiens noli-tangere L.		T	E-As	
Impatiens parviflora DC.[I)]		T	Cul-ad	
Betulaceae				
Alnus glutinosa (L.) Gaertner		P	E-As	
Alnus incana (L.) Moench.		P	Cul-ad	
Betula pendula Roth *	7	P	E-As	
Boraginaceae				
Anchusa arvensis (L.) M.Bieb.		T	E-As	
Anchusa officinalis L.		H	E	
Cerinthe minor L.*	10	T	S-Eur	
Cynoglossum officinale L.		H	E-As	
Echium vulgare L.*	10	H	E	
Heliotropium europaeum L.*	11	T	Med	
Lithospermum arvense L.*	10	T	E-As	
Lithospermum officinale L.*	8	H	E-As	
Myosotis arvensis (L.) Hill.		T	E-As	
Myosotis laxa Lehm. ssp. *Caespitosa* (C. F. Schultz) Nordh.		T	Cir-H	
Myosotis ramosissima Rochel		T	E-As	
Myosotis scorpioides L.		H	Cir-H	
Pulmonaria officinalis L.*	8	H	E	
Symphytum officinale L.		H	E	
Symphytum tuberosum L.		G	Ce	
Brassicaceae				
Alliaria petiolata (M. Bieb.) Cavara et Grande*	8	H	E-As	

List of taxa	Investigated locality	Life form	Floral element	Risk category / Protection statusw
Alyssum alyssoides (L.) L.		T	S-Eur	
Arabidopsis thalliana (L.) Heynh.		T	Cosm	
Arabis glabra (L.) Bernhardt		H	Cosm	
Arabis hirsuta (L.) Scop.*	8	H	Cosm	
Brassica napus L.		T	Cul-ad	
Calepina irregularis (Asso) Thell.*	8	T	E	
Capsella bursa-pastoris (L.) Med.		H	Cosm	
Cardamine bulbifera (L.) Crantz*	8	G	E	
Cardamine pratensis L. ssp. *dentata* (Schult.) Čelak		H	Cir-H	
Cardaria draba (L.) Desv		G	Cosm	
Coronopus squamatus (Forssk.) Asch.		T	Cosm	
Descurainia sophia (L.) Webb ex Parntl		T	E-As	
Diplotaxis muralis (L.) DC.		T	Cosm	
Diplotaxis tenuifolia (L.) DC.		H	Cosm	
Lepidium ruderale L.		T	E-As	
Rorippa amphibia (L.) Besser		Hy	E-As	
Rorippa sylvestris (L.) Besser		H	E-As	
Sinapis arvensis L.		T	Cosm	
Sisymbrium officinale (L.) Scop.		T	Cosm	
Thlaspi alliaceum L.*	8	T	S-Eur	
Callitrichaceae				
Callitriche palustris L.		Hy	Cir-H	SP
Campanulaceae				
Campanula patula L. *	8	H	E-As	
Campanula sibirica L.*	11	H	Se-E	
Campanula trachelium L. ssp. *trachelium**	7	H	E-As	DD
Cannabaceae				
Humulus lupulus L.*	2	P	E-As	
Caprifoliaceae				
Sambucus nigra L.		P	Cosm	
Viburnum opulus L.		P	E-As	
Caryophyllaceae				
Agrostemma githago L.*	2	T	Cosm	
Arenaria serpyllifolia L.		T	Cosm	
Cerastium brachypetallum Pers.		T	S-Eur	
Cerastium glomeratum Thuill.		T	Cosm	
Cerastium semidecandrum L.		T	S-Eur	
Lychnis flos-cuculi L.*	8	H	E-As	
Lychnis viscaria L.		H	E-As	
Myosoton aquaticum (L.) Moench.		H	E-As	
Petrorhagia prolifera (L.) P. W. Ball et Heywood		T	E-As	
Silene latifolia Poir. ssp. *alba* (Mill.) Greuter et Bourdet		H	E-As	
Silene otites (L.) Wibel		H	E-As	
Silene vulgaris (Moench) Garcke		H	E-As	
Stellaria media (L.) Vill.		T	Cosm	
Celastraceae				
Euonymus europaeus L.		P	E-As	

List of taxa	Investigated locality	Life form	Floral element	Risk category / Protection statusw
Ceratophyllaceae				
Ceratophyllum demersum L		Hy	Cosm	
Chenopodiaceae				
Chenopodium album L.		T	Cosm	
Chenopodium polyspermum L.		T	Cosm	
Chenopodium rubrum L.		T	Cosm	DD SP
Cichoriaceae				
Cichorium intybus L.		H	Cosm	
Crepis foetida L. ssp. *rhoeadifolia* (M. Bieb.) Čelak.		T	Ee-P	
Hieracium caespitosum Dumort.*	8	H	E-As	
Lactuca serriola L.		H	Cosm	
Mycelis muralis (L.) Dumort.		H	E-As	
Picris hieracioides L.		H	E-As	
Sonchus arvensis L.		H	Cosm	
Sonchus asper (L.) Hill		T	E-As	
Taraxacum officinale Weber		H	Cosm	
Tragopogon pratensis L. ssp. *orientalis* (L.) Čelak.		H	E-As	
Tragopogon pratensis L. ssp. *pratensis*		H	E-As	
Clusiaceae				
Hypericum hirsutum L.		H	Cosm	
Hypericum perforatum L.		H	Cosm	
Convolvulaceae				
Calystegia sepium (L.) R. Br.		H	Cosm	
Convolvulus arvensis L.		G	Cosm	
Cornaceae				
Cornus mas L.		P	S-Eur	
Cornus sanguinea L.		P	E	
Corylaceae				
Carpinus betulus L.		P	Ce	
Corylus avellana L.		P	E	
Cucurbitaceae				
Echinocystis lobata (Michx.) Torr. et Gray[1)]		T	Cul-ad	
Cuscutaceae				
Cuscuta australis R. Br. ssp. *cesatiana** (Bertol.) Feinbrun	4	T	S-Eur	
Dipsacaceae				
Dipsacus fullonum L.		H	S-Eur	
Dipsacus laciniatus L.*	2	H	E-As	
Dipsacus pilosus L		H	E-As	
Scabiosa ochroleuca L		H	E	
Euphorbiaceae				
Euphorbia amygdaloides L.		Ch	Ce	
Euphorbia cyparissias L.		H	E-As	
Euphorbia lucida Waldst. et Kit.*	1	H	Ce	
Euphorbia palustris L.		G	Cosm	
Euphorbia salicifolia Host		H	Ee-P	
Euphorbia virgata Waldst. et Kit.*	1	H	E-As	
Fabaceae				
Amorpha fruticosa L.[1)]		P	Cul-ad	

List of taxa	Investigated locality	Life form	Floral element	Risk category / Protection statusw
Astragalus glycyphyllos L.		H	E-As	
Coronilla varia L.		H	E	
Galega officinalis L.		H	Ee-P	
Lathyrus hirsutus L.*	2	T	S-Eur	
Lathyrus palustris L.*	2	H	Cir-H	DD SP
Lathyrus pratensis L.		H	E-As	
Lathyrus tuberosus L.		H	E-As	
Lotus corniculatus L.		H	Cosm	
Medicago lupulina L.		T	Cosm	
Melilotus albus Medik.		T	E-As	
Melilotus officinalis (L.) Lam.		H	E-As	
Ononis arvensis L.		Ch	E-As	
Ononis spinosa L.		Ch	E	
Robinia pseudoacacia L.[1)]		P	Cul-ad	
Trifolium campestre Schreber		T	Cosm	
Trifolium hybridum L.		H	S-Eur	
Trifolium patens Schreb.*	8	T	S-Eur	
Trifolium pratense L.		H	E-As	
Trifolium repens L.		H	Cosm	
Vicia angustifolia L.		T	E	
Vicia grandiflora Scop.		H	Ee-P	
Vicia sativa L.		T	Cosm	
Fagaceae				
Quercus cerris L.		P	S-Eur	
Quercus robur L.		P	E	
Fumariaceae				
Corydalis intermedia (L.) Mérat*	8	G	Ce	
Gentianaceae				
Centaurium pulchellum (Sw.) Druce		T	E-As	
Gentiana pneumonanthe L.*	1	H	E-As	EN SP
Geraniaceae				
Erodium cicutarium (L.) L' Her.		T	Cosm	
Geranium dissectum L.*	1	T	Cosm	
Geranium molle L.*	7	T	Cosm	
Geranium robertianum L.		T	Cosm	
Haloragaceae				
Myriophyllum spicatum L.		Hy	Cosm	
Myriophyllum verticillatum L.		Hy	Cir-H	
Hippuridaceae				
Hippuris vulgaris L.		Hy	Cir-H	EN SP
Juglandaceae				
Juglans nigra L.		P	Cul-ad	
Juglans regia L.*	8	P	Cul-ad	
Lamiaceae				
Ajuga genevensis L.*	8	H	E-As	
Ajuga reptans L.		H	E-As	
Ballota nigra L.		H	E	
Calamintha sylvatica Bromf.		H	E	
Clinopodium vulgare L.		H	Cosm	
Galeopsis speciosa Mill.		T	E	
Galeopsis tetrahit L.		T	E-As	

List of taxa	Investigated locality	Life form	Floral element	Risk category / Protection statusw
Glechoma hederacea L.		H	Cir-H	
Glechoma hirsuta Waldst. et Kit.		H	S-Eur	
Lamium amplexicaule L.*	7	T	E-As	
Lamium maculatum L.		H	E-As	
Lamium purpureum L.		T	E-As	
Leonurus cardiaca L.		H	E-As	
Leonurus marrubiastrum L.		H	E-As	
Lycopus europaeus L.		H	E-As	
Mentha aquatica L.		H	Cosm	
Mentha arvensis L.		H	Cir-H	
Mentha longifolia (L.) Huds.		H	Cosm	
Mentha piperita L.		H	Cosm	
Mentha pulegium L.		H	E-As	
Mentha x *verticillata* L.		H	E	
Nepeta cataria L.*	10	H	Cosm	
Prunella laciniata (L.) L.		H	S-Eur	
Prunella vulgaris L.		H	Cosm	
Salvia glutinosa L.*	7	H	E-As	
Salvia nemorosa L.*	3	H	Ee-P	EN SP
Salvia pratensis L.*	8	H	E	
Scutellaria galericulata L.		G	Cir-H	
Scutellaria hastifolia L.		G	Se-E	
Stachys palustris L.		H	Cir-H	
Stachys recta L.*	8	G	S-Eur	
Stachys sylvatica L.*	7	H	E-As	
Teucrium scordium L.		H	E	
Thymus pulegioides L.		Ch	S-Eur	
Lentibulariaceae				
Utricularia vulgaris L.		Hy	Cir-H	SP
Loranthaceae				
Loranthus europaeus Jacq.		P	E-As	
Lythraceae				
Lythrum hyssopifolia L.		T	Cosm	
Lythrum salicaria L.		H	Cosm	
Malvaceae				
Abutilon theophrasti Medik.[1)]		T	Cosm	
Althaea officinalis L.		H	Cosm	
Hibiscus trionum L.*	6	T	S-Eur	EN SP
Lavatera thuringiaca L.*	6	H	E-As	
Malva sylvestris L.		P	Ce	
Menyanthaceae				
Nymphoides peltata (S. G. Gmelin) Kuntze		Hy	E-As	
Moraceae				
Morus alba L.		P	Cul-ad	
Morus nigra L.		P	Cul-ad	
Nymphaeaceae				
Nuphar lutea Sibth. et Sm.		Hy	E-As	
Nymphaea alba L.		Hy	E-As	
Oleaceae				
Fraxinus americana L.		P	Cul-ad	
Fraxinus angustifolia Vahl		P	S-Eur	

List of taxa	Investigated locality	Life form	Floral element	Risk category / Protection statusw
Fraxinus pennsylvanica Marshall		P	Cul-ad	
Ligustrum vulgare L.		P	Ce	
Onagraceae				
Circaea lutetiana L.		H	Cosm	
Epilobium parviflorum Schreber*	3	H	E-As	
Oxalidaceae				
Oxalis acetosella L.		G	Cosm	
Oxalis fontana Bunge		H	Cul-ad	
Papaveraceae				
Chelidonium majus L.		Hy	Cosm	
Papaver dubium L.*	2	T	Cosm	
Papaver rhoeas L.		T	Cosm	
Phytolaccaceae				
Phytolacca americana L.[1)]		G	Cul-ad	
Plantaginaceae				
Littorella uniflora (L.) Asch.*	5	Hy	E-As	DD SP
Plantago altissima L.		H	S-Eur	
Plantago lanceolata L.		H	Cosm	
Plantago major L. ssp. *intermedia* (Gilib.) Lange		H	E-As	
Plantago major L. ssp. *major*		H	Cosm	
Polygalaceae				
Polygala comosa Schkuhr*	8	H	E-As	
Polygonaceae				
Polygonum amphibium L.		G	Cosm	
Polygonum arenastrum Boreau*	6	T	Cosm	
Polygonum aviculare L.*	9	T	Cosm	
Polygonum hydropiper L.		T	Cir-H	
Polygonum lapathifolium L.*	2	T	Cosm	
Polygonum minus Hudson		T	Cosm	
Polygonum mite Schrank		T	E	
Polygonum persicaria L.		T	Cosm	
Reynoutria japonica Houtt.[1)]		G	Cul-ad	
Rumex conglomeratus Murray		H	Cosm	
Rumex crispus L.		H	Cosm	
Rumex hydrolapathum Hudson		Hy	E	
Rumex maritimus L.		T	E-As	DD SP
Rumex obtusifolius L.		H	Cosm	
Rumex palustris Sm.		T	E-As	
Portulacaceae				
Portulaca oleracea L.*	6	T	Cosm	
Primulaceae				
Anagallis arvensis L.*	8	T	Cosm	
Hottonia palustris L.		Hy	E-As	EN SP
Lysimachia nummularia L.		H	E	
Lysimachia vulgaris L.		H	E-As	
Primula vulgaris Huds.		H	S-Eur	
Ranunculaceae				
Caltha palustris L.*	8	H	Cosm	
Clematis vitalba L.		P	E	
Consolida regalis S. F. Gray*	9	T	S-Eur	

List of taxa	Investigated locality	Life form	Floral element	Risk category / Protection statusw
Ranunculus acris L.		H	Cosm	
Ranunculus aquatilis L.		Hy	Cosm	
Ranunculus auricomus L.		H	E-As	
Ranunculus circinatus Sibth.		Hy	E-As	
Ranunculus ficaria L.		G	E	
Ranunculus flammula L.		H	E-As	
Ranunculus repens L.		H	Cosm	
Ranunculus sardous Crantz*	9	T	Cosm	
Ranunculus sceleratus L.		T	E-As	
Ranunculus trichophyllus Chaix in Vill.		Hy	E	
Thalictrum lucidum L.		H	E	
Resedaceae				
Reseda lutea L.		H	Cosm	
Rhamnaceae				
Frangula alnus Mill.		P	Ce	
Rhamnus catharticus L.*	7	P	E-As	
Rosaceae				
Agrimonia eupatoria L.		H	Cir-H	
Crataegus monogyna Jacq.		P	Ce	
Crataegus nigra Waldst. et Kit.		P	Ee-P	
Crataegus pentagyna Waldst. et Kit. ex Willd.		P	Ee-P	
Fragaria vesca L.		H	Cosm	
Geum urbanum L.*	7	H	Cosm	
Malus sylvestris Mill.*	7	P	Ce	
Potentilla anserina L.		H	Cosm	
Potentilla reptans L.		H	Med	
Potentilla supina L.		T	Cosm	
Prunus avium L.		P	E-As	
Pyrus pyraster (L.) Burgsd.*	10	P	E-As	
Rosa canina L.*	2	P	Cosm	
Rubus caesius L.		P	E-As	
Rubus plicatus Weihe et Nees		P	Ce	
Rubiaceae				
Cruciata glabra (L.) Ehrend.		H	E-As	
Cruciata laevipes Opiz		H	E-As	
Galium album Mill.		H	E-As	
Galium aparine L.*	2	T	Cosm	
Galium mollugo L.		H	E-As	
Galium odoratum (L.) Scop.*	7	G	E-As	
Galium palustre L.		H	E-As	
Galium verum L.		H	Cosm	
Salicaceae				
Populus alba L.		P	E-As	
Populus x canadensis Moench*	6	P	Cul-ad	
Populus nigra L.		P	E-As	
Salix alba L.		P	E-As	
Salix caprea L.		P	E-As	
Salix fragilis L.		P	E-As	
Salix purpurea L.		P	E-As	
Salix triandra L.		P	E-As	

List of taxa	Investigated locality	Life form	Floral element	Risk category / Protection statusw
Santalaceae				
Viscum album L.		P	E-As	
Scrophulariaceae				
Gratiola officinalis L.		H	Cosm	
Kickxia elatine (L.) Dumort. ssp. *elatine*		T	S-Eur	DD
Lathraea squamaria L.*	8	G	E-As	
Limosella aquatica L.		T	Cir-H	CR SP
Linaria genistifolia (L.) Mill.		H	E-As	
Linaria vulgaris Mill.		H	E-As	
Lindernia procumbens (Krock.) Philcox		T	E-As	VU SP
Odontites vernus (Bellardi) Dumort.*	10	T	E-As	
Pseudolysimachion longifolium (L.) Opiz		H	E-As	EN SP
Scrophularia nodosa L.		H	Cir-H	
Verbascum blattaria L.		H	Cosm	
Verbascum nigrum L.		H	E	
Verbascum phlomoides L.		H	E	
Veronica anagallis-aquatica L.		H	E	
Veronica austriaca L.		H	Ee-P	
Veronica catenata Pennell*	5	Hy	Cir-H	
Veronica chamaedrys L.		H	E-As	
Veronica hederifolia L.		T	E-As	
Veronica peregrina L.		T	Cul-ad	
Veronica persica Poir.[1)]		T	Cosm	
Veronica scutellata L.		H	E	
Veronica serpyllifolia L.*	8	H	Cosm	
Veronica teucrium L.		H	E-As	
Simaroubaceae				
Ailanthus altissima (Mill.) Swingle*[,1)]	2	P	Cul-ad	
Solanaceae				
Datura stramonium L.[1)]		T	Cosm	
Physalis alkekengi L.		H	E	
Solanum dulcamara L.		P	Cosm	
Solanum nigrum L.		T	Cosm	
Tiliaceae				
Tilia cordata Mill.*	7	P	E	
Tilia platyphyllos Scop.*	7	P	E	
Trapaceae				
Trapa natans L.		Hy	Cosm	NT SP
Ulmaceae				
Ulmus laevis Pall.		P	Ce	
Ulmus minor Miller		P	E	
Urticaceae				
Parietaria officinalis L.		H	S-Eur	
Urtica dioica L.		H	Cosm	
Urtica kioviensis Rogow.		H	E	
Valerianaceae				
Valeriana officinalis L.*	3	H	E-As	
Valerianella locusta (L.) Laterrade		T	Med	
Verbenaceae				
Verbena officinalis L.		H	Cosm	
Violaceae				
Viola alba Besser		H	S-Eur	

List of taxa	Investigated locality	Life form	Floral element	Risk category / Protection statusw
Viola arvensis Murray*	7	T	Cosm	
Viola elatior Fr.*	8	H	E-As	
Viola hirta L.		H	E-As	
Viola odorata L.		H	E	
Viola reichenbachiana Jord. ex Boreau		H	E-As	
Viola tricolor L.		T	Cul-ad	
Vitaceae				
Vitis vinifera L. ssp. *sylvestris* (C. C. Gmel) Hegi*	2	P	Cul-ad	
LILIOPSIDA (MONOCOTYLEDONAE)				
Acoraceae				
Acorus calamus L.		Hy	Cul-ad	
Alismataceae				
Alisma gramineum Lej.		Hy	E-As	EN SP
Alisma lanceolatum With.		Hy	Cosm	
Alisma plantago-aquatica L.		Hy	Cosm	
Sagittaria sagittifolia L.		Hy	E-As	
Amaryllidaceae				
Allium angulosum L.*	1	G	E-As	EN SP
Allium scorodoprasum L.		G	Ee-P	
Allium vineale L.*	8	G	Cosm	
Leucojum aestivum L.		G	E	
Asparagaceae				
Asparagus officinalis L.*	8	G	Cul-ad	
Convallaria majalis L.		G	Cir-H	
Muscari botryoides (L.) Mill.*	8	G	S-Eur	
Scilla bifolia L.		G	S-Eur	
Butomaceae				
Butomus umbellatus L.		Hy	E-As	NT
Colchicaceae				
Colchicum autumnale L.*	8	G	Ce	
Cyperaceae				
Bolboschoenus maritimus (L.) Palla*	9	Hy	Cosm	NT
Carex acuta L.		Hy	E-As	
Carex acutiformis Ehrh.		Hy	E-As	NT
Carex bohemica Schreb.		H	Cir-H	CR SP
Carex digitata L.		H	E-As	
Carex distans L.		H	E	
Carex divulsa Stokes		H	Cosm	
Carex elata All.		Hy	E	
Carex flacca Schreb.*	9	G	Cosm	
Carex hirta L.		G	E-As	
Carex nigra (L.) Reichard		G	Cosm	EN SP
Carex pendula Huds.		H	E-As	
Carex remota L.		H	E	
Carex riparia Curt.		G	E-As	VU SP
Carex spicata Huds.		H	E-As	
Carex sylvatica Huds.		H	E	
Carex vesicaria L.		G	Cir-H	VU SP
Carex vulpina L.		H	E	

List of taxa	Investigated locality	Life form	Floral element	Risk category / Protection statusw
Cyperus flavescens L.		T	Cosm	VU SP
Cyperus fuscus L.		T	E-As	VU SP
Cyperus glomeratus L.*	3	T	E-As	VU SP
Cyperus longus L.		Hy	Cosm	VU SP
Cyperus michelianus (L.) Link		T	E-As	VU SP
Eleocharis acicularis (L.) Roem. et Schult.		G	Cosm	
Eleocharis ovata (Roth) Roem. et Schult.		T	Cir-H	EN SP
Eleocharis palustris (L.) Roem. et Schult.		G	Cosm	
Scirpus lacustris L. ssp. *lacustris*		Hy	Cosm	
Scirpus mucronatus L.*	2	Hy	Cosm	CR SP
Scirpus pendulus Muhl.*	10	Hy	Cul-ad	
Scirpus supinus L.		T	Cosm	CR SP
Hydrocharitaceae				
Elodea canadensis Michx.*, [1)]	9	Hy	Cul-ad	
Elodea nuttallii (Planch.) H.St.John		Hy	Cul-ad	
Hydrocharis morsus-ranae L.		Hy	E-As	
Stratiotes aloides L.*	2	Hy	E-As	VU SP
Iridaceae				
Iris pseudacorus L.		G	E-As	SP
Iris sibirica L. ssp. *sibirica**	1	G	E-As	VU SP
Juncaceae				
Juncus articulatus L		G	Cir-H	
Juncus bufonius L.		T	Cosm	
Juncus compressus Jacq.		G	Cosm	
Juncus effusus L.w		H	E-As	
Juncus inflexus L.		H	E-As	
Juncus tenuis Willd.[1)]		H	Cosm	
Lemnaceae				
Lemna gibba L.	11	Hy	Cosm	EN SP
Lemna minor L.		Hy	Cosm	
Lemna minuta Kunth*	11	Hy	Cosm	
Lemna trisulca L.		Hy	Cosm	
Spirodela polyrhiza (L.) Schleiden		Hy	Cosm	
Wolffia arrhiza (L.) Horkel ex Wimm.		Hy	Cosm	VU SP
Liliaceae				
Fritillaria meleagris L.*	8	G	Med	VU SP
Najadaceae				
Najas marina L.		Hy	Cosm	
Najas minor All.		Hy	E-As	
Orchidaceae				
Anacamptis pyramidalis (L.) Rich.*	3	G	E	NT SP
Cephalanthera damasonium (Mill.) Druce		G	S-Eur	NT SP
Dactylorhiza incarnata (L.) Soó* ssp. *incarnata*	10	G	E-As	EN SP
Epipactis helleborine (L.) Crantz*	8	G	E-As	SP
Listera ovata (L.) R.Br.*	7	G	E-As	SP
Orchis laxiflora Lam. ssp. *palustris* (Jacq.) Bonnier et Layens		G	E	DD SP
Orchis purpurea Huds.*	8	G	E-As	VU SP

List of taxa	Investigated locality	Life form	Floral element	Risk category / Protection statusw
Platanthera bifolia (L.) Rich.*	8	G	E-As	VU SP
Platanthera chlorantha (Custer) Rchb.*	8	G	E-As	NT SP
Poaceae				
Agrostis stolonifera L.		H	Cir-H	
Alopecurus aequalis Sobol.		H	E	VU SP
Alopecurus geniculatus L.*	3	H	Cosm	VU SP
Alopecurus pratensis L.		H	E-As	
Dichanthium ischaemum (L.) Roberty		H	S-Eur	SP
Brachypodium sylvaticum (Huds.) P. Beauv.		H	E-As	
Bromus japonicus Thunb.		T	E-As	
Bromus squarossus L.		T	S-Eur	
Bromus sterillis L.		T	Cosm	
Calamagrostis epigejos (L.) Roth.		H	E	
Cynodon dactylon (L.) Pers.		G	Cosm	
Cynosurus cristatus L.		H	E	
Dactylis glomerata L.		H	E-As	
Echinochloa crus-galli (L.) P. Beauv.		T	Cosm	
Eleusine indica (L.) Gaertn*[,I)]	11	T	Cul-ad	
Elymus caninus (L.) L.		G	E-As	
Elymus hispidus (Opiz) Melderis		G	S-Eur	
Elymus repens (L.) Gould*	10	G	Cosm	
Festuca ovina L.		H	E	
Festuca pratensis Huds.*	8	H	Cosm	
Festuca rubra L.		H	Cir-H	
Glyceria fluitans (L.) R.Br.		Hy	Cosm	VU SP
Glyceria maxima (Hartm.) Holmb.		Hy	E-As	
Holcus lanatus L.		H	E-As	
Hordeum murinum L.		T	Cir-H	
Koeleria macrantha (Ledeb.) Schult.		H	E-As	
Koeleria pyramidata (Lam.) P. Beauv.		H	E	
Lolium perenne L.*	8	H	E	
Panicum capillare L.*[,I)]	3	T	Cul-ad	
Phalaris arundinacea L.		G	Cir-H	
Phleum paniculatum Huds.		T	Med	SP
Phragmites australis (Cav.) Trin. ex Steud.		Hy	Cosm	
Poa annua L.		T	Cosm	
Poa bulbosa L.		H	E-As	
Poa palustris L.		H	Cir-H	NT
Poa pratensis L.		H	Cosm	
Poa trivialis L.		H	E-As	
Sclerochloa dura (L.) P.Beauv		T	Med	
Setaria pumila (Poir.) Schult.		T	Cosm	
Setaria viridis (L.) P.Beauv.		T	E-As	
Potamogetonaceae				
Potamogeton coloratus Hornem.*	5	Hy	E	
Potamogeton crispus L.		Hy	Cosm	
Potamogeton gramineus L.		Hy	Cir-H	
Potamogeton lucens L.		Hy	Cir-H	
Potamogeton natans L.*	2	Hy	Cosm	
Potamogeton nodosus Poir.*	10	Hy	Cosm	

List of taxa	Investigated locality	Life form	Floral element	Risk category / Protection statusw
Potamogeton perfoliatus L.		Hy	Cosm	
Potamogeton pusillus L.		Hy	Cosm	
Potamogeton trichoides Cham. et Schltdl.		Hy	E-As	
Stuckenia pectinata (L.) Börner*	5	Hy	Cosm	
Sparganiaceae				
Sparganium erectum L.		Hy	E-As	
Sparganium erectum L. ssp. *neglectum* (Beeby) Schinz et Thell.		Hy	E-As	
Sparganium minimum Wallr.		Hy	E-As	DD
Typhaceae				
Typha angustifolia L.		G	Cir-H	
Typha latifolia L.		G	Cosm	
Typha laxmannii Lepech.		G	E-As	CR SP
Typha minima Funck		G	E-As	CR SP

From the taxonomic viewpoint, nine taxa (1.7%) belonged to ferns, while angiosperms were represented by 513 taxa: 381 (72.9%) belongs to dicotyledons and 132 (25.3%) to monocotyledons (Tab. 2).

Table 2: Taxonomic analyses of the flora of Kopački rit Nature Park.
Tabela 2: Taksonomske analize flore Naravnega parka Kopački rit.

Taxonomic category	Species and subspecies	Genus	Family
Pteridophyta	9	6	6
Magnoliopsida (Dicotyledonae)	381	226	72
Liliopsida (Monocotyledonae)	132	63	18
Total	522	295	96

The most diverse genera were: *Carex* (17 taxa), *Ranunculus* and *Veronica* (10 taxa each), *Potamogeton* (9), *Polygonum* (8) and *Viola* (7 taxa). The most frequent families were: Asteraceae (43 taxa), Poaceae (40), Lamiaceae (34), Cyperaceae (30), Fabaceae and Scrophulariaceae (23 taxa each).

Life-form analysis (Fig. 2a) showed that hemicryptophytes (39.3%) were dominant, followed by therophytes (23.8%), geophytes (12.6%), hydrophytes (12.5%) and phanerophytes (10.9%).

Phytogeographical analysis (Fig. 2b), showed the prevalence of Eurasian floral element (32.8%), followed by Cosmopolites (27.4%) and European floral element (10.7%).

Allochthonous flora was represented with 53 taxa (10.2% of the total flora) of which 12 (22.6%) were archaeophytes and 41 (77.4%) neophytes. The most of these taxa (22) have the North American origin, followed by 12 taxa of Asian origin (Fig. 3). Invasive alien plant species are represented by 26 taxa, which makes about 5% of the total flora.

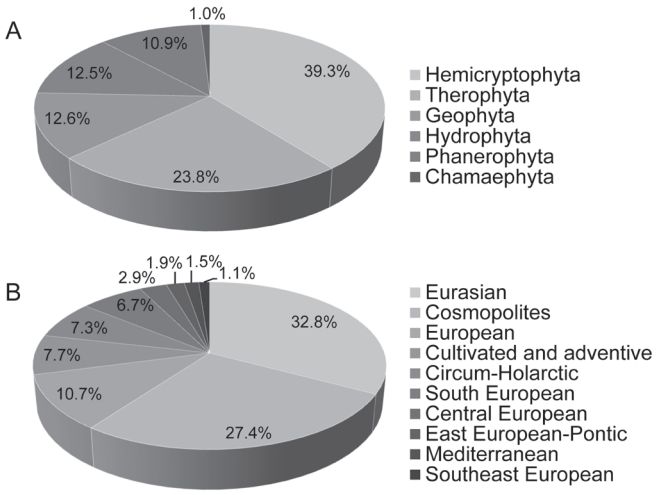

Figure 2: Life-form (A) and chorological spectrum (B) of the flora of Kopački rit Nature Park.
Slika 2: Življenjska oblika (A) in horološki spekter (B) flore Naravnega parka Kopački rit.

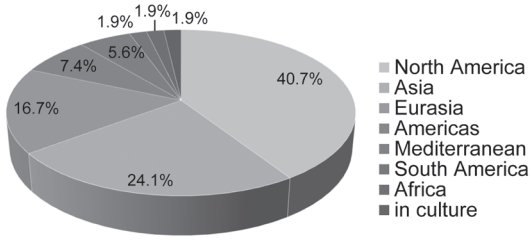

Figure 3: The ratio of geographical origin of allochthonous plants of Kopački rit Nature Park.
Slika 3: Delež geografskega izvora alohtonih rastlin Naravnega parka Kopački rit.

According to risk status assigned in the Red Book of Vascular Flora of Croatia (Nikolić and Topić 2005), 55 taxa (10.5% of the total flora) belongs to the following categories: critically endangered (6 taxa), endangered (13), vulnerable (17), near threatened (10), and 9 taxa as data deficient. Status of strictly protected species at the national level (Anonymous 2013b, 2016) was assigned to 53 taxa (10.2% of the total flora).

One species, *Marsilea quadrifolia* is listed in Annex II of the European Union Habitat Directive (Anonymous 1992, 2013c).

Discussion

The vascular plant diversity of Kopački rit Nature Park makes 10.4% of the total 5,034 taxa (species and subspecies) recorded for the vascular flora of Croatia (Nikolić 2018).

The floristic diversity of Kopački rit Nature Park is compared to that reported for selected protected areas in the Danube River basin (Tab. 3).

Biological spectrum confirms the phytogeographical position in the Pannonian sector of Central European Province, with hemicryptophytes indicating high plant resistance to the winter cold and adaptation to the moderate climate (Ellenberg 1988). For the comparison, therophytes (38.0%)

and hemicryptophytes (33.0%) are dominant in the Danube Delta, due to transitional position of this region, eastern of the Danubial Province and western of the Pontic Province (Ciocârlan 2011). A higher portion of therophytes (23.8%) indicates warm, and periodically dry climate conditions, as well as an impact of the human disturbance, because this life-form is usual in anthropogenic habitats (Dobrović et al. 2006). The agricultural land under intensive crop production (oilseed rape, wheat, barley, corn, sugar beet, sunflower and soybean) dominates in Baranja region (Kovačić et al. 2016) and cropland surrounds the western border of the Park. Percentage of hydrophytes (12.5%) is higher than 4% confirmed for the Baranja region (Panjković 1990).

This reflects the ecological features of Kopački rit as a large fluvial-marshy floodplain where an occurrence and spatial distribution of terrestrial, wetland and aquatic vegetation depends on the frequency, intensity and duration of floods, and drought periods.

The dominance of Eurasian floral element (32.8%) corresponds to 31.0% for the Baranja region (Panjković 1990) and 28.0% for the Danube Delta (Ciocârlan 2011).

The percentage of cosmopolites (27.4%) is much higher than in the Baranja region (6.2%), and the Danube Delta (8.3%). Oppositely, the percentage of the Central European floral element is much higher in the Baranja region (20.9%) than in Kopački rit Nature Park (2.9%). Percentage of European floral element is higher in the Danube Delta (14.0%).

The allochthonous flora includes 53 taxa, which makes 8.5% of 624 taxa registered for the allochthonous flora of Croatia. Invasive alien plants count 26 taxa or 34.7% of 75 taxa registered in the Croatian flora (Nikolić 2018). The presence of alien plants is higher (13.4%) in Donau-Auen National Park (Drescher and Magnes 2002), and lower (3.1%) in Special Nature Reserve Gornje Podunavlje (Panjković and Stojšić 2001), and Danube Delta Biosphere Reserve with 5.4% (Mihai et al. 2011). The richer allochthonous flora shows disturbance intensity caused by anthropogenic activities.

Wet meadows from the vegetation alliance *Cnidion dubii* are still present in the area of Kopački rit Nature Park, but under the high risk of extinction. This was confirmed by recording the presence of taxa: *Allium angulosum*, *Euphorbia lucida, Gentiana pneumonanthae*, *Iris sibirica* ssp. *sibirica* and *Pseudolysimachion longifolium*, as diagnostic species for this habitat type listed in Annex I of the EU Habitats Directive under the code: 6440 Alluvial meadows of river valleys of the *Cnidion dubii* (Anonymous 1992, 2013c).

Knowledge on the diversity of orchid family (*Orchidaceae*) expands from two previously re-

Table 3: A comparison of the floristic diversity between Kopački rit Nature Park and selected protected areas in the Danube catchment area.
Tabela 3: Primerjava florne raznovrstnosti Naravnega parka Kopački rit z izbranimi zavarovanimi območji v Donavskem porečju.

Protected area (Country)	Number of taxa	Reference
Kopački rit Nature Park (Croatia)	522	
Lonjsko Polje Nature Park (Croatia)	550	Gugić (2008)
Donau-Auen National Park (Croatia)	838	Drescher and Magnes (2002)
Gornje Podunavlje Special Nature Reserve (Serbia)	1,000	Panjković et al. (2000)
Đerdap National Park (Serbia)	1,013	Petrić et al. (2010)
Rusenski Lom Nature Park (Bulgaria)	877	Stoyanov (2005)
Danube Delta (Romania)	985	Ciocârlan (2011)
Danube Delta Biosphere Reserve (Romania)	1,215	Mihai et al. (2011)

ported taxa (*Cephalanthera damasonium*, *Orchis laxiflora* ssp. *palustris*) to currently known nine taxa. During the field surveys, following seven taxa were discovered: *Anacamptys pyramidalis*, *Dactylorhiza incarnata* ssp. *incarnata*, *Epipactis helleborine*, *Listera ovata*, *Orchis purpurea*, *Platanthera bifolia* and *Platanthera chlorantha*. All taxa of the *Orchidaceae* are strictly protected species in Croatia.

The macrophyte diversity in Kopački rit Nature Park comprises 158 taxa (30.3% of the total flora), which exceeds the number of only seven taxa recorded in the Danube main channel, and 37 taxa recorded in water bodies along the right bank in the Croatian reach of the Danube River (Ozimec and Topić 2018).

Stressors and threats to the flora of Kopački rit Nature Park are natural and anthropogenic. In recent decades, more frequent fluctuations in flooding intensity of the Danube River, and extension of a dry season affects to reduction in size of the inundated area. Accumulation of suspended solids and sediment in sidearms and channels disrupt hydrological connection and initiate the natural succession processes. Abandoned land, as well as habitats overgrown with shrubs or herbaceous ruderal vegetation under the natural succession, supports the colonisation and dispersal of the invasive alien plant species, which can threaten the native flora. Stressors such as air, soil and water pollutants, pests and pathogens, invasive species, fire, storms, land management and visitor use have a harmful impact at some point on plants and their habitats.

Conclusions

1. The diversity of vascular plants in Kopački rit Nature Park, with 522 currently known taxa, confirms significant ecological values of this floodplain area situated in the middle course of the Danube River.
2. The flora is characterised by high percentage of hemicryptophytes and therophytes, as well as of Eurasian floral element and Cosmopolites.
3. Regarding the plant conservation, 53 taxa have a status of strictly protected species, and 55 taxa are included in the Red Book of Vascular Flora of Croatia.
4. Allochthonous flora is represented with 53 taxa, among which 26 are invasive alien plant species.
5. Comprehensive knowledge on plant diversity is an important tool for planning and implementation of activities in conservation of rare and threatened plants and their habitats in Kopački rit Nature Park.

Povzetek

Naravni park Kopački rit se nahaja v severovzhodni Hrvaški, na območju sotočja Donave in reke Drave. Park pokriva območje 231 km^2 in se nahaja na nadmorski višino od 78 do 86 m. Glede na fitogeografsko razdelitev sodi območje v evrosibirsko-severnoameriško regijo, panonski sektor srednjeevropske province. Zaradi izjemne biološke in ekološke vrednosti tega poplavnega območja v srednjem toku reke Donave, je območje od leta 1967 zaščiteno. Floristične študije na območju Naravnega parka Kopački rit so bile v preteklosti razdrobljene. V prispevku so zbrani literaturni podatki in rezultati terenskih raziskav, ki so bile izvedene v obdobju od leta 2010 do leta 2018. V Naravnem parku Kopački rit je bilo ugotovljenih 522 taksonov vaskularnih rastlin, kar potrjuje ekološko vrednost tega poplavnega območja, ki se nahaja v srednjem toku reke Donave. Za floro je značilen visok odstotek hemikriptofitov in terofitov, ter evrazijskih flornih elementov in kozmopolitov. Kar 53 taksonov ima status strogo zaščitenih vrst, 55 pa jih je vključenih na Rdeči seznam flore Hrvaške. Tujerodne rastline so zastopane s 53 taksoni, med katerimi je 26 invazivnih tujerodnih rastlinskih vrst. V Naravnem parku Kopački rit so prisotni številni naravni in antropogeni pritiski. V zadnjih desetletjih so pogoste spemembe vodostajev reka Donave in podaljševanje suhe sezone kar vpliva na zmanjšanje obsega poplavljene površine. Kopičenje usedlin v stranskih rokavih in kanalih moti hidrološko povezavo med različnimi predeli kar pospešuje sukcesijske procese. Opuščena

zemljišča ter habitati poraščeni z grmovjem ali zeliščno ruderalno vegetacijo, podpirajo kolonizacijo in razširjanje invazivnih tujerodnih rastlinskih vrst, ki lahko ogrozijo domačo floro. Predstavljeni izsledki predstavljajo pomembno izhodišče za načrtovanje in izvajanje dejavnosti ohranjanja redkih in ogroženih rastlin ter njihovih habitatov v Naravnem parku Kopački rit in drugih podobnih območjih.

Acknowledgements

Management and staff from the Public Institution Kopački rit Nature Park supported research and provided technical assistance for the field activities.

References

Anonymous, 1992. Council Directive 92/43/EEC of 21 May 1992 on the Conservation of Natural Habitats and of Wild Fauna and Flora. Official Journal of the European Communities L 206, 35.

Anonymous, 1999. Zakon o Parku prirode „Kopački rit“. Narodne novine, 45.

Anonymous, 2006. Odluka o donošenju Prostornog plana Parka prirode „Kopački rit“. Narodne novine, 24.

Anonymous, 2013a. Uredba o ekološkoj mreži. Narodne novine, 124.

Anonymous, 2013b. Pravilnik o strogo zaštićenim vrstama. Narodne novine, 144.

Anonymous, 2013c. Council Directive 2013/17/EU of 13 May 2013 Adapting Certain Directives in the Field of Environment by Reason of the Accession of the Republic of Croatia. Official Journal of the European Union L 158, 56.

Anonymous, 2015. Uredba o izmjenama i dopunama Uredbe o ekološkoj mreži. Narodne novine, 105.

Anonymous, 2016. Pravilnik o izmjenama Pravilnika o strogo zaštićenim vrstama. Narodne novine, 73.

Balátová-Tuláčková, E., Knežević, M., 1975. Beitrag zur Kenntnis der Überschwemmungswiesen in der Drava- und Karašica-Aue (Nord-Jugoslawien). Acta Botanica Croatica 34(1), 63-80.

Bognar, A., 1990. Geomorfologija Baranje. Savez geografskih društava Hrvatske, Zagreb, 312 pp.

Boros, A., 1944a. A lápi csalán (Urtica kioviensis) a Drávaközben. Albertina 1, 113-122.

Boros, A., 1944b. A Veronica peregrina úabb magayroszági előfordulása. Botanikai Közlemények 41(3-5), 154.

Boros, A., 1946. A Kopácsi ártér növényvilága nagyvízálláskor. Botanikai Közlemények 43(1), 21-24.

Boršić, I., Milović, M., Dujmović, I., Bogdanović, S., Cigić, P., Rešetnik, I., Nikolić, T., Mitić, B., 2008. Preliminary check-list of invasive alien plant species (IAS) in Croatia. Natura Croatica 17(2), 55-71.

Ciocârlan, V., 2011. Vascular flora of the Danube Delta. Analele ştiinţifice ale Universităţii „Aexandru Ioan Cuza” Iaşi 57(1), 41-64.

Cvitan, L., 2014. Početne naznake o prostornoj raznolikosti klime šireg područja Parka prirode „Kopački rit“. Hrvatski meteorološki časopis 48/49, 63-91.

Domac, R., 2002. Flora Hrvatske. Priručnik za određivanje bilja. Školska knjiga, Zagreb, pp. 504.

Dobrović, I. Nikolić, T., Jelaska S.D., Plazibat, M., Hršak, V., Šoštarić, R., 2006. An evaluation of floristic diversity in Medvednica Nature Park (northwestern Croatia). Plant Biosystems 140(3), 234-244

Drescher, A., Magnes, M., 2002. Antropochoren im Nationalpark Donau-Auen – Ziel von Bekämpfungsmaßnahmen oder Bereicherung der Biodiversität? 10. Österreichisches Botanikertreffen, BAL Gumpenstein, Tagungsbd 141-144.

Ellenberg, H., 1988. Vegetation Ecology of Central Europe (4th Edition). Cambridge University Press, Cambridge, 731 pp.

Gugić, G., (ed.), 2008. Park prirode Lonjsko polje, živući krajobraz i poplavni ekosustav Srednje Posavine, Plan upravljanja. Bilten Parka prirode Lonjsko Polje 10(1), 1-161.

Horvatić, S., 1963. Vegetacijska karta otoka Paga s općim pregledom vegetacijskih jedinica Hrvatskog primorja. Prirodoslovna istraživanja 33, Jugoslavenska akademija znanosti i umjetnosti, Zagreb, 187 pp.

Horvatić, S., Ilijanić, Lj., Marković-Gospodarić, Lj., 1967–1968. Biljni pokrov okolice Senja. Senjski zbornik 3, 298-322.

Ilijanić, Lj., 1968. Die Ordnung Molinietalia in der Vegetation Nordostkroatiens. Acta Botanica Croatica 26-27(1), 161-180.

Jávorka, S., Csapody, V., 1991. Iconographia Florae Partis Austro-Orientalis Europae Centralis. Akadémiai Kiadó, Budapest, pp. 576.

Jovanović, B., 1965. Biljni svet – osnovne karakteristike autohtone flore i vegetacije Beljskog lovno-šumskog područja. Jelen 3, 61-78.

Knežević, M., 2006. Atlas korovne, ruderalne i travnjačke flore. Poljoprivredni fakultet u Osijeku, Osijek, 402 pp.

Kočić, A., Horvatić, J., Jelaska, S.D., 2014. Distribution and morphological variations of invasive macrophytes *Elodea nuttallii* (Planch.) H. St. John and *Elodea canadensis* Michx in Croatia. Acta Botanica Croatia 73(2), 437-446.

Kovačić, M., Puškadija, Z., Ozimec, S., Majić, I., Sarajlić, A., 2016. Importance of pollinating insects for maintaining sustainable agriculture in eastern Croatia. Journal of Environmental Protection and Ecology 17(4), 1408-1415.

Marsigli, A. F., 1726. Danubius Pannonico-Mysicus. Tomus Sextus. P. Gosse, R. Chr. Alberts, P. de Hond, Hague; H. Uytwerf, F. Changuion, Amsterdam.

Mihai, D., Oprea, A., Ştefan, N., Sârbu, I., 2011. Vascular wild flora of Danube Delta Biosphere Reserve. Scientific Annals of the Danube Delta Institute Tulcea, Romania 17, 15-52.

Mitić, B., Boršić, I., Dujmović, I., Bogdanović, S., Milović, M., Cigić, P., Rešetnik, I., Nikolić. T., 2008. Alien flora of Croatia: proposals for standards in terminology, criteria and related database. Natura Croatica 17(2), 73–90.

Neilreich, A., 1866. Aufzählung der in Ungarn und Slavonien bisher beobachteten gefässpflanzen nebst einer pflanzengeografischen uebersicht. Wilhelm Braumüller, Wien.

Nikolić, T., 2018. Flora Croatica Database. Department of Biology, Faculty of Science, University of Zagreb. Retrieved March 5, 2018 from http://hirc.botanic.hr/fcd

Nikolić, T., Mitić, B., Boršić, I., 2014. Flora Hrvatske – invazivne biljke. Alfa, Zagreb, 296 pp.

Nikolić, T., Topić, J. (eds.), 2005. Crvena knjiga vaskularne flore Hrvatske, kategorije EX, RE, CR, EN i VU. Ministarstvo kulture, Državni zavod za zaštitu prirode, Zagreb, 693 pp.

Ozimec, S., Topić, J., 2018. Macrophytes of the Croatian Danube Reach. In: Janauer, G.A., Kvet, J., Germ, M., Exler, N., Gaberščik, A. (eds.): Macrophytes of the River Danube Basin. Academia, Prague, pp. 252-267.

Panjković, B., 1990. Analiza životnih oblika i flornih elemenata u flori Baranje (Hrvatska). Acta Botanica Croatica 49(1), 107-123.

Panjković, B., Krizmanić, L., Puzović, S., Stojšić, V., Kovačević, B., Štetić, J., 2000. Significant biodiversity components at Apatinski and Monoštorski rit (YU). International Association for Danube Research, Limnological Reports 33, 171-178.

Panjković, B., Stojšić, V., 2001. Prilog poznavanju adventivne flore „Gornjeg Podunavlja“. Zaštita prirode 53(1), 21-27.

Petrić, I., Stojanović, V., Lazarević, P., Pećinar, I., Đorđević, V., 2010. Florističke karakteristike područja NP „Đerdap“ i njegove neposredne okoline. Zaštita prirode 61(1), 35-59.

Pignatti, S., 2002. Flora d'Italia, Vols. 1–3. Edagricole, Bologna.

Preston, C.D., 1995. Pondweeds of Great Britain and Ireland. Botanical Society of the British Isles, London, 350 pp.

Purger, D., Csiky, J. 2008. Biljke Banskog brda. University of Pécs, Pécs, 62 pp.

Raunkiaer, C., 1937. Plant life forms. The Clarendon Press, Oxford, 104 pp.

Rauš, Đ., 1995. Sto trajnih ploha Republike Hrvatske (Ekološka istraživanja). Glasnik za šumske pokuse 32, 225-376.

Rauš, Đ., Seletković, Z., Šegulja, N., Topić, J., 1980. Komparativna istraživanja ekosistema u Hrvatskoj. Šumarski list 104(5-6), 201-218,

Rauš, Đ., Šegulja, N., Topić, J., 1985. Vegetacija sjeveroistočne Hrvatske. Glasnik za šumske pokuse 23, 223-355.

Rothmaler, W., 2009. Exkursionsflora von Deutschland 3, Gefäβpflanzen: Atlasband. Spektrum Akademischer Verlag, Heidelberg, 822 pp.

Stoyanov, S., 2005. The vascular flora of the catchment basin of the river Roussenski Lom in the beginning of the 21st century. Flora Mediterranea 15, 51-383.

Tadić, Z., 1999. Hidrološke značajke.. In: Mihaljević, M., Martinčić, J. (eds.): Kopački rit, pregled istraživanja i bibliografija. Hrvatska akademija znanosti i umjetnosti, Centar za znanstveni rad Osijek, Zagreb-Osijek, pp. 24-28.

Tadić, L., Bonacci, O., Dadić, T., 2014. Dynamics of the Kopački rit (Croatia) wetland floodplain water regime. Environmental Earth Sciences 71(8), 3559-3570.

Topić, J., 1989. Vegetation of the Special Zoological Reserve of Kopački rit. Hydrobiologia 182, 149-160.

Topić, J., 1999: Flora i vegetacija. In: Mihaljević, M., Martinčić, J. (eds.): Kopački rit, pregled istraživanja i bibliografija. Hrvatska akademija znanosti i umjetnosti, Centar za znanstveni rad Osijek, Zagreb-Osijek, pp. 71-79.

Topić, J., Ozimec, S., 2001. *Typha laxmannii* Lepechin (Typhaceae), a new species in Croatian flora. Natura Croatica 10(1), 61-65.

Topić, J., Šegulja, N., 2005: Biljnogeografski položaj i raščlanjenost Hrvatske. In: Nikolić, T., Topić, J. (eds.): Crvena knjiga vaskularne flore Hrvatske, kategorije EX, RE, CR, EN i VU. Ministarstvo kulture, Državni zavod za zaštitu prirode, Zagreb, pp. 564-567.

Trinajstić, I., Pavletić, Z., 1978. *Azolla filiculoides* Lam. u vegetaciji vodenjara istočne Hrvatske. Acta Botanica Croatica 37(1), 159-162.

Zahirović, Ž., 2000. Rijetke i ugrožene biljne vrste sjeveroistočne Hrvatske. Magistarski rad. Sveučilište u Zagrebu, Prirodoslovno-matematički fakultet, Zagreb

ABS ACTA BIOLOGICA SLOVENICA
LJUBLJANA 2018 Vol. 61, Št. 2: 71–84

Elemental composition and fungal colonisation of decomposing *Phragmites australis* (Cav.) Trin. ex Steud. litter at different water regimes

Elementna sestava in glivna kolonizacija razpadajočega opada trsta *Phragmites australis* (Cav.) Trin. ex Steud. pri različnih vodnih režimih

Matevž Likar*, Nataša Dolinar, Katarina Vogel-Mikuš, Alenka Gaberščik, Marjana Regvar

Department of Biology, Biotechnical Faculty, University of Ljubljana, Večna pot 111, 1000 Ljubljana, Slovenia

*correspondence: matevz.likar@bf.uni-lj.si

Abstract: Plant litter decomposition in intermittent dry and wet habitats share decomposition mechanisms of both dry land and submerged habitats. The aims of the present study were therefore to compare fungal communities on the decomposing plant material regarding the water regime of the location. Furthermore we wanted to evaluate the effects of the water regime on the decomposition in combination with fungal decomposers. Litter decomposition was followed on selected sites of Lake Cerknica with different hydrological regimes, using the litterbag method. The elemental composition of the decomposing plant tissues of *Phragmites australis* and fungal communities developing on the decomposing plant material were analysed. The hydrological regime has an important role in defining the fungal community of *P. australis* leaf litter. Water regime affected the fungal communities, which exhibited higher diversity under more stable dry or submerged conditions (in contrast to intermittent). Decomposition rates were more affected by the environment as by the fungal community diversity or composition. But, despite differences in the fungal communities the elemental composition showed similar patterns of enrichment due to decreases in the organic fraction of the plant tissue.

Keywords: litter decomposition, fungal community, elemental composition, intermittent habitat, wetland

Izvleček: Razgradnja rastlinskega materiala v presihajočih habitatih kaže lastnosti razgradnje značilne tako za suha kot vlažna okolja. Namen naše raziskave je bil primerjati glivne združbe na razkrajajočem rastlinskem materialu glede na vlažnostne razmere v okolju in oceniti vplive vodnega režima na razgradnjo v kombinaciji z glivnimi združbami v presihajočih ekosistemih. Na izbranih lokacijah ob Cerkniškem jezeru, ki so se razlikovale v vodnem režimu, smo spremljali razgradnjo listov in stebel navadnega trsta (*Phragmites australis*) in ovrednotili razlike v elementni sestavi in glivnih združbah, ki so se razvile na razkrajajočem rastlinskem materialu. Hidrološki režim lokacije se je izkazal kot pomemben dejavnik pri oblikovanju glivnih združb na razkrajajočih listih trsta. Vodni režim je močno vplival na glivne združbe, ki so imele večjo diverziteto pri stabilnejših razmerah tj. suhih ali potopljenih razmerah v primerjavi s presihajočimi. Naši rezultati kažejo, da je okolje samo močneje vpli-

valo na hitrost razgradnje kot glivna združba, ki se je oblikovala na razkrajajočem se rastlinskem materialu. Kljub razlikam v glivnih združbah, je elementna sestava rastlinskega materiala sledila podobnim vzorcem koncentriranja elementov zaradi razgradnje organske matrice.

Ključne besede: razgradnja opada, glivna združba, elementna sestava, presihajoči habitat, mokrišče

Introduction

Wetlands with prevailing helophyte vegetation have high primary productivity of biomass (Cronk and Fennessy 2001), which is subjected to decomposition processes (Longhi et al. 2008). The decomposition of wetland plants starts when senescent leaves are still attached to the plant (Bärlocher 1997, Van Ryckegem et al. 2007), with colonisation of the dead plant parts by fungi and bacteria (Komínková et al. 2000, Van Ryckegem et al. 2006). Microbial colonisation is followed by fragmentation of the material, due to different physical factors (Wallis and Raulings 2011), which can include currents, wave action, and water-level fluctuations. In addition, macro-invertebrates that favour leaves colonised by microorganisms have important roles in the decomposition of this plant material (Webster and Benfield 1986).

During the decomposition processes, much of the carbon is released, as CO_2 or CH_4, depending on oxygen availability, although it is also incorporated into microbial biomass. In contrast, P, N and other elements such as Fe, Zn and Ni, are built into the microbial biomass, which results in increased nutrient content of the decomposing litter (Cleveland and Liptzin 2007, Bridgham and Lamberti 2009). During the decomposition, some element concentrations can reach more than 100-fold, and some even 1000-fold, their concentrations in the original plant tissue (Zawislanski et al. 2001, Windham et al. 2004, Du Laing et al. 2006). This element accumulation primarily occurs in the microbial biofilm that is formed on the decomposing plant material (Purchase et al. 2009), and less so in the actual matrix of the decomposing materials (Schaller et al. 2011). Ryckengem et al. 2006 concluded that fungi decomposing the plant litter are active immobilizers of nutrients from the external environment as in their study fungi often contained increased element concentration when compare to the original plant material. Therefore, fungi have a considerable impact on the organic matter dynamics and should be incorporated in any study trying to understand nutrient cycling in wetland ecosystems.

The element enrichment however also depends on environmental conditions and on the properties of the original plant material (Du Laing et al. 2006, Batty and Younger, 2007). Given the plant species richness and assuming equally chemically diversity of plant material, which can affect the decomposition (Loranger et al. 2002, Kasurinen et al. 2006), it is critical to further investigate the importance of litter quality in order to increase our ability to understand and predict the decomposition process in different environments.

The decomposition in intermittent ecosystems is highly affected by the periodical flooding (Bedford 2005, Dolinar et al. 2016), which change the availability of oxygen and moisture that are needed for aerobic decomposition. The most important factors affecting the decomposition process seem to be the frequency and the duration of the submergence (Neckles and Neill 1994, Langhans and Tockner 2006, Dolinar et al. 2016). At drier locations where oxygen is readily available, flooding accelerates decomposition by increasing moisture, whereas longer submergence creates anoxic conditions that slow decay (Neckles and Neill 1994). Anoxic conditions represent one of the possible reasons for low decomposition rates in permanently flooded wetlands (Ryder and Horwitz 1995). High flood frequency also supports high decomposition rates (Brinson et al. 1981), as it also affects the fungal communities that colonise plant litter (Capps et al. 2011).

Lake Cerknica (Slovenia) is an intermittent wetland that undergoes pronounced water-level fluctuations (Dolinar et al. 2010, 2011), which makes it an ideal model situation for studies of plant decomposition. The vegetation of Lake

Cerknica is characterised by wetland communities with *Phragmites australis* (Cav.) Trin. ex Steud. common reed and *Carex elata* All. tufted sedge as the dominant plant species. Both species contribute significantly to the primary production (Martinčič 2003, Martinčič and Leskovar 2003), and consequently also to the production of litter in this ecosystem.

The main aim of the present study was to assess the influence water regimes in intermittent environment on elemental composition of decomposing *P. australis* tissues and fungal communities forming on the litter during the decomposition process. We hypothesised that differences in water regimes during the decomposition will affect formation of fungal communities on the decomposing *P. australis* material, and directly or indirectly (through fungal community) also influence the decomposition rate and elemental composition of decomposing *P. australis* material and therefore change the litter quality.

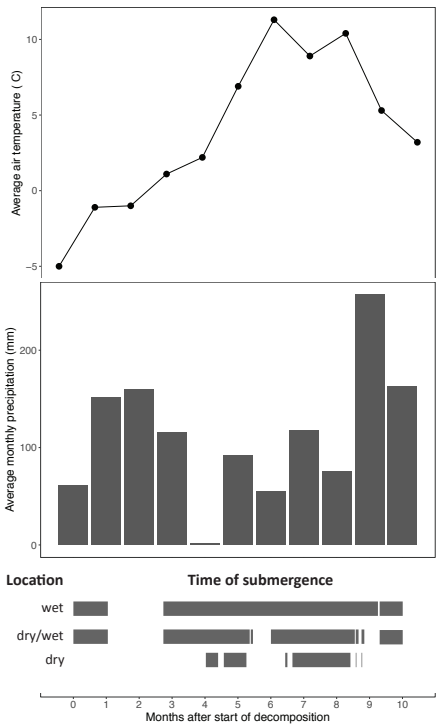

Figure 1: Average temperatures, precipitation and time of submergence for the locations with decomposing *Phragmites australis* material.

Slika1: Povprečne temperature, padavine in čas potopljenosti lokacije, na katerih je prihajalo do razgradnje materiala vrste *Phragmites australis*.

Material and methods

Site description

Lake Cerknica covers an area of 38 km^2 as an intermittent wetland that lies at the bottom of the Cerkniško polje depression (Slovenia). The annual precipitation for the locality is around 2000 mm and the average temperature is 10 °C. The monthly average temperatures and precipitation data is represented in Fig. 1.

In spring and usually in late autumn, Lake Cerknica reaches its normal level at 550 m above sea level, and covers the area of 26 km^2. The floodplain is flooded for 9 months to 10 months of the year, and dry for about 2 months, usually in summer. This provides a variable ecosystem that changes in both time and space. Its vegetation patterns show clear zonal distribution that depends on the extent and frequency of the flooding (Martinčič 2003, Martinčič and Leskovar 2003).

Decomposition analysis

The decomposition analysis was performed using the litterbag method (Webster and Benfield 1986). Here, 120 litterbags (15 × 30 cm) made from plastic mesh with 1 × 1 mm openings were filled with either 5 g leaves of *P. australis*, or 10 g culms of *P. australis*, that were collected at Lake Cerknica at the end of the vegetative period. Dry *P. australis* culms were cut to 25-cm-long pieces, while leaves were used as whole. In December 2007, the litterbags of *P. australlis* were placed at three experimental locations at Lake Cerknica (N45° 43’ 40’’, E14° 24’ 17’’) that differed according to the extent of water-level fluctuations, from habitats that were almost completely dry (termed dry), across intermittent (dry/wet), to almost always submerged (wet). Litterbags were attached to wooden poles that positioned them

5 cm above the ground, and they were collected five times as four replicates during the following year (for details see Dolinar et al. 2016). The selected locations were in the middle of the reed stand where sediment was stabilised by numerous rhizomes. In addition, the samples were fixed above the soil level to avoid the influence of sediment. During the decomposition study, the *P. australis* material at the wet location was submerged for the majority of the study time (Fig. 1). Material at dry/wet location was submerged 7-times: twice for longer than 60 days, and five times for under 30 days. At the dry location the material was submerged 6-times, with an average submergence time under 7 days.

The original plant material (termed 'Initial') was analysed prior to the decomposition experiment. After four months, samples for elemental composition analysis and analysis of fungal communities were collected. The material for elemental composition analysis was dried at 30 °C prior the analysis, whereas material for molecular analyses was frozen at – 20 °C until processed.

Elemental composition analysis

The composition of the plant materials was determined using energy dispersive X-ray fluorescence spectrometry, according to the protocol of Nečemer et al. (2008). In brief, 0.5 g to 1.0 g powdered sample material was used to form the sample pellets using a pellet die and hydraulic press. The primary excitation sources were [^{55}Fe] (10 mCi), [^{109}Cd] (25 mCi) and [^{241}Am] (20 mCi) annular radioisotope excitation sources (Isotope Products Laboratories, USA). The emitted fluorescence radiation was measured using an energy dispersive X-ray spectrometer that comprised a Si(Li) detector (Canberra), a spectroscopy amplifier (Canberra M2024), an analogue-to-digital converter (Canberra M8075) and a PC-based multichannel analyser (S-100, Canberra). The spectrometer was equipped with a vacuum chamber. The energy resolution of the spectrometer was 175 eV at 5.9 keV. The analysis of the X-ray spectra was performed using the analysis of X-ray spectra by an iterative least squares programme (Van Espen and Janssens 1993), as included in the quantitative X-ray analysis system software package (Vekemans et al. 1994). Element quantification from the measured spectra was performed using the quantitative analysis of environmental samples based on fundamental parameters (Kump et al. 2007). Quality assurance for the element analyses was performed using standard reference material NIST SRM 1573a (tomato leaves as a homogenised powder).

PCR amplification and temporal temperature gel electrophoresis

For the temporal temperature gel electrophoresis (TTGE) analysis, the protocol described by Likar et al. (2009) was followed, using GenElute Plant Genomic DNA miniprep kits (Sigma), according to the manufacturer instructions. The DNA was extracted from three subsamples from each plant (as 30 mg dry weight) that were combined prior to the amplification step.

All of the PCR reactions were carried out in a thermal cycler (MJ Research), using Taq DNA polymerase (Promega). The 25 µL reaction mixtures contained: 2.5 µL 10× PCR buffer, 2.5 mM $MgCl_2$, 200 µM of each nucleotide, 500 nM of each primer, 0.75 U DNA polymerase, and 12.5 µL diluted template. The PCR conditions for the ITS1F-ITS4 and ITS3-ITS4 primer pairs (Gardes and Bruns 1993; White et al. 1990) were 1 min at 94 °C, followed by 35 cycles of 35 s denaturation at 94 °C, followed by 53 s annealing at 55 °C, and 30 min elongation at 72 °C. The duration of the elongation step was increased by 5 s per cycle. A final elongation was performed at 72 °C for 10 min. A nested PCR approach was used, as a second PCR was performed with the ITS3-ITS4 primer pair after amplification of the DNA with the ITS1F-ITS4 primers.

The TTGE analysis of the fungal ITS region was carried out on a Dcode electrophoresis apparatus (BioRad, Hercules, CA, USA), as described by Likar et al. (2009). The polyacrylamide gel was composed of 8% (v/v) acrylamide-bisacrylamide mixture, 8 M urea, 0.25% 50× TAE buffer, 400 µL ammonium persulphate, and 40 µL TEMED. Electrophoresis was performed at a constant voltage of 100 V for 18 h, with a temperature gradient from 52 °C to 68 °C. A 100-bp ladder (Fermentas) was included in the first and last lanes on every gel, as the standards for the normalisation across the gels. The gels were stained with

ethidium bromide and photographed under a UV transilluminator.

Data analysis

The differences in the individual elements were compared using ANOVA. All tests were performed in R v3.3.2 statistical programme (R core team, 2016).

The effects of the hydrological regimes of the locations on the elemental contents of the decomposing *P. australis* material were visualised using non-metric multidimensional scaling with the *metaMDS* function of the Vegan v2.4-1 library (Oksanen et al. 2016).

Using the function *heatmap.2* in R package Gplots 2.10.1, a heatmap was generated for the z-scores of elemental composition data. Z-scores were obtained by subtracting the mean of all data points from each individual data point and then dividing those points by the standard deviation of all points with *scale* function. Using the function *hclust* in R package 2.15.1, the dendrograms of rows or columns were added on the margins of the heatmap. Hierarchical clustering with the complete linkage method was used for the dendrograms, based on the Euclidean distances among clusters in rows or among elements in columns.

The Euclidean distance matrices obtained from the elemental composition datasets were then analysed according to a hierarchical experimental design (with location of decomposing material as the grouping factor), using permutational multivariate analysis of variance (PERMANOVA; see Anderson 2001). Analysis of variance was performed with the *adonis* function of the R Vegan v2.4-1 library (Oksanen et al. 2016), with 999 permutations. The possibility of significant effects arising due to differences in multivariate dispersion rather than compositional changes was tested by calculation of the multivariate homogeneity of the group dispersions (variances), using the *betadisper* function of the Vegan package.

The TTGE gels were normalised, and similarity levels were calculated using the GelManager software package, version 1.5 (BioSystematica). GelManager 1.5 uses the Pearson product moment coefficient to generate the band similarity matrix using information about the apparent molecular weights of the bands and the band spacing. It should be noted that there is not necessarily a one-to-one correspondence between the number of bands and the number of unique sequences or fungal species, therefore we use term operational taxonomic units (OTUs). Chao Richness estimator (Chao 1984; 1987), Shannon diversity (Chao et al. 2013) and Gini-Simpson index (Good 1953, Chao et al. 2014) were calculated using package iNEXT 2.0.12 (Chao et al. 2014).

To calculate the unique and shared effects of water regime and fungal diversity, as well as how much variation in loss of mass of *P. australis* material during the decomposition was explained by each set of these variables, a variation partitioning analysis (partial RDA) was performed. Variation partitioning analysis by using *varpart* function and the significance of each testable fraction in variation partitioning analysis was obtained from the functions *rda* and *anova.cca*. The functions *varpart, rda* and *anova.cca* are all found in the package Vegan (Oksanen et al. 2016).

Results

Elemental analysis

The elemental analysis of the senescent plant material before the plant litter was exposed to decomposition was compared to the corresponding plant material after 4 months of decomposition. The initial concentrations of the elements K, Ca, Mn, Fe, Zn and Br in the plant material prior to decomposition are given in Tab. 1 (‘Initial’). The contents of the individual elements across *P. australis* culms and leaves were significantly different. Indeed, *P. australis* leaves showed K, Ca, Mn and Zn concentrations that were several times higher than for *P. australis* culms.

Table 1: Element concentrations in *Phragmites australis* culms and leaves before decomposition and at differ ent micro-locations after four months of decomposition.
Tabela 1: Elementna sestava poganjkov in listov trsta (*Phragmites australis*) pred poskusom in štiri mesece po začetku dekompozicije na različnih mikrolokacijah.

Organ	Location	Concentrations of elements [mg kg^{-1}]					
		K	**Ca**	**Mn**	**Fe**	**Zn**	**Br**
culms	Initial	166 ± 21	630 ± 104^{a}	83 ± 9	121 ± 27^{b}	20 ± 2	15 ± 2^{ab}
	dry	193 ± 93	1638 ± 273^{b}	100 ± 21	678 ± 112^{a}	14 ± 6	11 ± 2^{a}
	dry/wet	LOD	1490 ± 362^{b}	114 ± 8	228 ± 52^{b}	16 ± 4	15 ± 1^{ab}
	wet	193 ± 15	1913 ± 178^{b}	721 ± 111	416 ± 21^{a}	LOD	19 ± 4^{b}
leaves	Initial	1370 ± 193^{a}	10145 ± 942	474 ± 111^{a}	295 ± 67^{a}	36 ± 13^{b}	19 ± 2^{a}
	dry	2633 ± 705^{b}	10895 ± 1952	721 ± 111^{b}	5120 ± 269^{b}	77 ± 16^{a}	36 ± 2^{b}
	dry/wet	1998 ± 396^{ab}	9805 ± 597	743 ± 57^{b}	4230 ± 625^{b}	56 ± 9^{ab}	49 ± 6^{b}
	wet	1708 ± 494^{b}	10618 ± 2004	739 ± 157^{b}	3047 ± 618^{b}	46 ± 7^{b}	73 ± 15^{c}

Numbers represent averages ± SD (n = 4). Data not sharing the same letter in superscript are statistically significantly different at $p < 0.05$. LOD, limit of detection.
Številke predstavljajo povprečno vrednost ± SD (n = 4). Rezultati z različnimi črkami so statistično značilno različnio pri $p < 0,05$. LOD, meja detekcije.

The elemental analysis of the samples after 4 months of decomposition showed statistically significant differences in individual measured elements (Tab. 1) and overall elemental composition of the samples (Tab. 2) across the different conditions (i.e., wet vs. wet /dry vs. dry). When element concentrations in culms from different locations were compared, however, lowest concentration of Fe was observed in culms on dry/wet location, whereas dry location had lowest Br concentration. (Tab. 1). Fe was concentrated in all of the decomposing *P. australis* samples, although to a greater degree in leaves (reaching 10-17-fold the initial values). In *P. australis* culms, the Fe concentrations did not differ significantly from the initial plant material if decomposition took place under the dry/wet conditions, but reached up to 6-fold the initial Fe concentrations under the dry conditions (Tab. 1). No statistically significant differences were seen for the Zn concentrations in the decomposing *P. australis* culms, whereas concentrations in the decomposing *P. australis* leaves increased with increasing dryness of the location (from wet through dry/wet to dry) (Tab. 1). The opposite was seen for the Br concentration in the decomposing *P. australis* culms, as it increased with increased duration of submergence, whereas no statistically significant differences were seen for the different conditions for Br concentrations in the decomposing *P. australis* leaves (Tab. 1).

Comparison of the element compositions of the decomposing *P. australis* culms and leaves prior to and after 4 months of decomposition was also analysed by the heatmap clustering of element composition z-scores (Fig. 2). This demonstrated clustering of the samples according to the plant organ. In contrast, the water status of location at which samples decomposed showed no clear trend on the elemental composition of decomposing material.

The non-metrical multidimensional scaling returned two-dimensional ordinations for element loss from the decomposing material with clear separation between the initial and decomposed samples for all of the plant tissues (Fig. 3). As decomposing *P. australis* culms showed less progress compared to leaves, there was more pronounced separation between the different culms conditions, whereas for decomposing *P. australis* leaves, the dry, dry/wet and wet conditions were overlapping, which again was particularly obvious for the wet and dry/wet condition.

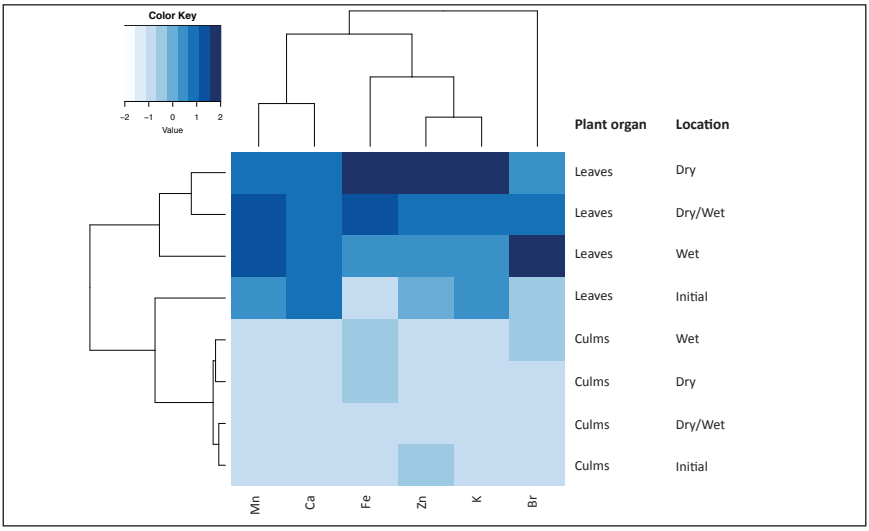

Figure 2: Z-scaled representation of element compositions in *Phragmites australis* culms and leaves after four months of decomposition under the different water conditions.

Slika 2: Z-lestvičena predstavitev elementne sestave stebel in listov vrste *Phragmites australis* po štirih mesecih dekompozicije pri različnih vodnih režimih.

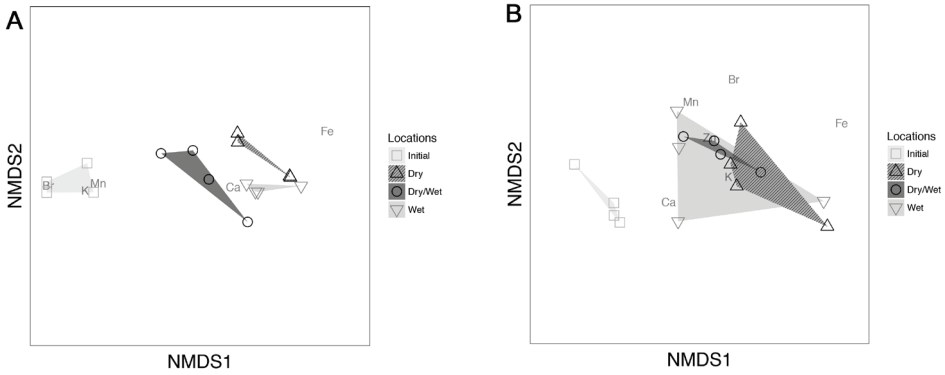

Figure 3: Ordination plot of the decomposing *Phragmites australis* culms (A) and leaves (B) along the dry, dry/wet and wet humidity gradient, based on the elemental contents, using non-metric multidimensional scaling.

Slika 3: Geometrična predstavitev elementne sestave razkrajajočih stebel (A) in listov (B) vrste *Phragmites australis* na lokacijah z različno vlažnostjo (suha, presihajoča in vlažna), pridobljen z nemetričnim večrazsežnostnimo lestvičenjem.

Relevance of fungal community and water regime for decomposition

Richness and diversity estimators showed that the highest richness/diversity of OTUs was observed in the initial *P. australis* material and fell during the decomposition process (Tab. 3). The lowest richness/diversity was observed in dry/wet location. Rank-abundance plots indicated that some of OTUs that were not present in the initial plant material were later found in all decomposing samples with high relative abundance (Fig. 4, marked with an asterisk). Also, some of the more abundant OTUs were observed to be missing from the samples decomposing in completely submerged conditions (Fig. 4, wet, marked with a cross) or dry/wet conditions (Fig. 4, dry/wet, marked with a double cross). In contrast, one of the OTUs was observed only in the initial material and was not found on any of the decomposing samples (Fig. 4, wet, marked with a double asterisk).

Table 3: Species richness and diversity estimators for fungal communities on *Phragmites australis* leaves prior to (initial) and after 7 months of decomposition at different locations (dry, dry/wet and wet). Values represent estimators ±SE (n=4).

Tabela 3: Vrstna pestrost in cenilci pestrosti za glivne združbe na listih trsta (*Phragmites australis*) pred in po 7 mesecih razgradnje na različnih mikrolokacijah. Vrednosti predstavljajo cenilko ±SN (n=4).

Location	Chao richness		Shannon diversity		Simpson diversity	
Initial	22.75 ±	20.72	23.79 ±	11.89	28.00 ±	9.08
Dry	13.53 ±	2.08	15.19 ±	2.53	18.07 ±	3.05
Dry/ Wet	8.00 ±	0.00	9.53 ±	1.29	11.77 ±	1.60
Wet	10.49 ±	2.03	12.79 ±	2.66	18.20 ±	2.87

Variation partitioning showed that water regime as average time of submergence together with frequency of submergence explained 96% of the total variation (with 52% of total variation shared by both factors), whereas fungal diversity explained only less than 1% and was not statistically significant.

Variation partitioning showed that variation in fungal communities was largely explained by the overall fungal diversity on the decomposing material (10% of total variation). Average time of submergence together with frequency of submergence together explained only 5% of total variation, but was not statistically significant.

Discussion

Periodical flooding can affect the decomposition in intermittent ecosystems as it changes the environmental conditions and thus affects the microbial communities and its activity (Bedford 2005, Dolinar et al. 2016).

In the present study, we observed differences in fungal communities on the decomposing *P. australis* leaves between locations with different water regimes. The majority of the OTUs on decomposing *P. australis* leaves was observed already in the initial leaf material collected from the plants, thus supporting observation that senescent leaves begin decomposition still attached to the plant (Bärlocher 1997, Van Ryckegem et al. 2007), when they are colonized by fungi and bacteria (Komínková et al. 2000, Van Ryckegem et al. 2006). Additional OTUs joined the fungal community of decomposers during the decomposition, while some disappeared. The later probably represented plant pathogens or less competitive

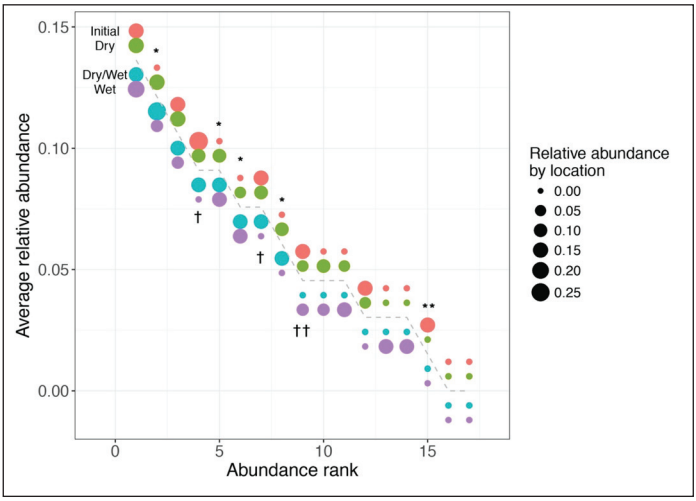

Figure 4: Rank abundance plot with average relative abundance for OTUs (dashed line) and relative abundance for individual OTUs from initial *Phragmites australis* leaves or leaves decomposing at dry, dry/wet and wet location (circles). The size of average relative abundance for OTUs is represented on the y-axis, whereas the relative abundance of the individual OTU at different locations is represented by the size of the circle. Legend: asterisks mark the OTUs that were not present in the initial plant material, double asterisks mark the OTUs that were missing at dry location, double crosses mark OTUs missing at the dry/wet location, and crosses mark OTUs that were absent in material decomposing at wet location.

Slika 4: Graf ranžirane številčnosti in povprečne relativne številčnosti operacijskih taksonomskih enot (črtkana črta) in relativna številčnost individualnih operacijskih taksonomskih enot iz izvornega materiala vrste *Phragmites australis* ali listov, ki so se razkrajali na suhi, presihajoči in vlažni lokaciji (krogci). Velikost povprečne relativne številčnosti operacijskih taksonomskih enot je predstavljena na y-osi, medtem ko je velikost relativne številčnosti posameznih operacijskih taksonomskih enot na različnih lokacijah predstavljena z velikostjo kroga. Legenda: zvezdica označuje operacijske taksonomske enote, ki niso bile prisotne v izvornem materialu, dvojna zvezdica označuje operacijske taksonomske enote, ki manjkajo na suhi lokaciji in križ označuje operacijske taksonomske enote, ki manjkajo na vlažni lokaciji.

saprophytes, which disappear with progression of decomposition (Berg and McClaugherty 2003). Our findings suggest that the contrasting environmental conditions to which these decomposing leaves were exposed might have lead to changes in the composition of fungal communities. The changes in fungal community composition were accompanied by difference in diversity, with the lowest diversity observed for *P. australis* leaves decomposing at dry/wet location. This suggests that the combination of submergence times and frequency of submergences at this location created an unstable community or at least the least favourable conditions for the development of a diverse community of fungal decomposers. This is in line with the observations of Kaisermann et al. (2015), who reported rapid changes in the fungal communities after changes in the soil moisture content. The reason for this might be the permanent disturbance and the variable environmental conditions in the shallower water, which might negatively affect the establishment of biotic communities on the decomposing plant parts (Collinson et al. 1995).

Differences in fungal communities could lead to changes in the metabolic performance of fungal community (Webster and Benfield 1986), resulting in changed decomposition rates. In line with this, Dolinar et al. (2016) reported that decomposition rate for *P. australis* leaves was faster under the wet conditions in comparison to the intermittent dry/wet conditions. But our results suggest that the main factor for differences was the environment (e.g. water regime), which

explained the majority of variation in weight loss during the decomposition. Fungal communities as an indirect effect of the environment were not a very strong factor, thus suggesting that changes in fungal communities did not heavily affect the decomposition efficiency.

The concentrations of elements in plant tissues depend on the properties of their habitat, as primarily on the amount of individual elements in the water and sediment, and also on environmental factors, and in particular, pH (Batty and Younger 2007). The initial values of the elements measured in these *P. australis* tissues in the present study were comparable to those in *P. australis* material collected from an acidic (pH 3) spoil heap discharge in Northumberland, UK (Batty and Younger 2007), and an urban district in Sicily (Bonanno 2011). This would suggest the importance of the plant species characteristics on their ionome independently from the growing locations and expand the comparability between different studies on *P. australis* elemental composition.

The element concentrations measured in the present study in *P. australis* leaves were much higher than in culms, which is in agreement with data from other studies (Vymazal et al. 2009, Bonanno 2011). Comparison of the contents of the elements K, Ca, Mn, Fe, Zn and Br in the dried plant tissues initially and the decomposition showed increases in most of the elements measured. Similarly to our observation, Windham et al. (2004) reported Zn and Cr concentration in *P. autralis* leaves increased 10-fold after 1 year of decomposition. In a similar study, Du Laing et al. (2006) reported approximately 5-fold higher Zn, Pb and Cu concentrations in leaves and about 10-fold higher Cd, Cr and Ni concentrations after 9-16 months of decomposition, while there was a much smaller accumulation of these elements in the culm. In the present study, decomposing materials differed depending on the conditions where they are decomposing, although the accumulation pattern of the individual elements showed no clear trend connected to the decomposition conditions. This suggests that the location where the element is incorporated in plant cell and tissue is more important for the resulting changes in its concentration during decomposition than environmental conditions at which the plant material is decomposing. The reasons for this accumulation of elements in decomposing plant tissues are numerous. One of the important reasons is that the dried tissue might retain some fine particles of sediment (Zawislanski et al. 2001, Windham et al. 2003, Du Laing et al. 2006), and another is the accumulation in the microbial biofilm that covers decomposing plant tissues (Batty and Younger 2007). As such, accumulation of individual element is greatly dependent on its availability in water, sediment and needs of the microbial communities in the biofilm. The greatly increased Fe concentrations during decomposition might also be a result for the formation of an oxalate complex. Oxalate crystals can adhere to fungal hyphae and chelate Fe and Al ions (Cromack et al. 1979), and consequently they increase these concentrations during decomposition of the plant matrix.

In conclusion, decomposition of *P. australis* tissues in intermittent environment showed differences in microbial communities and elemental concentrations, connected to the frequency and time of the submergence. The combination of submergence frequencies and submergence times at both extremes (longer submergence times or drier periods) seemed to form more stable conditions that promoted formation of more diverse communities. But, despite differences in the fungal communities the elemental composition showed similar patterns of enrichment due to decreases in the organic fraction of the plant tissue, which suggests that in different microbial communities, the same function during degradation of plant material can be performed by different representatives of the community.

Povzetek

Mokrišča s prevladujočo helofitsko vegetacijo imajo visoko produkcijo rastlinske biomase (Cronk and Fennessy 2001), ki se počasi razkraja (Longhi et al. 2008). Pri tem se razgradnja prične že na rastlinah samih, ko odmirajoče organe kolonizirajo bakterije in glive (Komínková et al. 2000, Van Ryckegem et al. 2006). Med mokrišči si posebno mesto zaslužijo presihajoči ekosistemi, saj je v njih razgradja močno odvisna od periodičnih poplav (Bedford 2005, Dolinar et al. 2016), med katerimi pride do večjih sprememb v vlagi in prezračenosti okolja. Razgradnja rastlinskega

materiala v presihajočih habitatih ima tako lastnosti razgradnje značilne za suha kot tudi vlažna okolja.

Glavni namen naše raziskave je bil primerjati glivne združbe na razkrajajočem materialu navadnega trsta (*Phragmites australis*) glede na vlažnostne razmere v okolju in oceniti vplive vodnega režima v kombinaciji z glivnimi združbami na razgradnjo. Predpostavili smo, da bodo različni vodni režimi vplivali na oblikovanje glivnih združb na razkrajajočem rastlinskem material in posredno ali neposredno (preko gliv) vplivali na hitrost razgradnje ter elementno sestavo ostankov trsta.

Na izbranih lokacijah ob Cerkniškem jezeru, ki so se razlikovale v vodnem režimu, smo spremljali razgradnjo rastlinskega materiala in ovrednotili razlike v elementni sestavi in glivnih združbah, ki so se razvile na razkrajajočem rastlinskem material. Elementno sestavo smo določili z metodo XRF (X-ray fluorescence spectrometry). Glivne združbe smo karakterizirali s pomnoževanjem ITS rDNA in elektroforezo v temperaturnem gradientu (TTGE, temporal temperature gel electrophoresis).

Hidrološki režim lokacije se je izkazal kot pomemben dejavnik pri oblikovanju glivnih združb na razkrajajočih listih navadnega trsta (*Phragmites australis*), pri čemer sta bila elementna sestava in profil glivnih združb odvisna od pogostosti in časa potopljenosti lokacije. Naši rezultati so pokazali, da so glivne združbe pestrejše v bolj stabilnih razmerah vodnega režima v ekostistemu tj. suhih ali potopljenih razmerah v primerjavi s presihajočimi. Kljub razlikam v glivnih združbah pa je elementna sestava pokazala podobnosti v koncentriranju nekaterih elementov zaradi razgradnje organske matrice, kar nakazuje, da lahko različne skupine gliv prevzamejo podobno funkcijo pri razgradnji rastlinske biomase v okoljih z izrazito različnimi vodnimi režimi.

Acknowledgement

This study was supported by the Ministry of Education, Science and Sport, Republic of Slovenia, through the programmes Biology of Plants (P1-0212) and Young Researchers (1000-06310153). Dr. Christopher Berrie is acknowledged for critical revision of the English language and grammar.

References

Anderson, M.J., 2001. A new method for non-parametric multivariate analysis of variance. Australian Ecology 26, 31-46.

Bärlocher, F., 1997. Pitfalls of traditional techniques when studying decomposition of vascular plant remains in aquatic habitats. Limnetica 13(2), 1-11.

Batty, L.C., Younger, P.L., 2007. The effect of pH on plant litter decomposition and metal cycling in wetland mesocosms supplied with mine drainage. Chemosphere 66, 158-164.

Bedford, A.P., 2005. Decomposition of *Phragmites australis* litter in seasonally flooded and exposed areas of a managed reedbed. Wetlands 25, 713-720.

Berg, B., McClaugherty, C., 2003. Plant litter, decomposition, humus formation, carbon sequestration. Springer Verlag, Berlin, 286 pp.

Bonanno, G., 2011. Trace element accumulation and distribution in the organs of *Phragmites australis* (common reed) and biomonitoring applications. Ecotoxicology and Environmental Safety 74, 1057-1064.

Bridgham, S.D., Lamberti, G.A., 2009. Ecological dynamics III: Decomposition in wetlands. In: Maltby, E., Barker, T. (eds,) The wetlands handbook, Blackwell Publishing Ltd, Chichester, 326-345.

Brinson, M.M., Lugo, A.E., Brown, S., 1981. Primary productivity, decomposition and consumer activity in freshwater wetlands. Annual Review of Ecology and Systematics 12, 123-161.

Capps, K.A., Graça, M.A.S., Encalada, A.C., Flecker, A.S., 2011. Leaf-litter decomposition across three flooding regimes in a seasonally flooded Amazonian watershed. Journal of Tropical Ecology 27, 205-210.

Chao, A., 1984. Nonparametric estimation of the number of classes in a population. Scandinavian Journal of Statistics 11, 265-270.

Chao, A., 1987. Estimating the population size for capture-recapture data with unequal catchability. Biometrics 43, 783-791.

Chao, A., Gotelli, N.J., Hsieh, T.C., Sander, E.L., Ma, K.H., Colwell, R.K., Ellison, A.M., 2014. Rarefaction and extrapolation with Hill numbers: a framework for sampling and estimation in species diversity studies. Ecological Monographs 84, 45-67.

Chao, A., Wang, Y.T., Jost, L., 2013. Entropy and the species accumulation curve: a novel entropy estimator via discovery rates of new species. Methods in Ecology and Evolution 4, 1091-1100.

Cleveland, C.C., Liptzin, D., 2007. C:N:P stoichiometry in soil: is there a "Redfield ratio" for the microbial biomass? Biogeochemistry 85, 235-252.

Collinson, N.H., Biggs, J., Corfield, A., Hodson, M.J., Walker, D., Whitfield, M., Williams, P.J., 1995. Temporary and permanent ponds: an assessment of the effects of drying out on the conservation value of aquatic macroinvertebrate communities. Biological Conservation 74, 125-133.

Cromack, K., Sollins, P., Graustein, W.C., Speidel, K., Todd, A.W., Spycher, G., Li, C.Y., Todd, R.L., 1979. Calcium oxalate accumulation and soil weathering in mats of *Hysterangium crassum*. Soil Biology and Biochemistry 11, 463-468.

Cronk, J.K., Fennessy, M.S., 2001. Wetland plants: biology and ecology. Lewis Publishers, Boca Raton, 462 pp.

Dolinar, N., Regvar, M., Abram, D., Gaberščik, A., 2016. Water-level fluctuations as a driver of *Phragmites australis* primary productivity, litter decomposition, and fungal root colonisation in an intermittent wetland. Hydrobiologia 774, 69-80.

Dolinar, N., Rudolf, M., Šraj, N., Gaberščik, A., 2010. Environmental changes affect ecosystem services of the intermittent Lake Cerknica. Ecological Complexity 7, 403-409.

Dolinar, N., Šraj, N., Gaberščik, A., 2011. Water regime changes and the function of an intermittent wetland. In: Vymazal, J. (ed.), Water and Nutrient Management in Natural and Constructed Wetlands. Springer, Dordrecht, pp. 251-262.

Du Laing, G., Van Ryckegem, G., Tack, F.M.G., Verloo, M.G., 2006. Metal accumulation in intertidal litter through decomposing leaf blades, sheaths and stems of *Phragmites australis*. Chemosphere 63, 1815-1823.

Gardes, M., Bruns, T.D., 1993. ITS primers with enhanced specificity of basidiomycetes: application to the identification of mycorrhizae and rusts. Molecular Ecology 2, 113-118.

Good, I.J., 1953. The population frequencies of species and the estimation of population parameters. Biometrika 40, 237-264.

Kaisermann, A., Maron, P.A., Beaumelle, L., Lata, J.C., 2015. Fungal communities are more sensitive indicators to non-extreme soil moisture variations than bacterial communities. Applied Soil Ecology 86, 158-164.

Kasurinen, A., Riikonen, J., Oksanen, E., Vapaavouri, E., Holopainen, T., 2006. Chemical composition and decomposition of silver birch leaf litter produced under elevated CO_2 and O_3. Plant and Soil 282, 261-280.

Komínková, D., Kuehn, K.A., Büsing, N., Steiner, D., Gessner, M.O., 2000. Microbial biomass, growth, and respiration associated with submerged litter of *Phragmites australis* decomposing in a littoral reed stand of a large lake. Aquatic Microbial Ecology 22, 271-282.

Kump, P., Nečemer, M., Vogel-Mikuš, K., Rupnik, Z., Ponikvar, D., Pelicon, P., Pongrac, P., Simčič, J., Budnar, M., 2007. Improvement of the XRF quantification and enhancement of the combined applications by EDXRF andMicro PIXE. In: First research coordination meeting under co-ordinated research project on "Unification of nuclear spectrometries: integrated techniques as a new tool for materials research": report: Vienna, 16–20 April, 2007, (IAEA/AL/, 181). IAEA, Vienna, pp. 91–95.

Langhans, S.D., Tockner, K., 2006. The role of timing, duration and frequency of inundation in controlling leaf litter decomposition in a river-floodplain ecosystem (Tagliamento, northeastern Italy). Oecologia 147, 501-509.

Likar, M., Regvar, M., Mandič-Mulec, I., Stres, B., Bothe, H., 2009. Diversity and seasonal variations of mycorrhiza and rhizosphere bacteria in three common plant species at the Slovenian Ljubljana Marsh. Biology and Fertility of Soils 45, 573-583.

Longhi, D., Bartoli, M., Viaroli, P., 2008. Decomposition of four macrophytes in wetland sediments: organic matter and nutrient decay and associated benthic processes. Aquatic Botany 89, 303-310.

Loranger, G., Ponge, J.F., Imbert, D., Lavelle, P., 2002. Leaf decomposition in two semi-evergreen tropical forests: influence of litter quality. Biology and Fertility of Soils 35, 247-252.

Martinčič, A., 2003. Praprotnice in semenke. In: Gaberščik A (ed) Jezero, ki izginja: Monografija o Cerkniškem jezeru. Ljubljana, Društvo ekologov Slovenije, pp. 72-80.

Martinčič, A., Leskovar, I., 2003. Vegetacija. In: Gaberščik A (ed) Jezero, ki izginja: Monografija o Cerkniškem jezeru. Ljubljana, Društvo ekologov Slovenije, pp. 80-96.

Neckles, H.A., Neill, C., 1994. Hydrologic control of litter decomposition in seasonally flooded prairie marshes. Hydrobiologia 286, 155–165.

Nečemer, M., Kump, P., Ščančar, J., Jaćimović, R., Simčič, J., Pelicon, P., Budnar, M., Jeran, Z., Pongrac, P., Regvar, M., Vogel-Mikuš, K., 2008. Application of X-ray fluorescence analytical techniques in phytoremediation and plant biology studies. Spectrochimica Acta B 63, 1240-1247.

Oksanen, J., Guillaume Blanchet, F., Friendly, M., Kindt, R., Legendre, P., McGlinn, D., Minchin, P.R., O›Hara, R.B., Simpson, G.L., Solymos, P., Stevens, M.H.H., Szoecs, E., Wagner, H., 2016. Vegan: Community Ecology Package. R package version 2.4-1. https://CRAN.R-project.org/package=vegan

Purchase, D., Scholes, L.N.L., Revitt, D.M., Shutes, R.B.E., 2009. Effects of temperature on metal tolerance and the accumulation of Zn and Pb by metal-tolerant fungi isolated from urban runoff treatment wetlands. Journal of Applied Microbiology 106, 1163-1174.

R Core Team, 2016. R: A language and environment for statistical computing. R Foundation for Statistical Computing, Vienna, Austria. URL https://www.R-project.org/.

Ryder, D.S., Horwitz, P., 1995. Seasonal water regimes and leaf litter processing in a wetland on the Swan Coastal Plain, Western Australia. Marine and Freshwater Research 46, 1077-1084.

Schaller, J., Brackhage, C., Mkandawire, M., Dudel, E.G., 2011. Metal/ metalloid accumulation/ remobilization during aquatic litter decomposition in freshwater: a review. Science of Total Environment 409, 4891-4898.

Van Espen, P., Janssens, K., 1993. Spectrum Evaluation. In: Van Grieken R, Markowicz A (eds) Handbook of X-ray Spectrometry, Methods and techniques. Marcel Dekker, New York, pp. 181–293.

Van Ryckegem, G., Gessner, M.O., Verbeken, A., 2007. Fungi on leaf blades of *Phragmites australis* in a brackish tidal marsh: diversity, succession and leaf decomposition. Microbial Ecology 53, 600-611.

Van Ryckegem, G., Van Driessche, G., Van Beeumen, J.J., Verbeken, A., 2006. The estimated impact of fungi on nutrient dynamics during decomposition of *Phragmites australis* leaf sheaths and stems. Microbial Ecology 52, 564-574.

Vekemans, B., Janssens, K., Vincze, L., Adams, F., Van Espen, P., 1994. Analysis of X-ray spectra by iterative least squares (AXIL): new developments. X-ray Spectrometry 23, 278–285.

Vymazal, J., Kröpfelová, L., Švehla, J., Chrastný, V., Štíchová, J., 2009. Trace elements in *Phragmites australis* growing in constructed wetlands for treatment of municipal wastewater. Ecological Engineering 53, 303-309.

Wallis, E., Raulings, E., 2011. Relationship between water regime and hummock-building by *Melaleuca ericifolia* and *Phragmites australis* in a brackish wetland. Aquatic Botany 95, 182-188.

Webster, J.R., Benfield, E.F., 1986. Vascular plant breakdown in freshwater ecosystems. Annual Reviews of Ecology and Systematics 17, 567-594.

White, T.J., Bruns, S., Lee, S., Taylor, J., 1990. Amplification and direct sequencing of fungal ribosomal RNA genes for phylogenetics. In: Innis, M., Gelfand, G., Sninsky, J., White, T. (eds.) PCR Protocols: A Guide to Methods Applications. Academic Press, Orlando, Florida, pp. 215-322.

Windham, L., Weis, J.S., Weis, P., 2003. Uptake and distribution of metals in two dominant salt marsh macrophytes, *Spartina alterniflora* (cordgrass) and *Phragmites australis* (common reed). Estuarine, Coastal and Shelf Science 56, 63-72.

Windham, L., Weis, J.S., Weis, P., 2004. Metal dynamics of plant litter of *Spartina alterniflora* and *Phragmites australis* in metal-contaminated salt marshes. Part 1: Patterns of decomposition and metal uptake. Environmental Toxicology and Chemistry 23, 1520-1528.

Zawislanski, P.T., Chau, S., Mountford, H., Wong, H.C., Sears, T.C., 2001. Accumulation of selenium and trace metals on plant litter in a tidal marsh. Estuarine, Coastal and Shelf Science 52, 589-603.

ACTA BIOLOGICA SLOVENICA
LJUBLJANA 2018 Vol. 61, Št. 2:85–92

Effect of selenium, iodine and their combination on development of Tartary buckwheat sprouts

Vpliv selena in joda ter njune kombinacije na razvoj kalic tatarske ajde

Sara Gorše, Aleksandra Golob, Mateja Germ*

Biotechnical Faculty, University of Ljubljana, Jamnikarjeva 101, SI-1000 Ljubljana, Slovenia

*correspondence: mateja.germ@bf.uni-lj.si

Abstract: Tartary buckwheat (*Fagopyrum tataricum* Gaertn) is becoming more and more popular due to its health benefits for humans. It contains important fibres, vitamins, certain minerals and antioxidants as rutin. Sprouts are a hot trend in the food production and nutrition. Enrichment of sprouts with iodine (I) and selenium (Se) may prevent endemic deficiency of these elements for humans and animals. The aim of the study was to found out the effect of selenate (Se(VI)), iodate (I(V)) and their combination on morphological, physiological and biochemical properties of Tartary buckwheat sprouts. Tartary seeds were soaked in solutions with Se(VI) (20 mg/L), I(V) (1500 mg/L) or in Se(VI) + I(V) (20 mg/L Se(VI) + 1500 mg/L (I(V)). Experiment was performed in growth chamber in two repetitions. Measurements were performed three weeks after germination. The solution of iodate and combination of selenate and iodate lowered germination rate of sprouts. There was no effect of the treatments on the amount of chlorophyll *a*, anthocynins and UV absorbing compounds. The amount of rutin was the highest in control sprouts. According to physiological measurements, control sprouts and sprouts from treated seeds were not stressed by the treatments.

Key words: Tartary buckwheat, sprouts, selenium, iodine

Izvleček: Tatarsko ajdo (*Fagopyrum tataricum* Gaertn) v zadnjem času spet bolj pogosto sejemo zaradi njenih pozitivnh učinkov za zdravje ljudi. Ajda vsebuje pomembne vlaknine, vitamine, nekatere minerale ter antioksidativne snovi, kot je rutin. Kalice so trenutno zelo popularne v prehrani ljudi. Obogatitev kalic s selenom (Se) in jodom (I) lahko prepreči znake pomanjkanja obeh elementov pri ljudjeh in živalih. Cilj dela je bil ugotoviti vpliv selenata, (Se(VI)), iodata (I(V)) in njune kombinacije na morfološke, fiziološke in biokemijske lastnosti kalic tatarske ajde. Semena tatarske ajde smo izpostavili raztopinam, ki so vsebovale Se(VI) (20 mg/L), I(V) (1500 mg/L) ali Se(VI) + I(V) (20 mg/L Se(VI) + 1500 mg/L (I(V)). Kalitev in razvoj kalic smo spremljali v rastnih komorah v dveh ponovitvah. Po treh tednih smo poskus prekinili in opravili morfološke, fiziološke in biokemijske meritve na kalicah. Semena tatarske ajde, ki so bila namočena v raztopinah iodata in kombinaciji selenata in iodata, so imela nižjo kalivost. Obravnavanja niso vplivala na vsebnost klorofila *a*, antocianov in UV absorbirajočih snovi. Vsebnost rutina je bila najvišja v kontrolnih kalicah. Glede na rezultate fizioloških meritev, namakanje smen v raztopinah selenata, jodata ter njune kombinacije, ni delovalo stresno na kalice.

Ključne besede: tatarska ajda, kalice, selen, jod

Introduction

Growing of buckwheat was in decline in the past century. However, recently cultivation has increased due to the growing interest in organic farming, alternative culture, old and traditional diets, outstanding nutritive properties and its positive effects on human health (Wieslander and Norback 2001). Cereals and pseudocereals are very important source of macronutrients and bioactive substances that have antioxidative activity. Buckwheat grains and groats contain numerous flavonoids and polyphenols, such as rutin, catechin, quercetin, p-coumaric acid, p-hydroxybenzoic acid and gallic acid (Dziedzic et al. 2018). Similarly to cereal crops, buckwheat seeds contain a lot of starch (Wronkowska and Haros 2014). Seeds, sprouts and fresh green parts of the plant are used in the diet (Golob et al. 2016). The presence of flavonoid rutin in buckwheat groats as well as in green parts of buckwheat plants is important due to its wide spectrum of pharmacological activities, including anti-inflammatory, anticancer, antiatherogenic, and antioxidant activity (Kreft et al. 2006, Starowicz et al. 2017).

Tartary buckwheat *(Fagopyrum tataricum*) is a dicot pseudocereal and belongs to family Polygonaceae. Currently, buckwheat sprouts are used as a novel source of vegetables due to the presence of enormous nutraceutical properties. Buckwheat sprouts are popular as a health food in Korea and Japan because of their high flavonoids content (Kim et al. 2004, Ji et al. 2016), especially rutin, and also short biological cycle (7–10 days) (Suzuki et al. 2005). Tartary buckwheat sprouts attracted a lot of attention because of their beneficial effects on blood pressure (Nakamura et al. 2013).

Although Se is not involved in vital metabolic processes in plants, it could help the plants to reduce the damage caused by oxidative stress if it is used in small doses (Seppänen et al. 2003). Se is on the list of beneficial elements for plants: it is not required by all plants but can promote plant growth and may be essential for particular taxa (Pilon-Smits et al. 2009). Soil and foliar addition of Se fertilizers (agronomic biofortification) are often used to improve the concentration of Se in diet (Nawaz et al. 2017). Iodine is a trace element, essential for mammalian life. The goal of iodine biofortification of plants is to obtain food, rich in this element, which may increase its consumption by various populations (Piątkowska et al. 2016).

Iodine and selenium together enable important functional roles in organisms of humans and animals. Biofortification (enrichment) of plants with these elements is justified to prevent endemic deficiency of I and Se in humans and animals (Smoleń et al. 2015). However, knowledge about the effects of simultaneous fortification with Se in I on plant's physiology and metabolism is lacking. Besides knowing the amount of Se and I in the sprouts, effect of elements on biochemical characteristics and growth is also very important before growing of fortified sprouts for human consumption. We assume that simultaneous fortification with Se in I, as well as fortification with both elements alone, will have an effect on the growth and physiological characteristics of Tartary buckwheat sprouts.

Materials and methods

Buckwheat seeds (cv. Darja) were soaked in solution for 8 h in 200 mL of distilled water (MilliQ) (control), or in solutions contained selenate (SeO_4^{2-}) with a concentration of 20 mg Se/L, iodate (IO_3-) with a concentration of 1500 mg I/L, and their combinations (SeO_4^{2-} + IO_3^-) with a concentration 20 mg Se/L and 1500 mg I/L respectively. Selenium was applied in the form of sodium selenate (Na_2SeO_4), and iodine was applied in the form of potassium iodate (KIO_3). After soaking, seeds were distributed to the plastic trays. Sprouts were grown in controlled conditions in the growth chamber with constant temperature 19 °C and 60% relative air humidity, and 160 µM $m^{-2}s^{-1}$ PAR, 16 h : 8 h. Measurements were done after 14 days of growing sprouts.

The contents of chlorophyll (Chl *a*, *b*) and carotenoids were determined following methods described by Lichtentaler and Buschman (2001a, b) and measured with a UV/Vis spectrometer. The anthocyanin contents were measured according to Drumm and Mohr (1978). The contents of UV-A and UV-B absorbing compounds were evaluated following the methodology of Caldwell (1968).

The potential photochemical efficiency of photosystem (PS)II was measured according to Schreiber et al. (1996) using a portable fluorometer

(PAM 2500 Chlorophyll Fluorometer; Heinz Walz GmbH, Germany). The respiratory potential of the mitochondria was determined *via* activity of terminal electron transport system (ETS) as described by Kenner and Ahmed (1975). For detailed description of the preparation of sprout tissue and extraction processes see Germ et al. (2005).

The normal distribution of the data was tested using Shapiro-Wilk tests. Differences between the conditions were tested using one-way analysis of variance followed by Duncan *post-hoc* tests. The level of significance was accepted at $p < 0.05$. The SPSS Statistics software, version 20.0 (IBM) was used for these calculations.

Results

Germination rate was lower in sprouts from seeds soaked in solution of iodate and combination with selenate and iodate comparing to control groups and sprouts emerged from seeds, soaked in selenate solution. Dry mass of the sprouts was the lowest in sprouts developed from selenate treated seeds in the first experiment, while between control and other two treatments there were no differences in dry mass of the sprouts (Table1).

Treatments did not affect the amount of chlorophyll *a*, anthocyanins, and UV-B and UV-A absorbing compounds, while the amount of carotenoids was the highest in sprouts from seeds, treated with combination of selenate and iodate in the first experiment. ETS activity was the lowest in control sprouts in the first experiment while there was no difference between control and treatments in the second experiment. There were no differences in the potential photochemical efficiency of PSII between control and sprouts from treated seeds in both experiments (Table 1).

The amount of rutin was the highest in control sprouts in the first experiment. In the second experiment, there was no difference between control and treated sprouts (Fig. 1).

Table 1: Biochemical and physiological responses of Tartary buckwheat sprouts grown from seeds previously soaked in solutions with addition of Se (Se(VI)) and I (I(V)) alone and simultaneous addition of Se and I (Se(VI) + I(V)).

Tabela 1: Biokemijski in fiziološki odziv kalic tatarske ajde zraslih iz semen, ki so bila predhodno namočena v raztopinah z dodatkom samo Se (Se(VI)), samo I (I(V)) in obeh elementov hkrati (Se(VI) + I(V)).

	Treatment				
First experiment	0	Se(VI)	I(V)	Se(VI) + I(V)	unit
germination	74.2 ± 4.4^{b}	71.9 ± 9.5^{b}	61.6 ± 1.5^{a}	59.8 ± 4.8^{a}	%
dry weight	15.5 ± 1.0^{b}	13.8 ± 0.7^{a}	16.8 ± 0.8^{b}	16.4 ± 0.7^{b}	%
chlorophyll *a*	$10.0 \pm 2.0^{a,b}$	8.5 ± 3.1^{a}	$8.9 \pm 2.1^{a,b}$	13.1 ± 3.0^{b}	mg/g d.w.
carotenoids	1.2 ± 0.2^{a}	1.1 ± 0.4^{a}	1.2 ± 0.3^{a}	2.0 ± 0.4^{b}	mg/g d.w.
anthocyanins per d.w.	262 ± 26^{a}	206 ± 66^{a}	284 ± 72^{a}	287 ± 75^{a}	rel. unit/g d.w.
UV-A abs	46 ± 4^{a}	38 ± 6^{a}	41 ± 10^{a}	35 ± 8^{a}	rel. unit/cm^2
UV-B abs	2.7 ± 0.2^{a}	2.2 ± 0.3^{a}	2.6 ± 0.6^{a}	2.1 ± 0.5^{a}	rel. unit/cm^2
F_v/F_m	0.8 ± 0.02^{a}	0.8 ± 0.01^{a}	0.8 ± 0.02^{a}	0.8 ± 0.01^{a}	
ETS activity	0.5 ± 0.09^{a}	0.7 ± 0.14^{b}	0.8 ± 0.12^{b}	0.7 ± 0.12^{b}	µL O_2/mg d.w./h

	Treatment				
Second experiment	0	Se(VI)	I(V)	Se(VI) + I(V)	unit
germination	85.7 ± 4.8^{b}	81.0 ± 7.9^{b}	68.5 ± 6.3^{a}	70.5 ± 2.5^{a}	%
dry weight	12.8 ± 0.5^{a}	13.2 ± 1.5^{a}	13.4 ± 2.0^{a}	16.5 ± 3.6^{a}	%
chlorophyll *a*	8.2 ± 1.0^{a}	7.9 ± 0.9^{a}	8.6 ± 1.3^{a}	7.8 ± 1.0^{a}	mg/g d.w.
carotenoids	1.1 ± 0.2^{a}	1.0 ± 0.2^{a}	1.0 ± 0.1^{a}	1.0 ± 0.1^{a}	mg/g d.w.
anthocyanins per d.w	439 ± 102^{a}	315 ± 103^{a}	294 ± 77^{a}	397 ± 156^{a}	rel. unit/g d.w.
UV-A abc	46 ± 4^{a}	38 ± 6^{a}	42 ± 10^{a}	35 ± 8^{a}	rel. unit/cm^2
UV-B abc	2.8 ± 0.3^{a}	2.6 ± 0.2^{a}	2.8 ± 0.5^{a}	2.6 ± 0.7^{a}	rel. unit/cm^2
F_v/F_m	0.6 ± 0.02^{a}	0.7 ± 0.08^{a}	0.7 ± 0.03^{a}	0.7± 0.4^{a}	
ETS activity	1.0 ± 0.3^{a}	0.8 ± 0.1^{a}	1.1 ± 0.3^{a}	1.0 ± 0.3^{a}	µL O_2/mg d.w./h

Data are means ± standard deviation (n = 4 for each treatment). Different letters indicate significant differences between the treatments, (p <0.05; Duncan test). Abbreviations: d.w., dry weight; ETS, electron transport system activity; abc, absorbing compounds.
Rezultati so predstavljeni kot povprečje ± standardna deviacija (n = 4 za vsak tretma). Različne črke označujejo statistično značilne razlike med tretmaji (p <0,05; Duncan test). Okrajšave: d.w., suha teža; ETS, aktivnost elektronskega transportnega sistema; abc, absorbirajoče snovi.

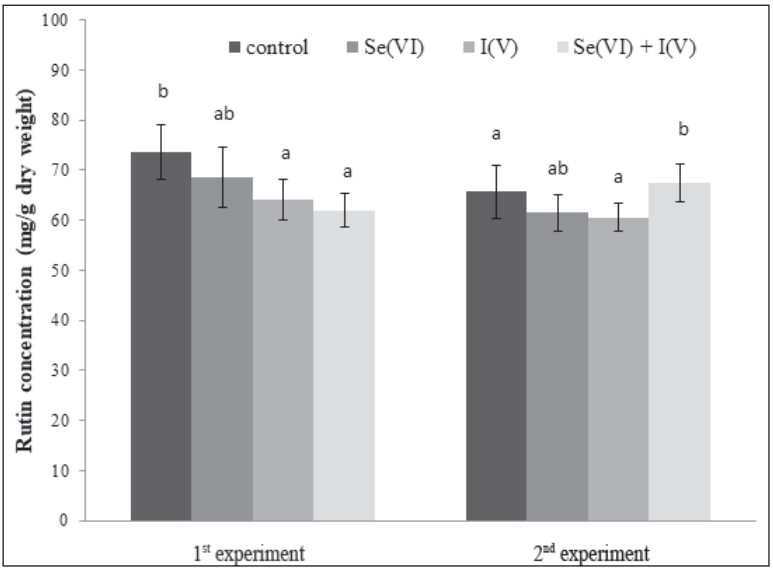

Figure 1: Rutin concentration in Tartary buckwheat sprouts grown from seeds previously soaked in solutions with addition of Se (Se(VI)) and I (I(V)) alone and simultaneous addition of Se and I (Se(VI) + I(V)). Different letters indicate significant differences between the treatments (p <0.05; Duncan test).

Slika 1: Vsebnost rutina v kalicah tatarske ajde zraslih iz semen, ki so bila predhodno namočena v raztopinah z dodatkom samo Se (Se(VI)), samo I (I(V)) in obeh elementov hkrati (Se(VI) + I(V)). Različne črke označujejo statistično značilne razlike med tretmaji (p <0,05; Duncan test).

Discussion

Germination is complex process in which a new plant emerges from a seed and is affected by a variety of environmental conditions (Todirascu-Ciornea et al. 2016). Treatment with iodate and combination of selenate and iodate negatively affected the germination of Tartary buckwheat sprouts. Iodate exerted negative effect on germination on wheat in the study from Todirascu-Ciornea and Dumitru (2015), where potassium iodate (KIO_3) solutions in 10^{-3}, 10^{-4} and 10^{-5} M concentrations were used. However, potassium iodate did not significantly influence the germination rate of the wheat seeds in the study from Todirascu-Ciornea et al. (2016) where two seed varieties, Putna and Gasparom, were treated with water (control) or 10^{-3}, 10^{-4} and 10^{-5} M solutions of KIO_3. Older study point out the positive role of low iodine concentrations on plants (Borst-Pauwels 1962). The author identified the positive effect of iodine on the growth of spinach, clover, tomato, turnip, barley, wheat and mustard. There was no effect of iodine on the growth of buckwheat, and a negative impact on oats. Dai et al. (2006) showed in their study that biomass productions of spinach was not affected by the addition of iodate and iodide.

Treatments in the present study did not affect the amount of chlorophyll *a* in the Tartary buckwheat sprouts. Amount of chlorophyll *a* was also not affected in pea sprouts, soaked in Se and I solution (Jerše et al. 2017). Similarly, in the study of Krzepilko et al. (2016) authors reported that in comparison with the control, KI did not affect chlorophyll content of lettuce seedlings. Amount of anthocyanins, which are often synthesised under stress conditions (Hawrylak-Nowak 2008) did not differ between the control sprouts and sprouts from treated seeds, which is consistent with results from study on pea sprouts (Jerše et al. 2017).

In the study on wheat seedlings Todirascu-Ciornea and Dumitru (2015) reported that 10^{-5} M solution of KIO_3 exerted significant strong influences, stimulating the chlorophyll *a* synthesis in comparison with the control. On the other hand, KIO_3 in concentration of 10^{-3} M did not affect content of chlorophyll *a*, while the KIO_3 10^{-4} M solution exerted even a slight inhibitory effect. Soaking seeds of common buckwheat in iodate solution increases the amount of chlorophyll *a* in common buckwheat while the treatment with selenate and combination of selenate and iodate also did not affect the amount of chlorophyll *a* comparing to control sprouts (Germ et al. 2015). The amount of UV-B and UV-A compounds were similar in control sprouts and sprouts from treated seeds as was previously evidenced for kohlrabi sprouts (Osmić et al. 2017).

Potential photochemical efficiency of photosystem II was close to theoretical maximum 0.83, especially in the first experiment which is typical for unstressed green plants (Schreiber et al. 1996) in both control and sprouts from treated seeds. Values were close to 0.7 in the second experiment and similar between control sprouts and sprouts from treated seeds. Values close to 0.83 was observed in the study from Germ et al. (2015) and Osmić et al. (2017) studying the effect of Se and I in different forms on common buckwheat (*Fagopyrum esculentum*) sprouts and kohlrabi sprouts (*Brassica oleracea* L. var. *gongylodes* L.) respectively. In addition ETS activity did not differ between control and treated groups in the second experiment. According to the results from potential photochemical efficiency of photosystem II, ETS activity and the amount of anthocyanins, none of the treatments presented stress conditions for Tartary buckwheat sprouts.

Rutin is a secondary metabolite that prevent herbivory by larvae of specific species of insects (Simmonds 2003). Rutin concentration in mature cotyledon in common buckwheat was very high in the study from Suzuki et al. (2005) which was much higher than other defence compounds of plant. Therefore, authors presumed that also in cotyledon rutin may have a role to prevent consumption by insects. Several researchers evidenced that rutin functions as a UV screen under high solar radiation (Mahdavian et al. 2008). However, in the study from Suzuki et al. (2005), rutin concentration was high even in buckwheat cotyledons that were grown under darkness. Authors proposed that this result suggests that rutin in buckwheat cotyledons may have other roles, such as enhancement of the defence system against cold stress or desiccation stress in Tartary buckwheat leaves in addition to protection against herbivory and UV screening. In the present study, the amount of rutin was the highest in control sprouts. Treatment with iodate and combination with selenate and iodate lowered

the amount of rutin comparing to control in the first experiment. However, the pattern did not repeat in the second experiment. The practical view of the research would be the recommendation, if the amount of Se and I in the sprouts from treated seeds, would be suitable for human consumption. Thus, the amount of Se and I have to be measured in sprouts from treated seeds before recommended them as functional food for humans.

Conclusions

The aim of our study was to found out effect of selenate (Se(VI)), iodate (I(V)) and their combination on morphological, physiological and biochemical properties of Tartary buckwheat sprouts. The soaking seeds in solution of iodate and combination between selenate and iodate lowered germination of sprouts. There was no effect of the treatments on the amount of chlorophyll *a,* anthocyanins and UV absorbing compounds. The amount of rutin was the highest in control sprouts. According to physiological measurements, the treatments did not impose stress to Tartary buckwheat sprouts. Biofortified plants with elements like Se are used in human diet. However, the amount of Se and I have to be measured in spouts from treated seeds before we can recommend them as food for humans.

Povzetek

Semena tatarske ajde so bogata z aminokislinami, vitamini, minerali in s fenolnimi snovmi kot je rutin. Rutin se nahaja večinoma v cvetovih in v zelenih delih rastline. Z raziskavo smo želeli ugotoviti, ali izpostavitev semen tatarske ajde Se(VI) in I(V) ter Se(VI) + I(V), vpliva na rast in biokemijske lastnosti kalic tatarske ajde. Selen je esencialen element za človeka in živali, saj omogoča normalno delovanje od selena odvisnih encimov, hkrati pa ima pozitivne lastnosti protivnetnega delovanja in deluje proti nastanku nekaterih vrst raka in srčnih bolezni. Selen in jod sta v tesni biološki povezavi, saj so od selena odvisni nekateri encimi družine jodotironin dejodinaze; pomanjkanje selena lahko učinkuje na presnovo joda v organizmu. Interakcija selena z jodom med privzemom v rastline ali v presnovnih procesih znotraj rastline še ni popolnoma pojasnjena.

Semena tatarske ajde smo izpostavili Se(VI), I(V) ter Se(VI) + I(V). Ko so semena vsrkala raztopine, smo jih prestavili v rastno komoro. Po treh tednih rasti smo opravili morfološke in biokemijske meritve. Izvedli smo dve ponovitvi. Kalivost semen je bila najvišja pri kontroli in pri kalicah tatarske ajde, katerih semena so bila izpostavljena Se(VI), nižja kalivost je bila izmerjena pri kalicah iz semen, izpostavljenih I(V) ali Se(VI) + I(V). Iz izmerjenega razmerja F_v/F_m sklepamo, da tretiranja semen tatarske ajde s Se(VI), I(V) ali Se(VI) + I(V) niso negativno vplivala na kalice, saj je bilo razmerje F_v/F_m podobno vrednostim kontrolne skupine. Aktivnost elektronskega transportnega sistema (ETS) je bila najnižja pri kontrolni skupini v prvem eksperimentu, v drugem treatiranje semen ni vplivalo na aktivnost ETS pri kalicah. Obravnavanja niso vplivala na vsebnost klorofila *a*, antocianov in UV zaščitnih snovi. Vsebnost rutina je bila najvišja v kontrolnih kalicah. Glede na rezultate fizioloških meritev, kalice tatarske ajde niso bile izpostavljene stresnim razmeram.

Acknowledgments

The authors acknowledge the financial support from the Slovenian Research Agency research core funding Biology of plants P1-0212 and the projects The effect of iodine and selenium on growth and quality of crops, J4-5524 and Optimisation of barley and buckwheat processing for sustainable use in high quality functional foods, L4-7552, Lokalno pridelana ajda kot surovina za proizvodnjo kakovostnih živil (Slovene), L4-9305, Raziskave ionoma kulturnih rastlin za pridelavo varne in kakovostne hrane (Slovene), J7-9418, were financially supported by the Slovenian Research Agency.

References

Borst Pauwels, G.W.F.H., 1962. An investigation into the effects of iodide and iodate on plant growth. Plant and Soil 16, 284–292.

Dai, J.L., Zhu, Y., Huang, Y.Z., Zhang, M., Song, J. L., 2006. Availability of iodide and iodate to spinach (Spinacia oleracea L.) in relation to total iodine in soil solution. Plant and Soil 289, 301–308. doi: 10.1007/s11104-006-9139-7

Drumm, H., Mohr, H., 1978. The mode of interaction between blue (UV) light photoreceptor and phytochrome in anthocyanin formation of the sorghum seedling. Photochemistry and Photobiology 27, 241–248.

Dziedzic, K., Górecka, D., Szwengiel, A., Olejnik, A., Rychlik, J., Kreft, I., Drożdżyńska, A., Walkowiak, J., 2018. The cytotoxic effect of artificially digested buckwheat products on HT-29 colon cancer cells. Journal of Cereal Science 83, 68–73.

Germ, M., Kacjan Maršić, N., Turk, J., Pirc, M., Golob, A., Jerše, A., Kroflič, A., Šircelj, H., Stibilj, V., 2015. The effect of different compounds of selenium and iodine on selected biochemical and physiological characteristics in common buckwheat and pumpkin sprouts. Acta Biologica Slovenica 58(1), 35–44.

Germ, M., Kreft, I., Osvald, J., 2005. Influence of UV-B exclusion and selenium treatment on photochemical efficiency of photosystem II; Yield and respiratory potential in pumpkins (*Cucurbita pepo* L.). Plant Physiology and Biochemistry 43, 445–448.

Golob, A., Germ, M., Kreft, I., Zelnik, I., Kristan, U., Stibilij, V., 2016. Selenium uptake and Se compounds in Se-treated buckwheat. Acta Botanica Croatica 75(1), 17–24.

Hawrylak-Nowak, B., 2008. Changes in anthocyanin content as indicator of maize sensitivity to selenium. Journal of Plant Nutrition 31, 1232–1242.

Jerše, A., Kacjan Maršić, N., Šircelj, H., Germ, M., Kroflič, A., Stibilj, V., 2017. Seed soaking in I and Se solutions increases concentrations of both elements and changes morphological and some physiological parameters of pea sprouts. Plant Physiology and Biochemistry 118, 285–294.

Ji, H., Tang, W., Zhou, X., Wu, Y., 2016. Combined effects of blue and ultraviolet lights on the accumulation of flavonoids in Tartary buckwheat sprouts. Polish Journal of Food and Nutrition Sciences 66(2), 93–98. doi: 10.1515/pjfns-2015-0042.

Kenner, A.A., Ahmed, S.I., 1975. Measurements of electron transport activities in marine phytoplankton. Marine Biology 33, 119–127.

Kim, S.L., Kim, S.K., Park, C.H., 2004. Introduction and nutritional evaluation of buckwheat sprouts as a new vegetable. Food Research International 37, 319–327.

Krzepilko, A., Zych-Wezyk, I., Swiecilo, A., Molas, J., Skwarylo-Bednarz, B. 2016. Effect of iodine biofortification of lettuce seedlings on their mineral composition and biological quality. Journal of Elementology 21(4), 1071–1080. doi: 10.5601/jelem.2015.20.4.1022

Kreft, I., Fabjan, N., Yasumoto, K., 2006. Rutin content in buckwheat (*Fagopyrum esculentum* Moench) food materials and products. Food Chemistry 98(3), 508–512. doi: 10.1016/j.foodchem.2005.05.081

Lichtenthaler, H.K., Buschmann, C., 2001a. Extraction of photosynthetic tissues: chlorophylls and carotenoids. Current Protocols in Food Analytical Chemistry, F4.2.1-F4.2.6. John Wiley in Sons Inc., New York.

Lichtenthaler, H.K., Buschmann, C., 2001b. Chlorophylls and carotenoids: measurement and characterisation by UV-VIS. Current Protocols in Food Analytical Chemistry, F4.3.1-F4.3.8. John Wiley in Sons Inc., New York.

Mahdavian, K., Kalantari, K.M., Ghorbanli, M., Torkzade, M., 2008. The effects of salicylic acid on pigment contents in ultraviolet radiation stressed pepper plants. Biologia Plantarum 52(1), 170–172.

Nakamura, K., Naramoto, K., Koyama, M., 2013. Blood-pressure-lowering effect of fermented buckwheat sprouts in spontaneously hypertensive rats. Journal of Functional Foods 5, 406–415.

Nawaz, F., Ashraf, M.Y., Ahmad, R., Waraich, E.A., Shabbir, R., Hussain, R.A., 2017. Selenium supply methods and time of application influence spring wheat (*Triticum aestivum* L.) yield under water deficit conditions. Journal of Agricultural Science 155, 643–656.

Osmić, A., Golob, A., Germ, M., 2017. The effect of selenium and iodine on selected biochemical and morphological characteristics in kohlrabi sprouts (*Brassica oleracea* L. var. *gongylodes* L.) Acta Biologica Slovenica 60(1), 41–51.

Piątkowska, E., Kopeć, A., Bieżanowska Kopeć R., Pysz, M., Kapusta-Duch, J., Koronowicz, A.A., Smoleń, S., Skoczylas, Ł., Ledwożyw-Smoleń, I., Rakoczy, R., Maślak, E., 2016. The impact of carrot enriched in iodine through soil fertilization on iodine concentration and selected biochemical parameters in Wistar rats. PLoS ONE 11(4), e0152680.

Pilon-Smits, E.A.H., Quinn, C.F., Tapken, W., Malagoli, M., Schiavon, M., 2009. Physiological functions of beneficial elements. Current Opinion in Plant Biology 12, 267–274.

Schreiber, U., Kühl, M., Klimant, I., Reising, H., 1996. Measurement of chlorophyll fluorescence within leaves using modified PAM fluorometer with a fiber-optic microprobe. Photosynthesis Research 47, 103–109.

Seppänen, M., Turakainen, M., Hartikainen, H., 2003. Selenium effects on oxidative stress in potato. Plant Science 165, 311–319.

Simmonds, M.S., 2003. Flavonoid–insect interactions: recent advances in our knowledge. Phytochemistry 64(1), 21–30.

Smoleń, S., Skoczylas, Ł., Rakoczy, R., Ledwożyw-Smoleń, I., Liszka-Skoczylas, M., Kopeć, A., Piątkowska, E., Bieżanowska-Kopeć, R., Pysz, M., Koronowicz, A., Kapusta-Duch, J., Sady, W., 2015. Selected aspects of nitrogen metabolism and quality of field-grown lettuce (*Lactuca sativa* L.) depending on the diversified fertilization with iodine and selenium compounds. Acta Scientiarum Polonorum Hortorum Cultus 14(5), 159–175.

Starowicz, M., Ciesarová, Z., Zieliński, H., 2017. Analysis of the antioxidative properties and Maillard reaction products in ginger cakes enriched with rutin. Madridge Journal of Food Technology 2(1), 44–52.

Suzuki, T., Kim, S.J., Yamauchi, H., Takigawa, S., Honda, Y., Mukasa, Y., 2005. Characterization of a flavonoid 3-O-glucosyltransferase and its activity during cotyledon growh in buckwheat (Fagopyrum esculentum). Plant Science 169, 943–948.

Todirascu-Ciornea, E., Dumitru, G., 2015. Effect of 2,4-dinitrophenol and potassium iodate on wheat. germination. International Journal of Latest Research in Science and Technology, 4(4), 93–100.

Todirascu-Ciornea, E., Drochioiu, G., Stefanescu, R., Axinte, E. V., Dumitru, G., 2016. Morphological and biochemical answer of the wheat seeds at treatment with 2,4-dinitrophenol and potassium iodate. Brazilian Archives of Biology and Technology 59, e16150580. doi: 10.1590/1678-4324-2016150580

Wieslander, G., Norback, D., 2001. Buckwheat allergy. Allergy 56, 703–704.

Wronkowska, M., Haros, M., 2014. Wet-milling of buckwheat with hull and dehulled - The properties of the obtained starch fraction. Journal of Cereal Science 60, 477–483.

ACTA BIOLOGICA SLOVENICA
LJUBLJANA 2018 Vol. 61, Št. 1: 93–102

Family Gammaridae (Crustacea: Amphipoda), mainly its *Echinogammarus* clade in SW Europe. Further elucidation of its phylogeny and taxonomy

Družina Gammaridae (Crustacea: Amphipoda), posebej njena veja *Echinogammarus* v JZ Evropi. Nadaljnja razjasnitev filogenetskih in taksonomskih odnosov

Boris Sket[a]*, Zhonge Hou[b]

[a] Biology department, Biotechnical faculty, University of Ljubljana, p.p. 2995, 1001 Ljubljana, Slovenia
[b] Institute of Zoology, Chinese Academy of Sciences, Beijing 100101, China

*correspondence: boris.sket@bf.uni-lj.si

Abstract: Most parts of the *Echinogammarus* clade of Gammaridae have been appropriately classified with the help of a molecular analysis, ultimately freed of the *Echinogammarus*-*Chaetogammarus* malediction. Among defining morphological characters, the gnathopod interrelations are comparatively well congruent with molecular markers. Genus *Homoeogammarus* distribution area extended from Mediterranean to Atlantic islands. *Chaetogammarus* and *Trichogammarus* are firm members of the morphologically very diversified Ponto-Caspian group genera, not closely related to the morphologically similar *Echinogammarus, Marinogammarus* or *Homoeogammarus*. Genus *Pectenogammarus* (along with *Neogammarus* and *Laurogammarus*) synonymized with *Homoeogammarus*. *Parhomoeogammarus* diagnose corrected, based on topotype samples of the type species. Freshwater species of the 'European *Eulimnogammarus*' in SW Europe defined as *Iberogammarus* gen. nov. Continental *Homoeogammarus*-like, but molecularly distinct group, defined as *Dinarogammarus* gen. nov. Some here accepted genera are molecularly well supported, some are morphologically difficult to distinguish, but each one is morphologically homogeneous; they are also geographically well defined. In both respects, the very speciose and widely spread *Homoeogammarus* is different.

Keywords: Amphipoda, Gammaridae, systematics, molecular phylogeny, biogeography, new genera

Izvleček: Večino taksonov klada *Echinogammarus* družine Gammaridae smo uspeli z molekulsko analizo primerno razvrstiti in končno rešiti prekletstva imen *Echinogammarus*-*Chaetogammarus*. Med morfološkimi znaki omogoča velikost gnatopodov I in II klasifikacijo, ki je dokaj skladna s klasifikacijo po molekulskih znakih. Izkazalo se je, da razširjenost rodu *Homoeogammarus* seže od sredozemskih otokov daleč v Atlantik. *Chaetogammarus* in *Trichogammarus* sta člana morfološko zelo razčlenjene ponto-kaspijske skupine rodov in nista blizu morfološko podobnim rodovom *Echinogammarus, Marinogammarus* ali *Homoeogammarus*. Rodovi *Pectenogammarus, Neogammarus* in *Laurogammarus* so sinonimni s *Homoeogammarus*.

Na osnovi topotipskih osebkov tipske vrste smo popravili diagnozo rodu *Parhomoeogammarus*. Sladkovodne vrste 'evropskega *Eulimnogammarus*' iz JZ Evrope smo definirali kot *Iberogammarus* gen. nov.. Kontinentalne populacije, podobne rodu *Homoeogammarus*, vendar molekulsko drugačne, smo definirali kot *Dinarogammarus* gen. nov.. Nekateri tukaj definirani rodovi so molekulsko podprti, nekatere je težko določiti morfološko, vsak zase pa je morfološko enoten; so tudi geografsko definirani. Vrstno razčlenjen in geografsko zelo razširjen rod *Homoeogammarus* je težko definirati le morfološko.

Ključne besede: Amphipoda, Gammaridae, sistematika, molekulska filogenija, biogeografija, novi rodovi.

Introduction

The previous attempt to classify the family Gammaridae on numerous samples from the entire distribution area, of the essentially entire ecological range and with most of its supposedly subordinate groups, has shown that a purely morphological characterisation can not give us a phylogenetically plausible system. The most surprising result of molecularly grounded studies is the nesting of endemic, highly aberrant (disparate) endemic 'families' from the lake Bajkal (e.g. Baikalogammaridae, Macrohectopidae, Pallaseidae; Lowry and Myers 2013, Kamaltynov 1999, Tahteev 2000), within the genus *Gammarus*; this had been pointed out by Macdonald et al. (2005) and verified by Hou and Sket (2016). Similar is the situation with Pontic families (Pontogammaridae beside Gammaridae; Grabowski 2014, Lowry and Myers 2013) which however still retained a phylogenetic status of genera, but within the family Gammaridae.

Gammaridae with shortened endopodite of uropod III make the family particularly difficult to classify. Even among the molecularly well supported genus *Gammarus* outside the strange Bajkal, there are species, which have erroneously been classified as separate genera, like *Fontogammarus* (S. Karaman 1931).

The majority of gammarids with shortened uropod III endopodite have been classified as species of *Echinogammarus* or *Chaetogammarus*, some of them changing their position between these two genera, occasionally completed by *Marinogammarus* and some others. The authors either did not make much effort with reasoning their decisions or the reasoning was not very convincing. But even the very serious attempt of Stock (1968) gave no happy result.

After the ancient Schellenberg's (1937a), among the most comprehensive revisions were made by Stock (1968) and by Karaman (1977a). Stock synonymized the taxa *Homoeogammarus, Parhomoeogammarus, Ostiogammarus* with *Echinogammarus,* while in *Chaetogammarus* he united the Pontocaspian member with some Mediterranean and Atlantic species. Karaman included *Chaetogammarus, Marinogammarus, Pectenogammarus,* the European *Eulimnogammarus* into *Echinogammarus* and rejected the majority of previously used taxonomical characters as not being genus specific. Later, Karaman (1977b) rejected also the genus *Neogammarus*. Nevertheless, Lowry and Myers (2013) revived all these genera (except *Eulimnogammarus*).

Only recently (Hou and Sket 2016) a molecularly based analysis separated most of above mentioned genera. However, some parts of the family still remained unresolved. The most confusing is the Stock's (1969) 'west European *Eulimnogammarus*', homonymous with a Bajkalian genus, but evidently being molecularly close to European genera. In this paper we are trying to solve this and some additional problems.

Material and methods

Samples

Animals were caught by a hand net and preserved in 96% ethanol, exchanged after the first fixation. At least taxonomically important parts

of the biochemically treated specimens have been preserved for a later morphological examination and/or study.

This paper is aimed to answer some phylogenetic and taxonomical questions left open in Hou and Sket (2016). We could direct our sampling mainly to areas of highest diversity at the genus level, which appeared to be the SW Europe and the shallow seas washing it. This includes the Macaronesian islands, Canaries and Madeira. The main subject of the analysis are groups of the clade *Echinogammarus*, while the clades *Gammarus* and *Sarothrogammarus* have only been used in some comparisons, evaluations.

As genera have been designated the sub-clades characterised by a high molecular or morphological singularity (e. g. *Iberogammarus*) or separated by other branches of such a character (e. g. *Chaetogammarus* within the Ponto-Caspian group of genera), if at least 80% support.

Therefore, our attention was focused on obtaining topotype samples of species, particularly type species of established or potential genera. We only attributed the species identity to samples from type localities and being morphologically adequate. The species identity can only be assured in topotype samples, since even the morphology of a population may change through the year (Pinkster 1988). For some details on sampling see Hou and Sket (2016).

Molecular methods

Total genomic DNA was extracted from specimens using the Tiangen Genomic DNA kit. Four different gene regions were amplified with primers in Hou *et al*. (2011), including nuclear fragments of 28S rRNA, 18S rRNA, elongation factor 1a (EF-1a), and a portion of mitochondrial cytochrome oxidase subunit I (COI). Sequence chromatograms were proofed and edited using Sequencher 4.2 DEMO (Gene Codes Corporation, Inc). Sequences were aligned using Clustal X (Thompson *et al*. 1997) and adjusted by eye using MacClade 4.06 (Maddison and Maddison 2000). The COI and EF-1a fragments were translated using *Drosophila* mitochondrial DNA or universal genetic code on MacClade to check for the pseudogenes.

The best-fitting partitioning schemes and nucleotide substitution models were selected using PartitionFinder 1.1.1 with the Bayesian information criterion (Lanfear *et al*. 2012). The four-partition scheme defined by gene region was selected as best-fitting scheme, 28S with SYM+I+G substitution model, COI with TIM+I+G model, 18S with GTR+I+G model and EF-1a with TrNef+I+G model. The phylogeny was reconstructed under maximum parsimony (MP) and maximum likelihood (ML). MP analyses were performed using PAUP* 4.0b10 (Swofford 2002). All phylogenetically uninformative characters were excluded from the analysis, and gaps were treated as missing data. Heuristic searches were conducted using tree bisection reconnection branch swapping, with a limit of one million rearrangements for each replicate. Bootstrap support indices were generated based on 1000 bootstrap replicates with ten random-addition sequences. ML analysis was performed using RAxML 8.2.9 (Stamatakis 2014), staring with 1000 rapid bootstrap replications followed by a thorough tree search. The GTR-GAMMA model of rate heterogeneity was used for the four-gene partition scheme. To compare the tree topology, ML analysis was implemented using GARLI 2.01 (Genetic Algorithm for Rapid Likelihood Inference; Zwickl, 2006), with four-gene partition model.

Results

The alignment of the combined data set contained 266 taxa (Table S1) with 5149 base pairs (bp), including 1507 bp for 28S, 656 bp for COI, 2385 bp for 18S, and 601 bp for EF-1a. All new sequences were deposited in GenBank (accession numbers MK159866–MK159939, MK176331, MK176332). The MP and ML analyses produced congruent phylogenetic trees, except for a few disagreements with lower support values. The main discrepancy was tip nodes within the Ponto-Caspian group of genera, with short branches.

A number of purposely collected new samples-taxa caused no substantial change in the previously (Hou and Sket 2016) constructed parts of the phylogram, but clarified some previously unclear situations (Fig. 1 and Suppl. Fig. 1).

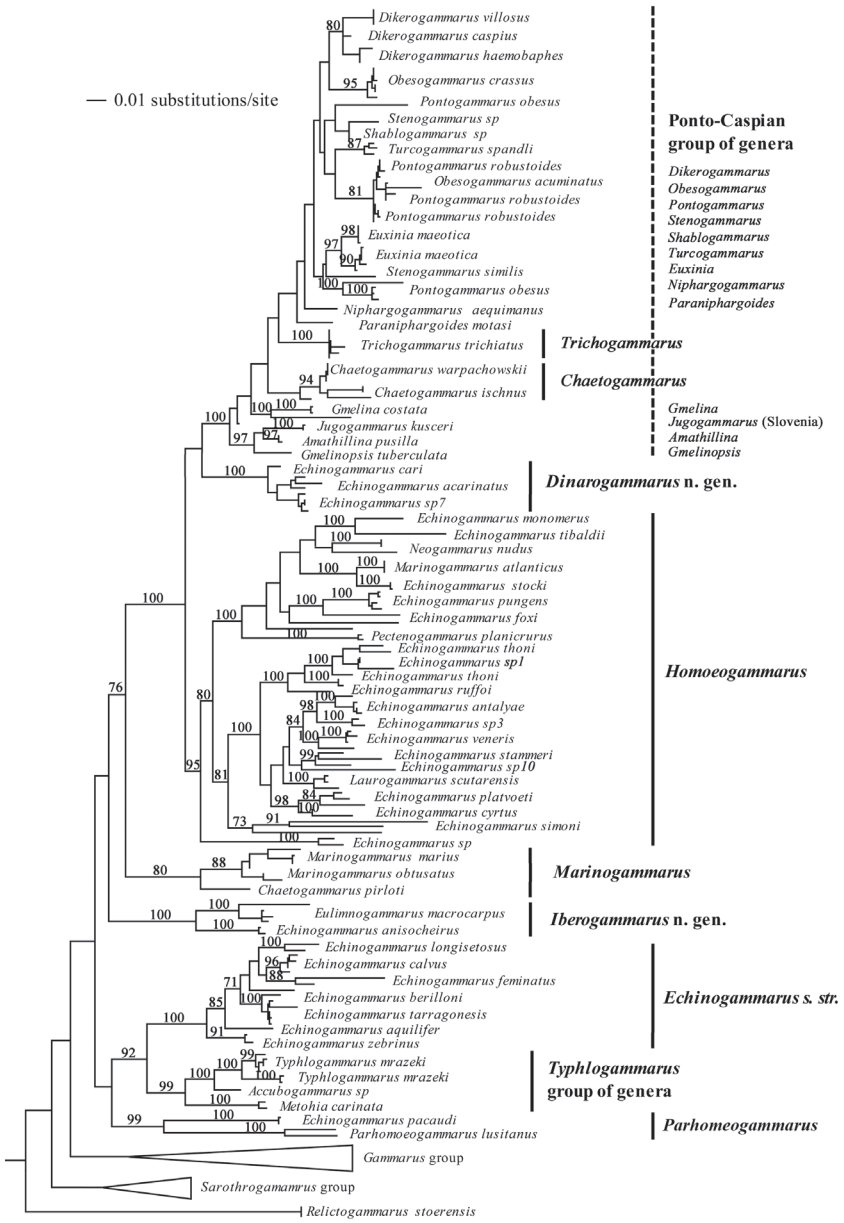

Figure 1: Maximum likelihood phylogenetic tree of *Echinogammarus* based on the combined analysis of mitochondrial (COI) and nuclear (28S, 18S and EF-1a) markers. Numbers represent statistical bootstrap supports of nodes. Taxonomical information is presented in S2.

Slika 1: Filogenetsko drevo veje *Echinogammarus* po analizi maximum likelihood (ML) na osnovi kombiniranih mitohondrijskih (COI) in jedrnih (28S, 18S and EF-1a) podatkov. Številke nad vejami so vrednosti ML bootstrap. Vrstna imena so provizorična, taksonomske rešitve so prikazane v S2.

After basally branching off of the *Relictogammarus* and the *Sarothrogammarus* clades, the gammarids divide into the *Gammarus* clade with generally plesiomorphic uropod III (with well developed endopodite) and the *Echinogammarus* clade with generally apomorphic uropod III (with more or less reduced endopodite). The plesiomorphy of the mentioned character (discussed by Hou and Sket 2016) is not in accord with the sequence of the tree branching.

The *Echinogammarus* clade is further clearly split into a number of well supported monophyla, while the sequence of branching off events is unclear, poorly supported. Well supported groups within the *Echinogammarus* large clade are:

- *Parhomoeogammarus* clade,
- *Echinogammarus* + *Typhlogammarus* group genera as well as each of both separately,
- 'W European *Eulimnogammarus*' (sensu Stock 1969) clade,
- *Marinogammarus* clade,
- *Homoeogammarus* + Dinaric + Pontocaspian genera group as well as each of the last mentioned branches separately; *Chaetogammarus* and *Trichogammarus* are morphologically similar to *Echinogammarus* or *Homoeogammarus*, but molecularly clearly nested within the morphologically very different and very diverse Pontocaspian group.

Beside the strong molecular similarity, there are rarely strong, but mostly weak morphological differences between these branches. Morphologically well distinguished are *Echinogammarus* s. str., *Typhlogammarus* group, '*Eulimnogammarus*'; less distinct are *Marinogammarus, Parhomoeogammarus*, while morphologically indistinct are geographically and molecularly well defined, mainly coastal *Homoeogammarus* and the continental Dinaric branch.

Discussion

Within the morphologically very diverse Ponto-Caspian group, there are again morphologically and molecularly distinct and well supported branchlets: *Chaetogammarus* and *Trichogammarus (sensu* Hou and Sket 2016); they are the only Ponto-Caspians morphologically similar to *Homoeogammarus*. We will be able to classify the morphologically and molecularly very diverse rest of Ponto-Caspian genera (and species) only when we obtain more complete series of samples from Caspian area. All authors agree that they have to be divided between a number of genera, but their definitions and species contents have been conceived highly diversely (Birštejn and Romanova 1968, Barnard and Barnard 1983, Karaman and Barnard 1979, Stock 1974).

It could be shown that *Gammarus anisocheirus* Ruffo which was (in the lack of the type sample of *E. lusitanus*) by Hou and Sket 2016 presented as a 'questionable *Parhomoeogammarus* member', is in fact not related to the type species *Gammarus (Parhomoeogammarus) lusitanus* Schellenberg 1943. Two populations of *P. lusitanus* form a well supported clade which includes also *Echinogammarus pacaudi* Hubault and Ruffo 1956, thus forming the genus *Parhomoeogammarus* Schellenberg 1943. On the other hand, *G. anisocheirus* could now be enthroned a type species of *Iberogammarus* **gen. nov.**, comprising species of the Stock's (1969) 'European *Eulimnogammarus*', which used to pose a particular phylogenetic and biogeographical enigma. *G. anisocheirus* has already been attributed to that group by Pinkster and Stock (1970) for its morphological similarity. In our new tree, *Iberogammarus* is a well supported monophyletic branch with *G. anisocherirus* and some populations resembling *E. grandimanus*.

(1) Genus *Homoeogammarus* Schellenberg 1937

(= *Echinogammarus* p. p.) remains the most speciose and the widely spread group of the *Echinogammarus* clade, its majority is relatively morphologically unified, with an extensive distribution area in Mediterranean and Atlantic.

Beside the previously (Hou and Sket 2016) listed species, according to further molecular analysis it includes also the following members: *Marinogammarus atlanticus* Dahl, 1958, *Neogammarus festae* Ruffo, 1937, *Pectenogammarus planicrurus* Reid, 1940. So, we can confirm the previous suppositions that the genus *Pectenogammarus* Reid, 1940 is superfluous, and so are

Neogammarus Ruffo, 1937 and *Laurogammarus* G. Karaman, 1984 (Karaman 1977, Hou and Sket 2016). But inclusion of the molecularly relevant species into *Homoeogammarus* makes it even more difficult to morphologically diagnose this genus. Opposite to the hint by Hou and Sket 2016, *Echinogammarus spinulicornis* Pinkster and Stock 1971 is not a member of *Parhomoeogammarus*, it is now a molecularly proven *Homoeogammarus* sp., inhabiting freshwater affluents of the Atlantic.

Biogeographically important is the fact that some *Homoeogammarus* spp. are present far within the Atlantic area. *H. planicrurus* reaches from French Mediterranean coast to the Great Britain. *H.* cf. *atlanticus* is present in the Atlantic Madeira, most probably (Dahl 1958; not molecularly proven) it is conspecific with *H. atlanticus* from Azores; its closest counterpart is the Adriatic *H.* cf. *stocki*, while we were not able to obtain the Canarian and topotypic samples of the Mediterranean '*Chaetogammarus*' *olivii* (H. Milne Edwards 1830) with which *H. atlanticus* might also be conspecific (Stock 1995). Our efforts to sample probably related *Gammarus nox* Stock 1995 (Madeira) and *Chaetogammarus chaetocerus* Beyer and Stock 1994 (La Gomera) were not successful. The Italian Peninsula and adjacent big islands are occupied by species of *Homoeogammarus* also inland (Ruffo and Stoch 2006), while in other parts of the Mediterranean, they are limited to narrow coastal belts (estuaries and coastal springs).

(2) The Stock's (1969) taxon 'western European (species of) *Eulimnogammarus*'

Stock (1969) classified his species *Eulimnogammarus macrocarpus* Stock 1969, along with *Gammarus anisocheirus* Ruffo 1959 and with the marine *Gammarus obtusatus* Dahl 1938 into the noted Bajkalian genus *Eulimnogammarus* Bazikalova 1945. Molecular analysis has shown that (1) the genuine Bajkalian *Eulimnogammarus* is phylogenetically a member of the genus *Gammarus* (Hou and Sket 2016) and endemic to lake Bajkal, well distinguished from *Echinogammarus* and its relatives, (2) *G. obtusatus* appears to be a member of *Marinogammarus* (Hou and Sket 2016), (3) *G. anisocheirus* is related to *E. macrocarpus*, but not closely related to *Gammarus* (or *Eulimnogammarus*). Our present tree clearly shows that *G. anisocheirus* and *E. macrocarpus* can form a separate genus, weakly related to *Marinogammarus* and *Homoeogammarus*, but not to *Gammarus*. This is the rationale of the here established *Iberogammarus* **gen. nov.**

***Iberogammarus* gen. nov.** syn. western European (species of) *Eulimnogammarus* Stock 1969 p. p. (Pinkster and Stock 1972).

Type species *Gammarus anisocheirus* Ruffo 1959; type locality is a hygropetric confluent of Neste d'Aure, at St. Lary-Soulan, Hautes-Pyrénées, France (825 m a.s.l.).

Additional species: molecularly proven *Eulimnogammarus* cf. *macrocarpus*. Not molecularly proven *Eulimnogammarus macrocarpus* Stock 1969, *Eulimnogammarus toletanus* Pinkster and Stock 1970.

Genus diagnosis. Gammariform amphipods from SW Europe (Iberian Peninsula), similar to *Homoeogammarus*, but with markedly different gnathopods; gnathopod propodite II only less than 80% length and up to 60% width of propodite I. Uropod III endopodite 20-50% exopodite length, linear, with a terminal and one or more marginal spines; exopodite with marginal groups of spines and variable setation.

Distribution. Fresh waters of Central and NE part of Iberian Peninsula, including central Pyrenees.

Remark. The most reliable marker of *Iberogammarus* is the smaller and particularly the narrower gnathopod II propodite, which also differs remarkably in shape with its very short palmar margin. Besides, the uropod III endopodite bears also a marginal spine which is normally absent in *Homoeogammarus*; the setation and the endopodite length are very variable.

(3) Correction of the *Parhomoeogammarus* definition

Before obtaining a sample of the *Parhomoeogammarus* type species, we (Hou and Sket 2016) overestimated the similarity of *G. anisocheirus* with it. In both, gnathopod I is somehow larger than gnathopod II, which is a comparatively rare character in gammarids. Additional sampling allowed a correction of that mistake. Here, we have samples of two distant populations of the type species while *G. anisocheirus* was moved to a new genus (*Iberogammarus*). Corrected data are given here.

***Parhomoeogammarus* Schellenberg 1943 (mended diagnosis)** syn. *Gammarus (Parhomoeogammarus)* Schellenberg 1943.

Type species *Gammarus (Parhomoeogammarus) lusitanus* Schellenberg 1943, type locality Lugar de Mantelães, Paredes de Coura, Portugal.

Additional molecularly proven species *Gammarus (Echinogammarus) pacaudi* Hubault and Ruffo 1956.

Genus diagnosis. Gammariform amphipods from Iberian peninsula and SW France, similar to *Homoeogammarus*, but gnathopod propodite II may be equal to or slightly shorter (only ca 80% length of) than propodite I, while they are approximately equally wide. Eyes elongated, more than twice as long as wide. Pereopod VII basis proximally convex, distally tapering, without a marked distoposterior lobe. Uropod III endopodite less than 25% exopodite long, scale-shaped to linear, with terminal and marginal spines; exopodite with marginal groups of spines and long setae.

Distribution. The genus seems to be limited to fresh waters in northern Portugal and adjacent NW Spain (all between Porto and A Coruña), SW France and NE Spain (Pinkster 1993).

Remarks. For *P. pacaudi*, the dentate posterior margin of pleonites ('l'armature caractéristique du métasome' Hubault and Ruffo 1956) was denoted the primary specific character. In fact, within the type population there are also individuals with unarmed pleonites. Both cohabiting (syntopic) morphs are molecularly indistinguishable.

Another putative candidate for this genus, *Echinogammarus spinulicornis* Pinkster and Stock 1971 (Hou and Sket 2016), appeared to be a *Homoeogammarus* (see above), although a very aberrant one.

(4) Continental Dinaric gammarids

Inland parts of the western Balkans host a group of gammarids, morphologically similar and provisionally attached to *Homoeogammarus*, making that genus paraphyletic. Some additional samples confirmed the geographical distinctness of this group and forced us to establish for it a separate genus.

***Dinarogammarus* gen. nov.**
Echinogammarus Stebbing, 1899 p.p.,
Ostiogammarus S. Karaman, 1931 p.p.
(e.g. *O. acarinatus*).

Type species *Ostiogammarus acarinatus* S. Karaman 1931a, Karaman 1970 (syn. *Gammarus pungens* forma *acarinata* Schäferna, 1922 p.p.), type locality spring Vrelo Bune, Blagaj, Mostar, Bosnia and Herzegovina. Additional species, molecularly confirmed: *Gammarus cari* S. Karaman, 1931b*, Ostiogammarus cari bosnensis* S. Karaman, 1934.

Genus diagnosis. Gammariform amphipods, morphologically indistinguishable from *Homoeogammarus.* Pereon and pleon dorsally smooth, each telson lobe less than twice as long as broad. Antennae I and II normal, antenna II shorter than antenna I; antena II with short or long, dense or sparse, straight setae. Mouth parts as in *Gammarus*. Gnathopods I and II subchelate, propodite II slightly longer than propodite I. Coxal plate IV distoposteriorly lobate. Pereopod VII basis without a distoposterior lobe. Uropods I and II usually normal, with distal and lateral spines. Uropod III exopodite with marginal groups of spines, usually accompanied by long setae that are always straight; endopodite diminished and scale-like, with terminal spine(s) only (without facial or marginal spines)

Distribution. Fresh waters (springs and rivers) in Dinaric karst from Ogulin in NW to Mostar in SE (within the rhomboid: Ogulin – Knin – Mostar - Travnik – Ogulin), away from the Adriatic coast. A local contact or shuffling with the coastal *Homoeogammarus* spp. is not impossible, but at the

moment, no case of shared locality of both genera was molecularly signalled. Some *Dinarogammarus* localities are in the Danube drainage (confluents of Sava river), the others in the confluents of the Adriatic. All *Homoeogammarus* localities in Dinaric area are in the Adriatic drainage, close to coast or even intertidal.

(5) The *Echinogammarus-Typhlogammarus* genera complex

appears now to consist of two biogeographically distinct (groups of) genera. The subgroup-genus *Echinogammarus* (s. str.) inhabits originally epigean fresh waters of SW Europe. The *Typhlogammarus* group seems to be limited to fresh subterranean waters of Dinaric karst; all species are highly troglomorph.

Acknowledgement

We are obliged to the collectors of many samples, their names are listed in Suppl. table 1. Thanks also to Pedro Oromi (La Laguna) for his help in the search for Canarian species. The study was financially supported by National Natural Sciences Foundation of China (NSFC-31372156/31422048) to ZH. Thanks to our colleagues Fabio Stoch, Rudi Verovnik and Christophe Piscart for some useful remarks. Thanks to Lučka Sket for her patience and manysided support during field work.

We must ask for excuse all colleagues who were or are not able to find some necessary data in Hou and Sket 2016. Due to some technical problems, some files disappeared from 'supporting files', prepared for that paper.

References

Barnard, J.L., Barnard, C.M., 1983. Freshwater Amphipoda of the world. Mt. Vernon, VA: Hayfield Associates.

Bazikalova, A.J., 1945. Amfipody ozera Bajkala. Trudy Bajkalskoj limnologičeskoj stancii, 11, 1-440.

Beyer, G., Stock, J.H., 1994. Epigean freshwater Gammaridae (Crustacea, Amphipoda) from La Gomera (Canary Islands). Bijdragen tot de Dierkunde 64(2), 101-114.

Birštejn, J.A., Romanova, N.N., 1968. Otrâd bokoplavy. Amphipoda. Atlas bezpozvonočnyh Kaspijskogo morâ. Moskva: Izdatelstvo Piščevaâ promyšlennost, 1–416.

Dahl, E., 1958. Fresh and brackish ater amphipods from the Azores and Madeira. Boletim do Museu municipal do Funchal 11(27), 5-25.

Grabowski, M., 2014. Check-list for Ponto-Caspian amphipods (brackish and freshwater) Caspian Sea Biodiversity Project under umbrella of Caspian Sea Environment Program. Available at: http://www.zin.ru/projects/caspdiv/caspian_amphipods.html (accessed 15 August 2017).

Hou, Z., Sket, B., Fišer, C., Li, S., 2011. Eocene habitat shift from saline to freshwater promoted Tethyan amphipod diversification. Proceedings of the National academy of sciences of the United States of America 108(35), 14533–14538.

Hou, Z., Sket, B., 2016. A review of Gammaridae (Crustacea: Amphipoda): the family extent, its evolutionary history, and taxonomic redefinition of genera. Zoological journal of the Linnean society 176(2), 323–348.

Hubault, E., Ruffo, S., 1956. *Gammarus (Echinogammarus) pacaudi* nov. sp. Bulletin societe zoologique France 81, 99-106.

Kamaltynov, R.M., 1999. On the higher classification of Lake Baikal amphipods. Crustaceana 72, 933–944.

Karaman, G.S., 1970. XXV. prilog poznavanju Amphipoda. Kritička zapažanja o vrstama *Echinogammarus acarinatus* (S. Kar. 1931) i *Echinogammarus stocki* n. sp. Poljoprivreda I Šumarstvo, Titograd 16, 1-2, pp. 193-214.

Karaman, G.S., 1977a. Revision of the *Echinogammarus* genera-complex (Fam. Gammaridae). Arhiv bioloških nauka (Beograd) 27(1957) (1-2), 69-93.

Karaman, G.S., 1977b. The value of genus *Neogammarus* (Ruffo 1937) and its relation to the genus *Echinogammarus* Stebb. 1889 (Fam. Gammaridae). Animalia 4(1/2), 109-121.

Karaman, G.S., 1984. The genus *Laurogammarus*, n. gen. (fa. Gammaridae) in Yugoslavia (Contribution to the knowledge of the Amphipoda 135). Bilten Društva ekologa Bosne i Hercegovine, Ser. B, 3, 29-35.

Karaman, G.S., Barnard, J.L., 1979. Classificatory revisions in Gammaridean Amphipoda (Crustacea), Part 1. Proceedings Biological society Washington 92(1), 106-165.

Karaman, S., 1931a. III. Beitrag zur Kenntnis der Amphipoden Jugoslaviens, sowie einiger Arten aus Griechenland. Prirodoslovne razprave 1, 31-66.

Karaman, S., 1931b. *Gammarus cari* n. sp. aus Westjugoslawien. Zoologischer Anzeiger 94, 265-268.

Karaman, S., 1934. VI. Beitrag zur Kenntnis jugoslawischer Süsswasseramphipoden. Zoologischer Anzeiger 107, 325-333.

Lanfear, R., Calcott, B., Ho, S.Y.W., Guindon, S., 2012. PartitionFinder: combined selection of partitioning schemes and substitution models for phylogenetic analyses. *Molecular Biology and Evolution* 29, 1695–1701.

Lowry, J.K., Myers, A.A., 2013. A Phylogeny and Classification of the Senticaudata subord. nov. (Crustacea, Amphipoda). *Zootaxa* 3610, 1–80.

Macdonald, K.S., Yampolsky, L., Duffy, J.E., 2005. Molecular and morphological evolution of the amphipod radiation of Lake Baikal. Molecular Phylogenetics and Evolution 35, 323–343.

Maddison, D.R., Maddison, W.P., 2000. MacClade 4: analysis of phylogeny and character evolution. Sunderland, MA: Sinauer Associates.

Pinkster, S., Stock, J., 1970. Western European species of the presumed Baikal - genus *Eulimnogammarus* (Crustacea - Amphipoda) with description of a new species from Spain. Bulletin Zoologisch Museum Universiteit van Amsterdam 1(14), 205-219.

Pinkster, S., Stock, J., 1971. Sur deux *Echinogammarus* limniques nouveaux du Bassin d'Aquitaine. Bijdragen tot de dierkunde 41(1), 37-51.

Pinkster, S., Stock J., 1972. Members of the *Echinogammarus simoni*-group and the genus *Eulimnogammarus* (Crustacea - Amphipoda) from Iberian Peninsula and North Africa, with descriptions of a new species. Bulletin Zoologisch Museum Universiteit van Amsterdam 2(10), 85-115.

Pinkster, S., 1993. A revision of the genus *Echinogammarus* Stebbing, 1899 with some notes on related genera (Crustacea, Amphipoda). Memorie del Museo Civico di Storia Naturale (serie 2a) Sezione Scienze della Vita, Verona 10, 1–185.

Pinkster, S., 1988. Problems in the taxonomy of the freshwater gammarids with special emphasis on the genus *Echinogammarus* in Italy. Crustaceana, Suppl. 13, 245-255.

Reid, D., 1940. On *Gamarus (Pectenogammarus) planicrurus* subg. et sp. n. (Crust. Amph.). Annals and magazine of natural history 11(6), 287-292.

Ruffo, S., 1937. Studi su Crostacei anfipodi V. Una nuova species di *Gammarus* del Mar Ligure. Annali del Museo civico di storia naturale di Genova 49, 438-446. *Neogammarus*

Ruffo, S., 1959. Una nuova specie di *Gammarus* (s. lato) della fauna francese (*Gammarus anisocheirus* n. sp.). Bulletin Museum Histoire Naturale, Paris 31, 435 – 439.

Ruffo, S., Stoch, F., 2006. Crustacea Malacostraca Amphipoda. In: Ruffo S., Stoch F. (eds.), Checklist and distribution of the Italian fauna. 10,000 terrestrial and inland waters species. Memorie del Museo Civico di Storia Naturale di Verona, 2. serie, Sezione Scienze della Vita 17, 109-111 (data on CD-ROM).

Schäferna, K., 1922. Amphipoda balcanica. Vestnik kralovske české společnosti nauk, Praha, 1921-1922, 12, 1-111.

Schellenberg, A., 1937a. Kritische Bemerkungen zur Systematik der Süsswassergammariden. Zoologische Jahrbücher, Abteilung Systematik 69, 469–516.

Schellenberg, A., 1937b. Schlüssel und Diagnosen der dem Süsswasser-*Gammarus* nahestehenden Einheiten ausschliesslich der Arten des Baikalsees und Australiens. Zoologischer Anzeiger 117, 267–280.

Schellenberg, A., 1943. Portugiesische Süsswasser-Amphipoden. Memorias e estudos do Museu zoologico da Universidade de Coimbra 139, 1–5.

Sexton, E.W., Spooner, G.M., 1940. An account of *Marinogammarus* (Schellenberg) gen. nov. (Amphipoda), with a description of a new species, *M. pirloti*. Journal of the marine biological association of the United Kingdom 24, 634– 682.

Stamatakis, A., 2014. RAxML version 8: a tool for phylogenetic analysis and post-analysis of large phylogenies. Bioinformatics 30, 1312.

Stock, J.H., 1968. A revision of the European species of the *Echinogammarus pungens* - group (Crustacea, Amphipoda). *Beaufortia* 16, 13–78.

Stock, J.H., 1969. Member of Baikal amphipod genera in European waters, with description of a new species, *Eulimnogammarus macrocarpus*, from Spain. Koninkl. Nederl. Akademie van Wetenschappen - Amsterdam, Ser. C 72(1), 66-75.

Stock, J.H., 1974. The systematics of certain Ponto-Caspian Gammaridae (Crustacea, Amphipoda). Mitteilungen Hamburg Zoologisches Museum Institut 70, 75-95.

Stock, J.H., 1995. *Gammarus* and *Chaetogammarus* (Crustacea, Amphipoda) from Macaronesia. Boletim do Museu municipal do Funchal 247(1993/1995), 41-52.

Swofford, D.L., 2002. PAUP*: Phylogenetic analysis using parsimony (and other methods). Sunderland, MA: Sinauer Associates.

Tahteev, V.V., 2000. Očerki o bokoplavah ozera Bajkal. Izdatelstvo Irkutskogo universiteta.

Thompson, J.D., Gibason, T.J., Plewniak, F., Jeanmougin, F., Higgins, D.G., 1997. The Clustal_X windows interface: flexible strategies for multiple sequence alignment aided by quality analysis tools. Nucleic Acids Research 25, 4876–4882.

Zwickl, D.J., 2006. Genetic algorithm approaches for the phylogenetic analysis of large biological sequence datasets under the maximum likelihood criterion. PhD thesis, University of Texas at Austin, Austin, TX. GARLI, version 1.0. Published by the author. Available at: http://www.nescent.org/wg_garli

ABS ACTA BIOLOGICA SLOVENICA
LJUBLJANA 2018 Vol. 61, Št. 2: 103–104

Slovenski simpozij o rastlinski biologiji z mednarodno udeležbo

Slovene symposium on plant biology with international participtaion

Raziskovalke Nacionalnega inštituta za biologijo (od leve proti desni: dr. Tjaša Lukan, dr. Anna Coll, dr. Tjaša Stare, Špela Tomaž in dr. Maruša Pompe Novak) so na simpoziju predstavile raziskave interakcije krompirja s krompirjevim virusom Y. (Foto: Marko Petek)

Slovensko društvo za biologijo rastlin je 17. in 18. septembra 2018 v Biološkem središču v Ljubljani organiziralo že 7. simpozij o rastlinski biologiji z mednarodno udeležbo. Zanimiv program z dvanajstimi vabljenimi predavatelji je privabil preko 100 udeležencev iz kar 12 držav, ki so svoje delo predstavili še v okviru 19 kratkih predavanj in 40 posterjev.

Slovensko društvo za biologijo rastlin, ki se bilo sicer ustanovljeno kot Slovensko društvo za rastlinsko fiziologijo, je aktivno od leta 1993 in združuje rastlinske biologe, ki delujejo na različnih področjih. Društvo simpozije organizira vsake 4 leta, prvi je bil organiziran leta 1993. Tokratni simpozij je pokrival različne tematike povezane z biologijo rastlin, od rastlinske filogenije, ekofiziologije, molekulske, celične in sistemske biologije do modernih tehnik rastlinske biologije.

Simpozij je otvoril prof. Johan Burger iz Stellenboch University iz Južne Afrike, ki je nazorno predstavil novo metodo žlahtnjenja rastlin, CRISPR/Cas9, ter uporabo te metode pri žlahtnjenju vinske trte. V diskusiji smo se dotaknili tudi izredno pereče teme regulacije novih tehnik žlahtnjenja v Evropski Uniji. V sekciji "Moderne tehnologije« so nato sledila predavanja o različnih tehnologijah, ki jih uporabljamo za spremljanje stanja rastlin na daljavo, njihovo zaščito pred škodljivci, žlahtnjenje in tudi ohranjanje ogroženih rastlinskih vrst. V sekciji »Rastlinska filogenija« so predavatelji predstavili uporabo visokozmogljivih metod transkriptomike in genomike v filogeniji ter

nakazali tudi na uporabnost filogenetskih dognanj biotehnologiji. V sekciji »Struktura in funkcija rastlin« so bile predstavljene različne metode za odkrivanje strukture rastlin ter povezave le-te z njihovo funkcijo pri rasti in razvoju ter odzivu na dejavnike okolja. V sekciji »Interakcije rastlin z okoljem« so predavatelji predstavili odgovor rastlin na sušo, svetlobo in težke kovine na strukturnem, molekulskem in ekološkem nivoju. V najobsežnejši sekciji, »Interakcije rastlin z drugimi organizmi« je dobršen del predavanj obravnaval različne vidike interakcije krompirja s krompirjevim virusom Y, ostala predavanja pa se dotaknila interakcij poljščin z drugimi povzročitelji bolezni, simbioz zelene hidre in biološke aktivnosti invazivnih rastlin. Simpozij smo vizionarsko zaključili s sklepnim predavanjem dr. Daniela Jacobsona iz Oak Ridge National Laboratory v ZDA, ki je predstavil pristope umetne inteligence in visokozmogljivega računalništva pri raziskavah različnih fenotipov in genotipov topola.

Simpozij je finančno podprlo sedem podjetij, Mediline d.o.o., Mettler Toledo d.o.o., VWR International GmbH, Omega d.o.o., Bia do.o.o., Chemass do.o. in Kemomed do.o.o. Biotehniška fakulteta Univerze v Ljubljani nam je odstopila predavalnice, založba Silva Slovenica pa je izdala zbornik. Vsem sponzorjem se zahvaljujemo.

Udeleženci smo se strinjali, da je simpozij pomemben tudi za povezovanje rastlinskih biologov v Sloveniji, saj je vzajemno razumevanje ekspertiz ključno za vzpostavitev formalnih sodelovanj. Ne dvomimo, da je sproščeno druženje o kavi, kosilu ali večerji spodbudilo veliko novih idej za bodoča sodelovanja.

Špela Baebler,
predsednica organizacijskega odbora

INSTRUCTIONS FOR AUTHORS

1. Types of Articles

SCIENTIFIC ARTICLES are comprehensive descriptions of original research and include a theoretical survey of the topic, a detailed presentation of results with discussion and conclusion, and a bibliography according to the IMRAD outline (Introduction, Methods, Results, and Discussion). In this category ABS also publishes methodological articles, in so far as they present an original method, which was not previously published elsewhere, or they present a new and original usage of an established method. The originality is judged by the editorial board if necessary after a consultation with the referees. The recommended length of an article including tables, graphs, and illustrations is up to fifteen (15) pages; lines must be double-spaced. Scientific articles shall be subject to peer review by two experts in the field.

REVIEW ARTICLES will be published in the journal after consultation between the editorial board and the author. Review articles may be longer than fifteen (15) pages.

BRIEF NOTES are original articles from various biological fields (systematics, biochemistry, genetics, physiology, microbiology, ecology, etc.) that do not include a detailed theoretical discussion. Their aim is to acquaint readers with preliminary or partial results of research. They should not be longer than five (5) pages. Brief note articles shall be subject to peer review by one expert in the field.

CONGRESS NEWS acquaints readers with the content and conclusions of important congresses and seminars at home and abroad.

ASSOCIATION NEWS reports on the work of Slovene biology associations.

2. Originality of Articles

Manuscripts submitted for publication in *Acta Biologica Slovenica* should not contain previously published material and should not be under consideration for publication elsewhere.

3. Language

Articles and notes should be submitted in English, or as an exception in Slovene if the topic is very local. As a rule, congress and association news will appear in Slovene.

4. Titles of Articles

Title must be short, informative, and understandable. It must be written in English and in Slovene language. The title should be followed by the name and full address of the authors (and if possible, fax number and/or e-mail address). The affiliation and address of each author should be clearly marked as well as who is the corresponding author.

5. Abstract

The abstract must give concise information about the objective, the methods used, the results obtained, and the conclusions. The suitable length for scientific articles is up to 250 words, and for brief note articles, 100 words. Article must have an abstract in both English and Slovene.

6. Keywords

There should be no more than ten (10) keywords; they must reflect the field of research covered in the article. Authors must add keywords in English to articles written in Slovene.

7. Running title

This is a shorter version of the title that should contain no more than 60 characters with spaces.

8. Introduction
The introduction must refer only to topics presented in the article or brief note.

9. Illustrations and Tables
Articles should not contain more than ten (10) illustrations (graphs, dendrograms, pictures, photos etc.) and tables, and their positions in the article should be clearly indicated. All illustrative material should be provided in electronic form. Tables should be submitted on separate pages (only horizontal lines should be used in tables). Titles of tables and illustrations and their legends should be in both Slovene and English. Tables and illustrations should be cited shortly in the text (Tab. 1 or Tabs. 1-2, Fig. 1 or Figs. 1-2; Tab. 1 and Sl. 1). A full name is used in the legend title (e.g. Figure 1, Table 2 etc.), written bold, followed by a short title of the figure or table, also in bold. Subpanels of a figure have to be unambiguously indicated with capital letters (A, B, …). Explanations associated with subpanels are given alphabetically, each starting with bold capital letter, a hyphen and followed by the text (A - text...).

10. The quality of graphic material
All the figures have to be submitted in the electronic form. The ABS publishes figures either in pure black and white or in halftones. Authors are kindly asked to prepare their figures in the correct form to avoid unnecessary delays in preparation for print, especially due to problems with insufficient contrast and resolution. Clarity and resolution of the information presented in graphical form is the responsibility of the author. Editors reserve the right to reject unclear and poorly readable pictures and graphical depictions. The resolution should be 300 d.p.i. minimum for halftones and 600 d.p.i. for pure black and white. The smallest numbers and lettering on the figure should not be smaller than 8 points (2 mm height). The thickness of lines should not be smaller than 0.5 points. The permitted font families are Times, Times New Roman, Helvetica and Arial, whereby all figures in the same article should have the same font type. The figures should be prepared in TIFF, EPS or PDF format, whereby TIFF (ending *.tif) is the preferred type. When saving figures in TIFF format we recommend the use of LZW or ZIP compression in order to reduce the file sizes. The photographs can be submitted in JPEG format (ending *.jpg) with low compression ratio. Editors reserve the right to reject the photos of poor quality. Before submitting a figure in EPS format make sure first, that all the characters are rendered correctly (e.g. by opening the file first in the programs Ghostview or GSview – depending on the operation system or in Adobe Photoshop). With PDF format make sure that lossless compression (LZW or ZIP) was used in the creation of the *.pdf file (JPEG, the default setting, is not suitable). Figures created in Microsoft Word, Excel, PowerPoint etc. will not be accepted without the conversion into one of the before mentioned formats. The same goes for graphics from other graphical programs (CorelDraw, Adobe Illustrator, etc.). The figures should be prepared in final size, published in the magazine. The dimensions are 12.5 cm maximum width and 19 cm maximum height (width and height of the text on a page).

11. Conclusions
Articles shall end with a summary of the main findings which may be written in point form.

12. Summary
Articles written in Slovene must contain a more extensive English summary. The reverse also applies.

13. Literature
References shall be cited in the text. If a reference work by one author is cited, we write Allan (1995) or (Allan 1995); if a work by two authors is cited, (Trinajstić and Franjić 1994); if a work by three or more authors is cited, (Pullin et al. 1995); and if the reference appears in several works, (Honsig-Erlenburg et al. 1992, Ward 1994a, Allan 1995, Pullin et al. 1995). If several works by the same author published in the same year are cited, the individual works are indicated with the added letters a, b, c,

etc.: (Ward 1994a,b). If direct quotations are used, the page numbers should be included: Toman (1992: 5) or (Toman 1992: 5–6).The bibliography shall be arranged in alphabetical order beginning with the surname of the first author, comma, the initials of the name(s) and continued in the same way with the rest of the authors, separated by commas. The names are followed by the year of publication, the title of the article, the full name of the journal (periodical), the volume, the number in parenthesis (optional), and the pages. Example:

Mielke, M.S., Almeida, A.A.F., Gomes, F.P., Aguilar, M.A.G., Mangabeira, P.A.O., 2003. Leaf gas exchange, chlorophyll fluorescence and growth responses of Genipa americana seedlings to soil flooding. Experimental Botany, 50(1), 221–231.

Books, chapters from books, reports, and congress anthologies use the following forms:

Allan, J.D., 1995. Stream Ecology. Structure and Function of Running Waters, 1st ed. Chapman & Hall, London, 388 pp.

Pullin, A.S., McLean, I.F.G., Webb, M.R., 1995. Ecology and Conservation of *Lycaena dispar*: British and European Perspectives. In: Pullin A. S. (ed.): Ecology and Conservation of Butterflies, 1st ed. Chapman & Hall, London, pp. 150-164.

Toman, M.J., 1992. Mikrobiološke značilnosti bioloških čistilnih naprav. Zbornik referatov s posvetovanja DZVS, Gozd Martuljek, pp. 1-7.

14. Format and Form of Articles

The manuscripts should be sent exclusively in electronic form. The format should be Microsoft Word (*.doc) or Rich text format (*.rtf) using Times New Roman 12 font with double spacing, align left only and margins of 3 cm on all sides on A4 pages. Paragraphs should be separated by an empty line. The title and chapters should be written bold in font size 14, also Times New Roman. Possible sub-chapter titles should be written in italic. All scientific names must be properly italicized. Used nomenclature source should be cited in the Methods section. The text and graphic material should be sent to the editor-in-chief as an e-mail attachment. For the purpose of review the main *.doc or *.rtf file should contain figures and tables included (each on its own page). However, when submitting the manuscript the figures also have to be sent as separate attached files in the form described under paragraph 10. All the pages (including tables and figures) have to be numbered. All articles must be proofread for professional and language errors before submission.

A manuscript element checklist (For a manuscript in Slovene language the same checklist is appropriately applied with a mirroring sequence of Slovene and English parts):
English title – (Times New Roman 14, bold)
Slovene title – (Times New Roman 14, bold)

Names of authors with clearly indicated addresses, affiliations and the name of the corresponding author – (Times New Roman 12)
Author(s) address(es) / institutional addresses – (Times New Roman 12)
Fax and/or e-mail of the corresponding author – (Times New Roman 12)
Keywords in English – (Times New Roman 12)
Keywords in Slovene – (Times New Roman 12)
Running title – (Times New Roman 12)
Abstract in English (Times New Roman 12, title – Times New Roman 14 bold)
Abstract in Slovene – (Times New Roman 12, title – Times New Roman 14 bold)

Introduction – (Times New Roman 12, title – Times New Roman 14 bold)
Material and methods – (Times New Roman 12, title – Times New Roman 14 bold)
Results – (Times New Roman 12, title – Times New Roman 14 bold)
Discussion – (Times New Roman 12, title – Times New Roman 14 bold)
Summary in Slovene – (Times New Roman 12, title – Times New Roman 14 bold)
Figure legends; each in English and in Slovene – (Times New Roman 12, title – Times New Roman 14 bold, figure designation and figure title – Times New Roman 12 bold)
Table legends; each in English and in Slovene – (Times New Roman 12, title – Times New Roman 14 bold, table designation and table title – Times New Roman 12 bold)
Acknowledgements – (Times New Roman 12, title – Times New Roman 14 bold)
Literature – (Times New Roman 12, title – Times New Roman 14 bold)
Figures, one per page; figure designation indicated top left – (Times New Roman 12 bold)
Tables, one per page; table designation indicated top left – (Times New Roman 12 bold)
Page numbering – bottom right – (Times New Roman 12)

15. Peer Review

All Scientific Articles shall be subject to peer review by two experts in the field (one Slovene and one foreign) and Brief Note articles by one Slovene expert in the field. With articles written in Slovene and dealing with a very local topic, both reviewers will be Slovene. In the compulsory accompanying letter to the editor the authors must nominate one foreign and one Slovene reviewer. However, the final choice of referees is at the discretion of the Editorial Board. The referees will remain anonymous to the author. The possible outcomes of the review are: 1. Fully acceptable in its present form, 2. Basically acceptable, but requires minor revision, 3. Basically acceptable, but requires important revision, 4. May be acceptable, but only after major revision, 5. Unacceptable in anything like its present form. In the case of marks 3 and 4 the reviewers that have requested revisions have to accept the suitability of the corrections made. In case of rejection the corresponding author will receive a written negative decision of the editor-in-chief. The original material will be erased from the ABS archives and can be returned to the submitting author on special request. After publication the corresponding author will receive the *.pdf version of the paper.

Acta Biologica Slovenica (2018) – Vol. 61: št. 2

ČLANKI – ARTICLES:

NOVICE – NEWS